AWARD NUMBER: W81XWH-14-1-0271

TITLE: Targeting GPR30 in Abiraterone- and MDV3100-Resistant Prostate Cancer

PRINCIPAL INVESTIGATOR: Hung-Ming Lam, PhD

CONTRACTING ORGANIZATION: University of Washington
Seattle, WA 98195

REPORT DATE: December 2017

TYPE OF REPORT: Final

PREPARED FOR: U.S. Army Medical Research and Materiel Command
Fort Detrick, Maryland 21702-5012

REPORT DOCUMENTATION PAGE

Form Approved
OMB No. 0704-0188

1. REPORT DATE	2. REPORT TYPE	3. DATES COVERED
December 2017	Final	30Sept2014 - 29Sept2017

4. TITLE AND SUBTITLE
Targeting GPR30 in Abiraterone- and MDV3100-Resistant Prostate Cancer

5a. CONTRACT NUMBER

5b. GRANT NUMBER W81XWH-14-1-0271

5c. PROGRAM ELEMENT NUMBER

6. AUTHOR(S)
Hung-Ming Lam

E-Mail: minglam@uw.edu

5d. PROJECT NUMBER

5e. TASK NUMBER

5f. WORK UNIT NUMBER

7. PERFORMING ORGANIZATION NAME(S) AND ADDRESS(ES)

University of Washington
1959 NE Pacific St
Seattle WA98195

8. PERFORMING ORGANIZATION REPORT NUMBER

9. SPONSORING / MONITORING AGENCY NAME(S) AND ADDRESS(ES)

U.S. Army Medical Research and Materiel Command
Fort Detrick, Maryland 21702-5012

10. SPONSOR/MONITOR'S ACRONYM(S)

11. SPONSOR/MONITOR'S REPORT NUMBER(S)

12. DISTRIBUTION / AVAILABILITY STATEMENT

Approved for Public Release; Distribution Unlimited

13. SUPPLEMENTARY NOTES

14. ABSTRACT
Little information is available on the novel treatment for abiraterone (Abi)- and MDV3100 (MDV)-resistant disease. G protein-coupled receptor 30 (GPR30) is a seven-transmembrane estrogen receptor and activation by its specific agonist G-1 inhibited growth in multiple castration-resistant prostate cancer (CRPC) xenograft models that were resistant to the first-generation androgen deprivation therapy. More importantly, GPR30 is an androgen-repressed target and its expression increased in clinical CRPC when compared to primary prostate cancer. Here, we showed that G-1 significantly inhibited the growth and extended the progression-free survival of patient-derived xenograft models that are sensitive (LuCaP 136CR, P=0.046) or minimally responsive to Abi and MDV (LuCaP 35CR, P=0.005). Interesting, no survival benefit was observed with G-1 when these mice had been pre-treated with Abi or MDV. However, G-1 delayed the development of Abi resistance in the Abi-sensitive LuCaP 136CR, suggesting a defined window for the G-1 therapy. Together with our previous findings, G-1 invariably inhibited 5 models of CRPC, independent of their sensitivity to Abi or MDV. No adverse side effect of G-1 was detected in these preclinical studies. Clinically, GPR30 expression was detected in >90% of CRPC metastases, whereas 80% showed a moderate to high expression level. In rapid autopsy patients who were treated with Abi- and/or MDV, GPR30 was highly expressed in both lung and bone metastases. The high level of GPR30 in CRPC receiving Abi and MDV highlights the potential in effective G-1 therapy on CRPC patients either in combination with Abi, or on CRPC that is minimally responsive to Abi and MDV.

15. SUBJECT TERMS
Prostate Cancer, Abiraterone, MDV3100, GPR30, Estrogen receptor, G-1, Patient derived xenografts, Treatment resistance

16. SECURITY CLASSIFICATION OF:			17. LIMITATION OF ABSTRACT	18. NUMBER OF PAGES	19a. NAME OF RESPONSIBLE PERSON
a. REPORT	b. ABSTRACT	c. THIS PAGE			USAMRMC
U	U	U	Unclassified	56	19b. TELEPHONE NUMBER *(include area code)*

Table of Contents

1. ABSTRACT

Targeting GPR30 in Abiraterone- and MDV3100-Resistant Prostate Cancer

Tseona O, Nguyen HM, Heide J, de Frates R, Morrissey C, Corey E, Vessella RL, Lam HM

Department of Urology, University of Washington, 1959 Pacific Street, Seattle, WA 98195

Period 9/30/16-9/29/17

Little information is available on the novel treatment for abiraterone (Abi)- and MDV3100 (MDV)-resistant disease. G protein-coupled receptor 30 (GPR30) is a seven-transmembrane estrogen receptor and activation by its specific agonist G-1 inhibited growth in multiple castration-resistant prostate cancer (CRPC) xenograft models that were resistant to the first-generation androgen deprivation therapy. More importantly, GPR30 is an androgen-repressed target and its expression increased in clinical CRPC when compared to primary prostate cancer. Here, we showed that G-1 significantly inhibited the growth and extended the progression-free survival of patient-derived xenograft models that are sensitive (LuCaP 136CR, P=0.046) or minimally responsive to Abi and MDV (LuCaP 35CR, P=0.005). Interesting, no survival benefit was observed with G-1 when these mice had been pre-treated with Abi or MDV. However, G-1 delayed the development of Abi resistance in the Abi-sensitive LuCaP 136CR, suggesting a defined window for the G-1 therapy. Together with our previous findings, G-1 invariably inhibited 5 models of CRPC, independent of their sensitivity to Abi or MDV. No adverse side effect of G-1 was detected in these preclinical studies. Clinically, GPR30 expression was detected in >90% of CRPC metastases, whereas 80% showed a moderate to high expression level. In rapid autopsy patients who were treated with Abi- and/or MDV, GPR30 was highly expressed in both lung and bone metastases. The high level of GPR30 in CRPC patients receiving Abi and MDV highlights the potential in effective G-1 therapy on CRPC either in combination with Abi, or on CRPC that is minimally responsive to Abi and MDV.

2. INTRODUCTION

Castration-resistant prostate cancer (CRPC) is evolving fast and developing resistance to the most recent treatments including abiraterone (Abi) and MDV3100 (MDV). Treatments to these newly resistant tumors have not been explored. While research efforts continue to abolish the residue androgen signaling in these resistant cells, we propose to focus on androgen-repressed therapeutic targets whose expression is now high under the ultra-low androgen milieu in Abi- and MDV-resistant cancer. G protein-coupled receptor 30 (GPR30) is a seven-transmembrane estrogen receptor and it elicits cell growth or death depending on the cellular context. We showed GPR30 activation by its specific agonist G-1 inhibited prostate cancer growth through G2 arrest and apoptosis. We further showed that GPR30 expression was suppressed by androgen and importantly its expression was increased in castration-resistant prostate cancer (CRPC) in both preclinical setting and clinical specimens. G-1 inhibited the growth of multiple CRPC xenografts that were resistant to the first-generation ADT (i.e. castration). We hypothesize that for CRPC resistant to the second-generation ADT including Abi and MDV, the expression of the androgen-suppressed target GPR30 is high, and hence the anti-tumor effect of G-1 will be maximized.

In this proposal, we will perform preclinical testing on the efficacy and the safety of the GPR30-targeted therapy in our newly developed Abi- and MDV-resistant patient-derived xenografts, and investigate the frequency of GPR30 expression in patient specimens. This study will also provide information on the mechanism underlying GPR30 responsiveness and resistance.

3. KEYWORDS

Prostate Cancer, Abiraterone, MDV3100, GPR30, Estrogen receptor, G-1, Patient derived xenografts, Treatment resistance

4. ACCOMPLISHMENTS

4.1. G-1 inhibited the growth of CRPC in the absence of prior Abi and MDV treatment

G-1 invariably inhibited growth of 5 CRPC models including LNCaP, C4-2, PC-3 (*Lam et al, Endocrine-related Cancer, 2014*), LuCaP 136CR, and LuCaP 35CR **(Figure 1)**. We completed the G-1 efficacy studies on the growth inhibition in abiraterone (Abi)- and MDV3100 (MDV)-resistant LuCaP xenografts. In both LuCaP 35CR and LuCaP 86.2, tumors took more than expected (take rate 78% and 83%, respectively). The mice were treated with Abi or MDV and resistance to drugs developed as anticipated **(Figure 2).** No toxicity or weight loss due to treatment was detected **(Figure 3)**. Tumor growth was monitored twice weekly. Although G-1 consistently inhibited growth of CRPC, G-1 did not inhibit growth once tumors received prior treatment with Abi **(Figure 4)** and MDV **(Figure 5)**. It is likely attributed to the diverse survival mechanisms in Abi-resistant tumors (*Lam et al., Clin Can Res, 2017*). The lack of G-1-induced growth inhibition post-Abi and MDV is not dependent on whether the Abi resistance was acquired (LuCaP 136CR) or *de novo* (LuCaP 35CR, **Figure 1**),

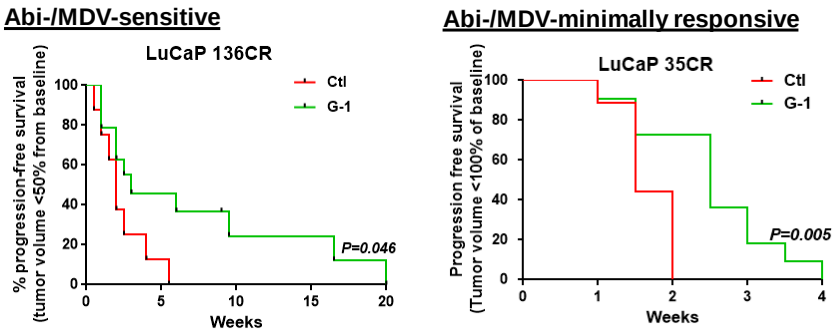

Figure 1. G-1 delayed progression in both Abi/MDV – sensitive and – minimally responsive CRPC.

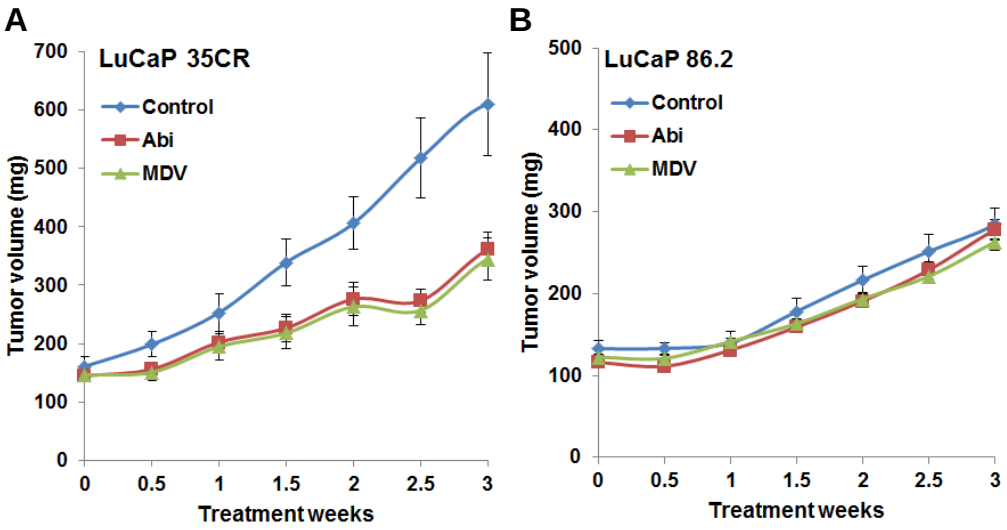

Figure 2. Tumor growth upon Abi and MDV resistance in **A)** LuCaP 35CR and **B)** LuCaP 86.2 patient-derived prostate cancer xenografts. Control, n=9; Abi, n=29-40 due to the rolling enrollment; MDV, n=21-37 due to the rolling enrollment.

Next, we evaluated the tumor characteristics associated with G-1 treatment in Abi- and MDV-resistant CRPC. G-1 did not generally alter proliferation except it induced a slight increase in proliferation in LuCaP 136CR ($P<0.01$) upon Abi resistance, suggesting a tumor model specific induction of proliferation upon G-1 resistance **(Figure 6)**. G-1 inhibited apoptosis in LuCaP 136CR and LuCaP 35CR ($P=0.02$ and $P=0.09$, respectively), but not in LuCaP 86.2 upon Abi resistance **(Figure 7)**. In contrast, G-1 increased apoptosis in LuCaP 86.2 ($P=0.01$) upon MDV resistance **(Figure 7)**. Finally, G-1 treatment did not alter the number of CD34+ blood vessels in both Abi- and MDV-resistant CRPCs, suggesting G-1 had no detectable effects on angiogenesis in these CRPC models **(Figure 8)**.

Interestingly, we noticed for the first time that the antiandrogen MDV inhibited angiogenesis in both LuCaP 35CR and LuCaP 86.2 (**Figure 8**; P=0.08 and P=0.03, respectively), arguing that MDV-resistant tumor may develop mechanisms to survive under a nutrient-deprived environment.

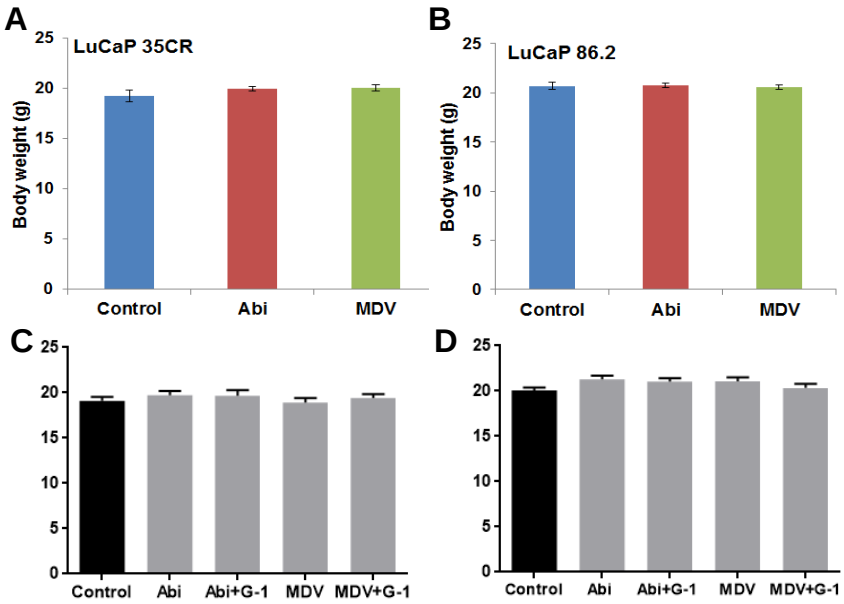

Figure 3. Body weight upon Abi and MDV resistance in **A)** LuCaP 35CR and **B)** LuCaP 86.2 patient-derived prostate cancer xenografts. Body weight at the end of study (tumor exceeded 1000mm^3) in **C)** LuCaP 35CR and **D)** LuCaP 86.2. Error bars represents mean±SEM. Treatment n=11-16/group; control n= 8/group.

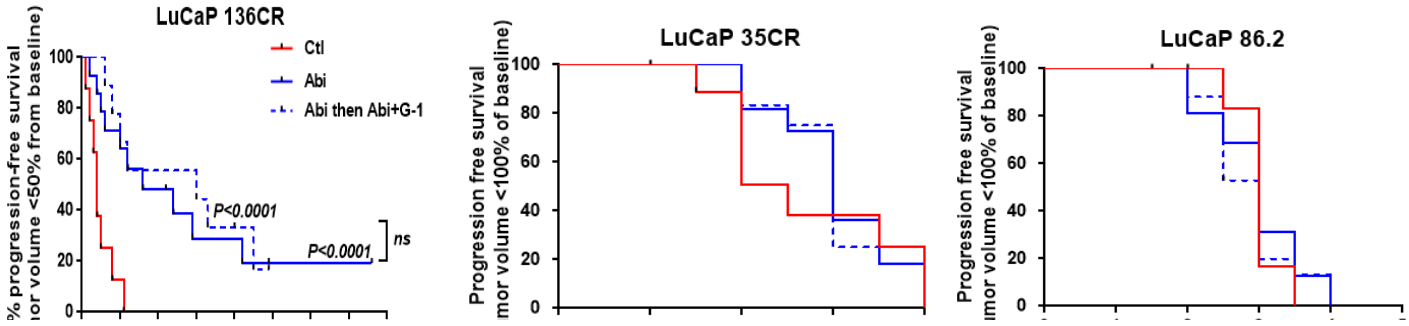

Figure 4. G-1 did not delay progression of PDXs that exhibited acquired (LuCaP 136CR) or de novo resistance (LuCaP 35CR and LuCaP 86.2) to Abi.

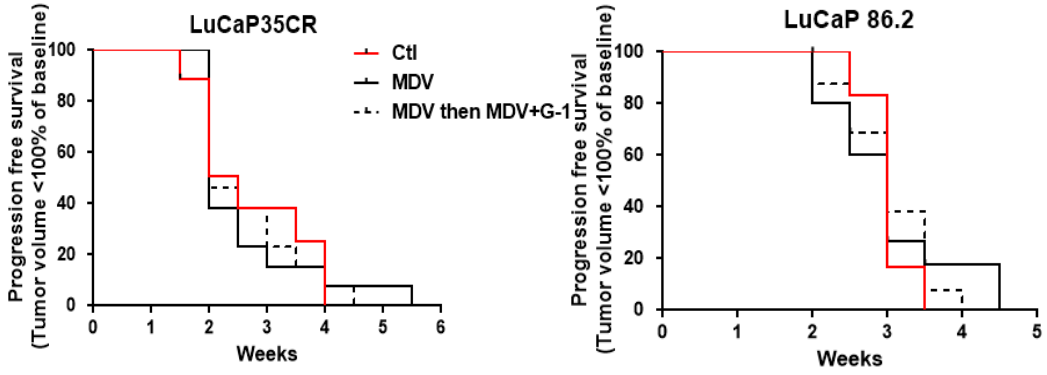

Figure 5. G-1 did not delay progression of MDV-resistant PDXs.

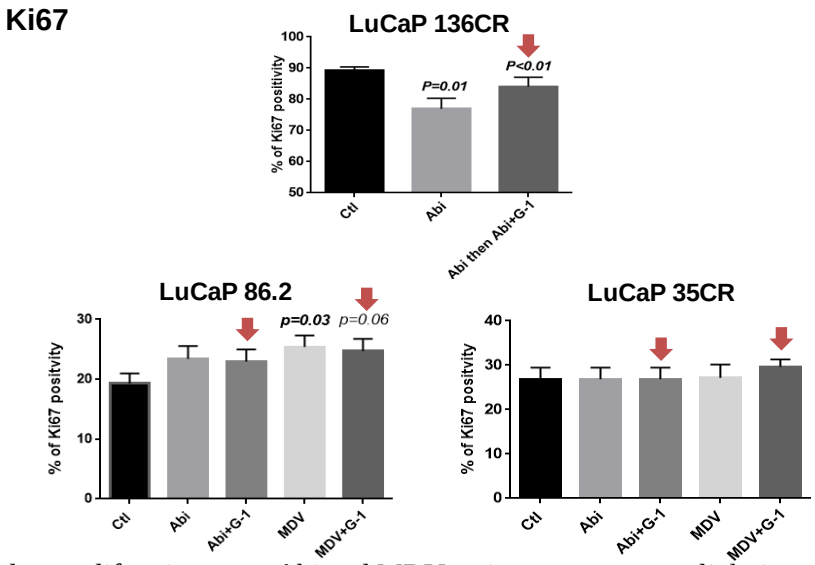

Figure 6. G-1 did not alter proliferation upon Abi and MDV resistance, except a slight increase in proliferation was detected in LuCaP 136CR.

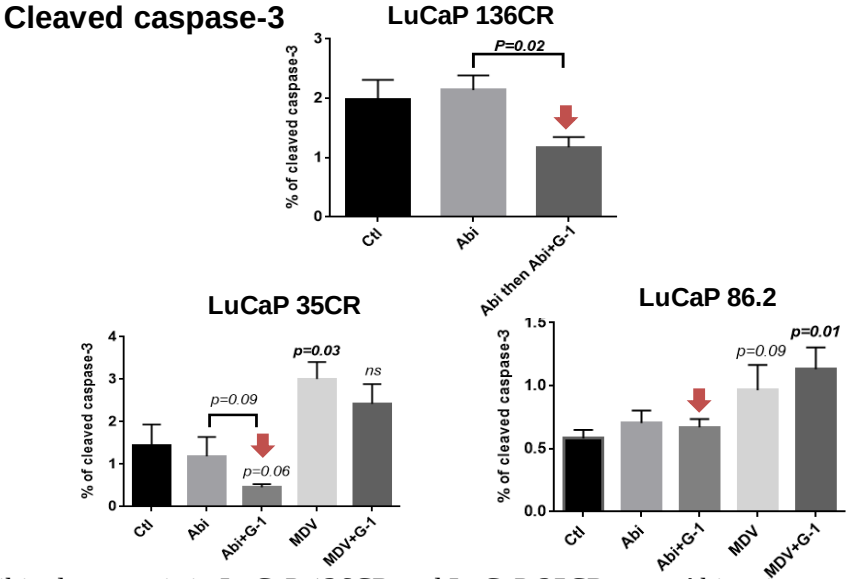

Figure 7. G-1 inhibited apoptosis in LuCaP 136CR and LuCaP 35CR upon Abi resistance. G-1 increased apoptosis in LuCaP 86.2 upon MDV resistance.

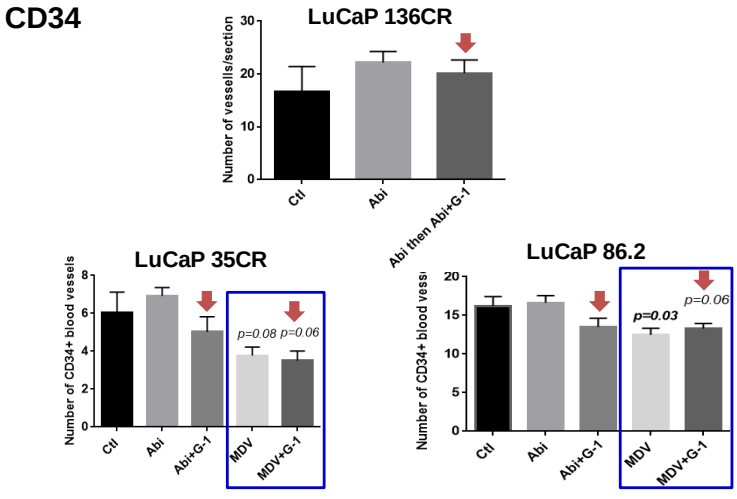

Figure 8. MDV inhibited angiogenesis in LuCaP 35CR (p=0.08) and LuCaP 86.2 (p=0.03, blue box). G-1 did not alter angiogenesis upon Abi and MDV resistance.

4.2. G-1 delayed Abi resistance and the rate *of de novo* resistance is low in G-1 and Abi combination treatment

The above results showed that G-1 inhibited growth of CRPC but was not able to delay progression in CRPC that acquired resistance to Abi and MDV, therefore we attempted to introduce G-1 earlier in the treatment course by combining Abi and G-1 to investigate if G-1 can delay the development of Abi resistance. In **Figure 9**, G-1 delayed Abi resistance in both LuCaP 136CR and C4-2 CRPC xenograft models. Most importantly, the *de novo* resistance rate to Abi+G-1 combination treatment is very low (8% compared to 43-50% for Abi or G-1 single treatment; **Table 1**). Gene expression studies showed that Abi increased GPR30 expression level in these xenografts, suggesting the high level of GPR30 may enhance the cell growth inhibition by G-1 **(Figure 10)**. Global gene expression analysis on how G-1 inhibited growth of CRPC showed genes that were differentially expressed in the responsive phase were abrogated upon G-1 resistance **(Figure 11)**.

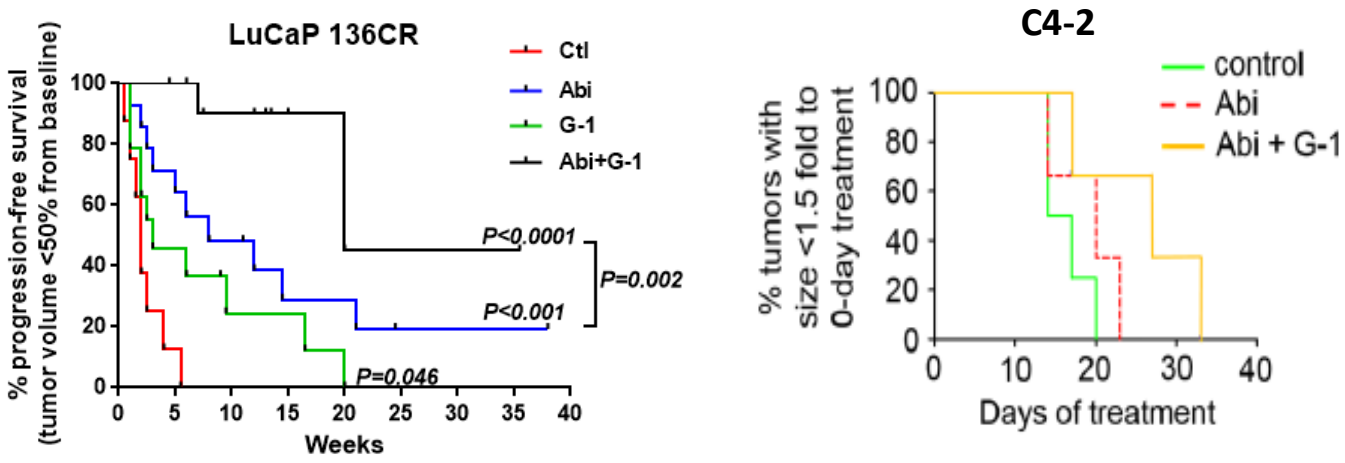

Figure 9. G-1 in combination with Abi delayed CRPC progression in LuCaP 136CR and C4-2.

Table 1. *De novo* resistance rate is low in G-1 and Abi combination treatment

Treatment	**De novo* resistance/total # of animals (%)
Control	8/8 (100%)
Abi	6/14 (43%)
G-1	7/14 (50%)
Abi+G-1	1/12 (8%)

**De novo* resistance is defined by tumor progression >50% from baseline at 6 weeks of treatment

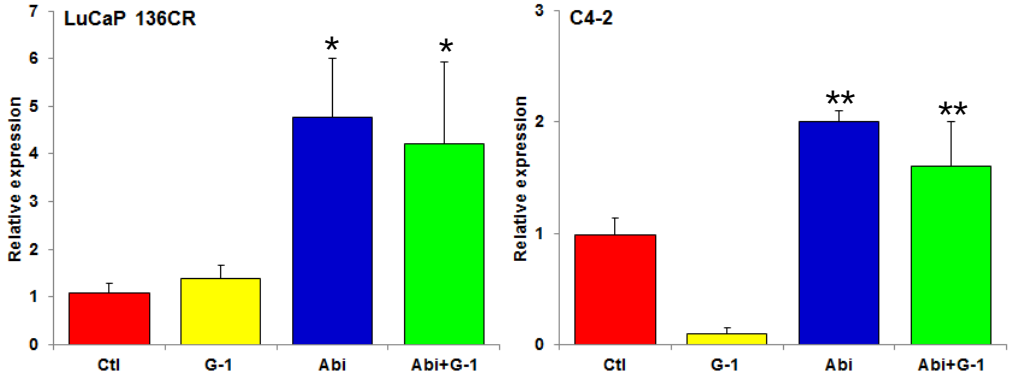

Figure 10. Abi increase GPR30 expression in PCa xenografts.

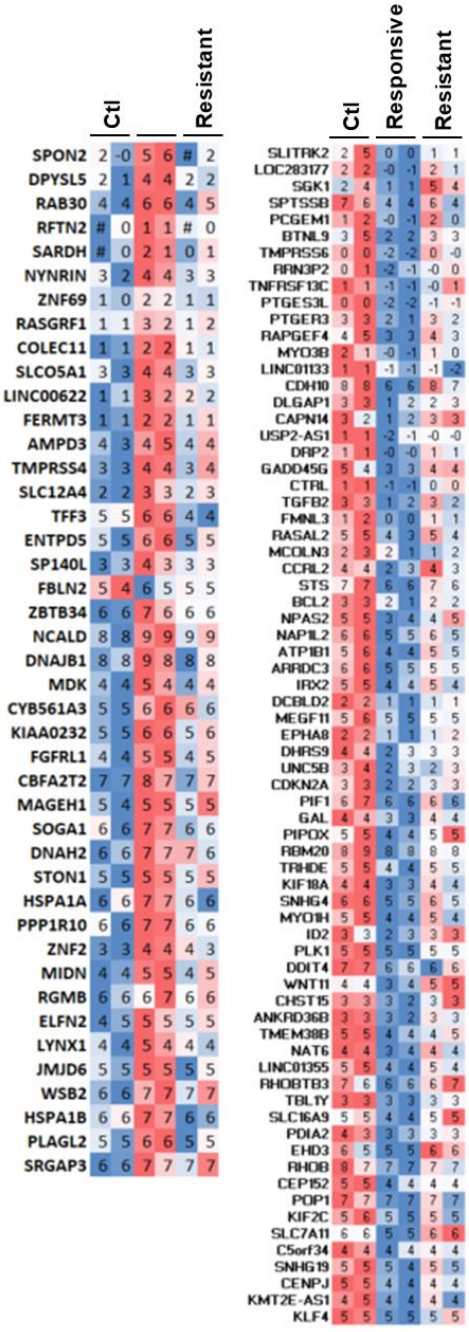

Figure 11. RNA sequencing analysis showing genes differentially expressed in G-1-responsive LuCaP35CR, which were abrogated upon resistance. G-1. Left panel: upregulated by G-1in the responsive phase; right panel: downregulated by G-1 in the responsive phase. Red: upregulated; blue: downregulated.

4.3. GPR30 expression is high in clinical CRPC metastases treated with Abi and MDV

Next, we sought to examine whether the GPR30 level is high post-Abi/MDV treatment in clinical metastases. We performed 12 rapid autopsies as anticipated. From the rapid autopsy, 5/12 patients had been treated with Abi only, 2/12 with MDV only, and 5/12 with both Abi and MDV. We performed immunohistochemistry staining of GPR30 and found high levels of GPR30 in both bone and soft tissue metastases (including lymph node, lung, and liver) in the patients who received Abi and/or MDV treatment **(Figures 12 and 13)**. Comparing between CRPC metastases from patients who had expired in the pre- and post-Abi/MDV era, we found that in the absence of Abi/MDV treatment, GPR30 expression was detected in >90% of CRPC metastases, whereas 80% showed a moderate to high expression level **(Figure 12, upper panel)**. In the recent patients who had received Abi and/or MDV, GPR30 expression remained high in both bone and soft tissue metastases in 92% of these patients **(Figure 12, lower panel)**. Collectively, *the consistent high level of GPR30 expression in CRPC metastasis upon treatment with Abi and/or MDV, and the effective growth inhibition of G-1 in combination with Abi highlighted the potential for an effective combination therapy of Abi+G-1 in >90% of patients.* Since GPR30 is an androgen-repressed target, we attempted to correlate the intratumoral androgen levels with the GPR30 level in both pre- and post-Abi/Enz patients. Intratumoral androgens were evaluated using mass spectrometry in collaboration with Dr. Elahe Mostaghel. Ten patients in both pre- and post-Abi/Enz settings had evaluable tumor androgens including testosterone (T) and dihydrotestosterone (DHT). In the pre-Abi/Enz patients, GPR30 protein level (detected by IHC) did not achieve a significant inverse correlation with the intratumoral T (Pearson r=-0.43, p=0.25) and DHT level (Pearson r = -0.32, p=0.40). In the post-Abi/Enz patients, GPR30 level was not correlated with the intratumoral T (Pearson r=0.43, p=0.23) and DHT level (Pearson r=0.52, p=0.12). In fact, while GPR30 level is fairly consistent across metastatic sites **(Figure 12)**, the intratumoral androgen levels are not universal within a patient. As shown in **Figure 14**, a subset of patients showed variable intratumoral T (patients 1-4, 18-20) whereas others showed a very consistent level of intratumoral T across metastatic sites (patients 7-10, 11-15). The variation in the intratumoral T within patients did not appear to be associated with Abi/Enz treatment **(Figure 14A)**. In contrast, intratumoral DHT levels were more heterogeneous across metastatic sites, and appeared to be more heterogeneous within Abi/Enz-resistant patients **(Figure 14B)**.

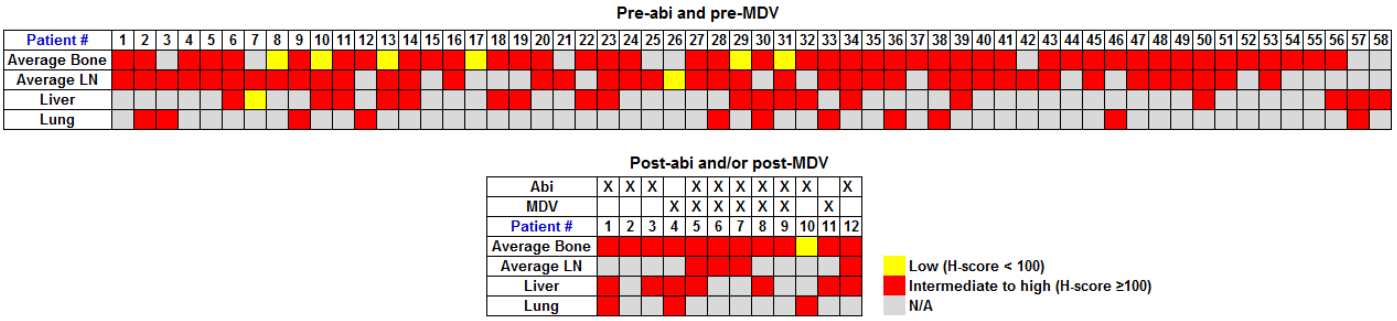

Figure 12. GPR30 expression is high in CRPC metastases from patients in the pre- and post-Abi/MDV era.

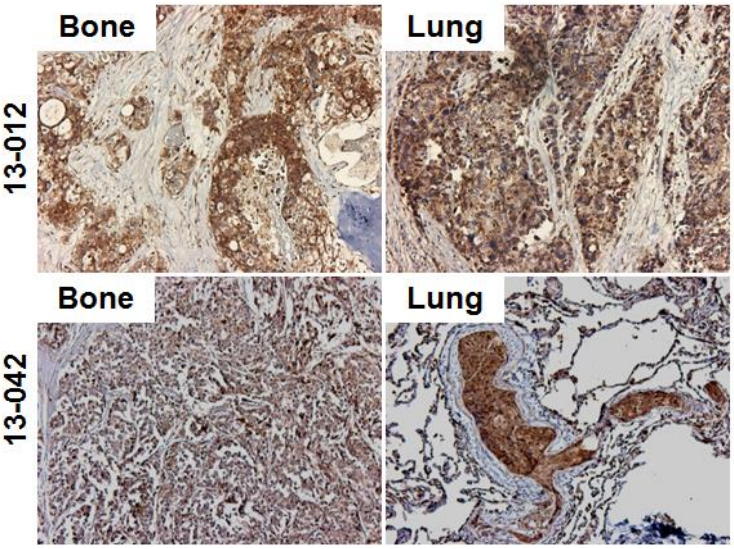

Figure 13. Representative pictures showing high expression of GPR30 in both bone and lung metastases in prostate cancer rapid autopsy patients who had received Abi and MDV treatment.

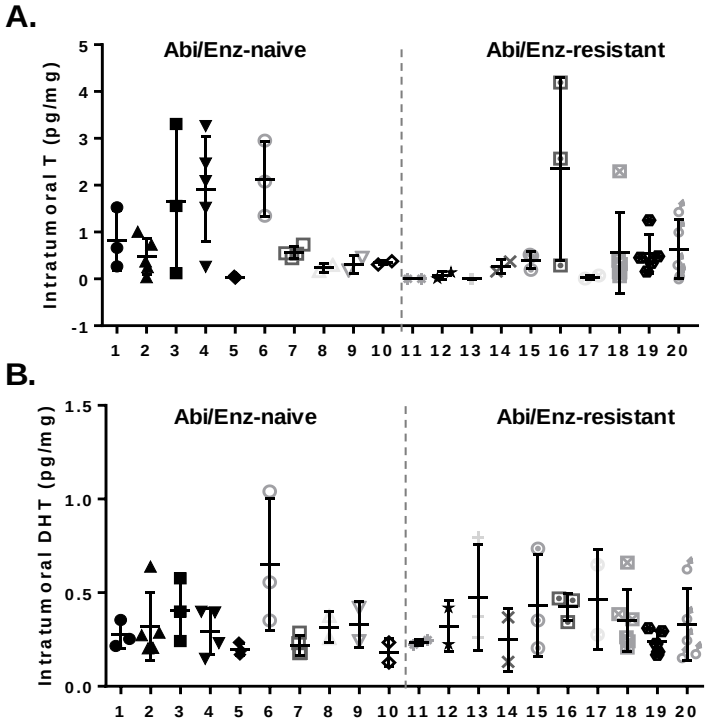

Figure 14. Intratumoral androgen measurement in multiple metastatic sites of Abi/Enz-naïve and Abi/Enz-resistant patients from rapid autopsy. **(A)** Intratumoral T level is variable in a subset of patients whereas consistent in others across metastatic sites. **(B)** Intratumoral DHT displayed a greater heterogeneity within patients. Patients with two or more evaluable metastatic sites were included.

Opportunities for training and professional development
I participated in preclinical study meetings to gain knowledge on the different responses to Abi and MDV, and studied the molecular mechanisms underlying the response and resistance to Abi and MDV in various in-house patient-derived xenograft models, resulting in a publication in the journal *Clinical Cancer Research* (Lam et al., 2017). The information has provided a basis for examining intratumoral androgens and drug resistance outlined in this project. This project has attracted interests in the prostate cancer community and was selected to be presented in the plenary session of the Prostate Cancer Foundation Scientific Retreat in 2015. In 2016, I attended and presented in the PCRP IMPaCT meeting to advance the knowledge on the most recent prostate cancer work, and grant applications and reviews. This project also provided on-hand training for Olena Tseona, a research scientist, on specimen identification and sectioning, immunohistochemistry staining and quantification, and tumor characterization. Ms. Tseona was then successfully applied to medical school in 2017.

Results disseminated to community of interest
1. Presented advances in exploring estrogen receptors as a therapeutic target in CRPC in a Prostate Cancer Foundation teleconference in November 2014.
2. Presented signaling mechanisms involved in prostate cancer cell escape from dormancy in a Prostate Cancer Foundation international webinar in August 2015.
3. Presented part of the proposal in the plenary lecture in the Prostate Cancer Foundation Annual Retreat in October 2015.
4. Presented the molecular characterization of abiraterone ultra-responders in CRPC patient-derived xenograft models in Pacific Northwest Prostate Cancer SPORE meeting in March 2016.
5. Presented interim results in the PCRP IMPaCT meeting in August 2016.
6. Prepared a brief description of the project to 2016 PCRP program materials.

Plan to do during the next reporting period to accomplish the goals
The experiments were on track and we are preparing the final manuscript for submission.

5. IMPACT
Impact on the development of the principal discipline of the project
Nothing to report

Impact on other disciplines
Nothing to report

Impact on technology transfer
Nothing to report

Impact on society beyond science and technology
Nothing to report

6. CHANGES/PROBLEMS
Nothing to report

7. PRODUCTS
Publications, conference papers, and presentations

A) Publications:

1. **Lam H.M.**, Ouyang B., Chen J., Ying J., Wang J., Wu C.L., Li J., Medvedovic M., Vessella, R.L., Ho S.M. (2014) Targeting GPR30 with G-1: a new therapeutic target for castration-resistant prostate cancer. Endocr Relat Cancer. 21(6):903-914.

2. Ruppender N., Larson S., Lakely B., Kollath L., Brown L., Coleman I., Coleman R., Nguyen H.M., Nelson P.S., Corey E., Snyder L.A., Vessella R.L., Morrissey C., **Lam H.M.** (2015) Cellular adhesion promotes prostate cancer cells escape from dormancy. PLoS One. 10(6):e0130565.

3. **Lam H.M.**, McMullin R., Nguyen H.M., Coleman I., Gormley M., Gulati R., Brown L., Holt S.K., Li W., Ricci D., Verstraeten K., Thomas S., Mostaghel E.A., Nelson P.S., Vessella R.L., Corey E. (2017) Characterization of an abiraterone ultraresponsive phenotype in castration-resistant prostate cancer patient-derived xenografts. Clin Can Res. 23(9):2301-2312.

   ► Highlighted in Nature Reviews Urology

B) Conferences abstracts:

1. **Lam H.M.**, Zhang X., Nguyen H., Olson J., Corey E., Ho S.M., Vessella R.L., "Targeting GPR30 delayed Abiraterone resistance in castration-resistant prostate cancer", 21st Annual Prostate Cancer Foundation Scientific Retreat, San Diego, CA. October 2014.

2. Ruppender N., Larson S., Lakely B., Kollath L., Brown L., Coleman I., Coleman R., Nguyen H.M., Nelson P.S., Corey E., Snyder L.A., Vessella R.L., Morrissey C., **Lam H.M.**, "Cellular adhesion promotes prostate cancer cells escape from dormancy", Society for Basic Biological Research, Dallas, TX. November 2014.

3. **Lam H.M.**, McMullin R., Nguyen H.M., Gormley M., Gulati R., Li W., Ricci D., Verstraeten K., Thomas S., Mostaghel E.A., Nelson P.S., Vessella R.L., Corey E. "Abiraterone acetate (AA) treatment of prostate cancer patient-derived xenografts (PDXs) demonstrates heterogeneity of responses and identifies potential biomarkers of adaptive resistance", AACR Annual Meeting, Philadelphia, PA . April 2015.

4. Tseona O., Nguyen H.M., Heide J., de Frates R., Morrissey C., Corey E., **Lam H.M.,** ''Targeting estrogen receptors in castration-resistant prostate cancer'', 22nd Annual Prostate Cancer Foundation Scientific Retreat, Washington D.C., October 2015

5. Tseona O., Nguyen H.M., Heide J., de Frates R., Morrissey C., Corey E., **Lam H.M.**, "Targeting GPR30 in Abiraterone- and MDV3100-resistant Prostate Cancer", DoD PCRP IMPaCT Meeting, Towson, MD. August 2016.

6. Tseona O., Nguyen H.M., Heide J., de Frates R., Morrissey C., Corey E., **Lam H.M.**, "GPR30 as a Therapeutic Target in Abiraterone- and MDV3100-resistant Prostate Cancer", SBUR Fall Meeting, Scottsdale, AZ. November 2016.

C) Presentations:

1. *The biological implication of single disseminated prostate cancer cells from patient*s, Prostate Cancer Foundation Tumor Microenvironment Working Group, International Webinar, November 2014.
2. *The challenges and value of interrogating the transcriptome of a single disseminated prostate cancer cell from a patient*, SBUR Fall Symposium, Dallas, TX. November 2014.
3. *Activation of GPR30 by G-1 provides a novel strategy in targeting CRPC,* Prostate Cancer Foundation. Teleconference, November 2014.
4. 11. *Cellular adhesion promotes prostate cancer cells escape from dormancy*, Prostate Cancer Foundation. International webinar, August 2015.
5. 12. *Targeting estrogen receptors in castration-resistant prostate cancer*, Prostate Cancer Foundation 22nd Scientific Retreat, Washington DC. October 2015.
6. 13. *Characterization of the abiraterone ultraresponder in castration-resistant prostate cancer*, Pacific NW Prostate Cancer SPORE Meeting, Seattle, WA. March 2016.
7. 14. *Targeting GPR30 in abiraterone- and MDV3100-resistant prostate cancer*, DoD PCRP IMPaCT meeting, Towson, MD. August 2016.

8. PARTICIPANTS AND OTHER COLLABORATING ORGANIZATIONS

Name	Hung-Ming Lam
Project role	PD/PI
Nearest person month worked	8
Contribution to project	Prepare documents for IACUC, ACURO, and HRPO approvals, and

	IRB exemptions; design and oversee preclinical studies; analyze and interpret results; clear documents required for abiraterone acetate and MDV3100 transfer; present findings; prepare reports and manuscripts

Name	Eva Corey
Project role	Co-I
Nearest person month worked	1
Contribution to project	Assist in preclinical study setup and result interpretation

Name	Olena Tseona
Project role	Research scientist
Nearest person month worked	4
Contribution to project	Conduct tumor characterization experiments including tissue sectioning, and immunohistochemistry staining and quantification; acquire abiraterone- and MDV3100-resistant specimens in the prostate cancer rapid autopsy program; prepare tissue microarray and stain for GPR30 in rapid autopsy specimens.
Funding support	NIH/NCI

Name	Jessica Olson
Project role	Research scientist
Nearest person month worked	5
Contribution to project	Perform preclinical studies including castration of the mouse, tumor inoculation, tumor measurement, drug administration, PSA measurement, mouse sacrifice, and tissue acquisition; acquire abiraterone- and MDV3100-resistant specimens in the prostate cancer rapid autopsy program

Name	Holly Nguyen
Project role	Research scientist
Nearest person month worked	3
Contribution to project	Submit IACUC protocol; perform preclinical studies and organize results; acquire abiraterone- and MDV3100-resistant specimens in the prostate cancer rapid autopsy program

Name	Bryce Lakely
Project role	Research scientist
Nearest person month worked	5
Contribution to project	Identify specimens, extract RNA, RNA sequencing.

Name	Belinda Nghiem
Project role	Research scientist
Nearest person month worked	1
Contribution to project	Prepare tumor specimens for intratumoral androgen analysis

Changes in active support
Nothing to report

Other organizations involved as partners

Organization name	Janssen Pharmaceuticals
Location of organization	Raritan, NJ
Contribution to the project	Provided abiraterone acetate for the study

Organization name	Astella/Medivation
Location of organization	San Francisco, CA
Contribution to the project	Provided MDV3100 for the study

9. SPECIAL REPORTING REQUIREMENTS

N/A

10. APPENDICES

Next page

Targeting GPR30 with G-1: a new therapeutic target for castration-resistant prostate cancer

Hung-Ming Lam[1,†], Bin Ouyang[1], Jing Chen[1], Jun Ying[1], Jiang Wang[2], Chin-Lee Wu[3], Li Jia[4,‡], Mario Medvedovic[1,5], Robert L Vessella[6] and Shuk-Mei Ho[1,5,7,8]

[1]Department of Environmental Health, University of Cincinnati Medical Center, Room 128 Kettering Complex, Cincinnati, Ohio 45267-0056, USA
[2]Department of Pathology and Laboratory Medicine, University of Cincinnati Medical Center, Cincinnati, Ohio, USA
[3]Department of Pathology, Massachusetts General Hospital and Harvard Medical School, Boston, Massachusetts, USA
[4]Department of Medicine, Center for Pharmacogenomics, Washington University School of Medicine, St Louis, Missouri, USA
[5]Center for Environmental Genetics, University of Cincinnati Medical Center, Cincinnati, Ohio, USA
[6]Department of Urology, University of Washington, Seattle, Washington, USA
[7]Cincinnati Veterans Affairs Medical Center, Cincinnati, Ohio, USA
[8]Cincinnati Cancer Center, Cincinnati, Ohio, USA
[†]H-M Lam is now at Department of Urology, University of Washington, Box 356510, Seattle, Washington 98195, USA
[‡]L Jia is now at Division of Urology, Department of Surgery, Brigham and Women's Hospital, Boston, Massachusetts 02115, USA

Correspondence should be addressed to S-M Ho
Email
Shuk-mei.Ho@uc.edu

Abstract

Castration-resistant prostate cancer (CRPC) is an advanced-stage prostate cancer (PC) associated with high mortality. We reported that G-1, a selective agonist of G protein-coupled receptor 30 (GPR30), inhibited PC cell growth by inducing G2 cell cycle arrest and arrested PC-3 xenograft growth. However, the therapeutic actions of G-1 and their relationships with androgen *in vivo* are unclear. Using the LNCaP xenograft to model PC growth during the androgen-sensitive (AS) versus the castration-resistant (CR) phase, we found that G-1 inhibited growth of CR but not AS tumors with no observable toxicity to the host. Substantial necrosis (approximately 65%) accompanied by marked intratumoral infiltration of neutrophils was observed only in CR tumors. Global transcriptome profiling of human genes identified 99 differentially expressed genes with 'interplay between innate and adaptive immune responses' as the top pathway. Quantitative PCR confirmed upregulation of neutrophil-related chemokines and inflammation-mediated cytokines only in the G-1-treated CR tumors. Expression of murine neutrophil-related cytokines also was elevated in these tumors. *GPR30* (*GPER1*) expression was significantly higher in CR tumors than in AS tumors. In cell-based experiments, androgen repressed *GPR30* expression, a response reversible by anti-androgen or siRNA-induced androgen receptor silencing. Finally, in clinical specimens, 80% of CRPC metastases ($n=123$) expressed a high level of GPR30, whereas only 54% of the primary PCs ($n=232$) showed high GPR30 expression. Together, these results provide the first evidence, to our knowledge, that GPR30 is an androgen-repressed target and G-1 mediates the anti-tumor effect via

Key Words
- androgen deprivation therapy
- androgen-repressed gene
- metastases
- tumor-infiltrating neutrophils

http://erc.endocrinology-journals.org
DOI: 10.1530/ERC-14-0402

Published by Bioscientifica Ltd.

neutrophil-infiltration-associated necrosis in CRPC. Additional studies are warranted to firmly establish GPR30 as a therapeutic target in CRPC.

Endocrine-Related Cancer
(2014) **21**, 903–914

Introduction

Androgen ablation therapies are mainstay treatments for advanced prostate cancer (PC; Tannock *et al*. 2004, Higano *et al*. 2009, de Bono *et al*. 2011). Unfortunately, almost all patients ultimately fail to respond to these therapies and develop castration-resistant PC (CRPC) that grows in the presence of castration levels of circulating testosterone (de Bono *et al*. 2011). Although chemotherapy (docetaxel or cabazitaxel; Tannock *et al*. 2004, de Bono *et al*. 2010), immunotherapy (e.g. sipuleucel-T; Higano *et al*. 2009, Kantoff *et al*. 2010), or complete androgen blockade (e.g. abiraterone; de Bono *et al*. 2011) may extend the lives of some patients, these treatments all have documented side effects and a relatively short duration of response. Hence, the development of new CRPC therapies with durable efficacy and low toxicity is warranted.

Estrogens have a long history of efficacy for advanced PC (Oh 2002). Huggins & Hodges (2002) first reported the use of diethylstilbestrol for advanced PC in 1941. However, severe cardiovascular toxicity of oral estrogens limited their use in PC (Norman *et al*. 2008). The early efficacy of parenteral estrogen in recent studies (Schellhammer 2012, Langley *et al*. 2013) and especially the better toxicity profiles owing to hepatic bypass (Norman *et al*. 2008) reinvigorated interest in the use of estrogens as a therapy for PC. In addition to the suppression of testosterone effects by estrogens, estrogens are also directly cytotoxic to PC cells (Ho *et al*. 2011). The actions of parenteral estrogens are believed to be mediated by the classical estrogen receptors (ERs), ESR1 and ESR2. However, the exact effects of the two ERs and their isoforms on PC growth and metastases may vary according to cellular contexts (Claessens & Tilley 2014, Nelson *et al*. 2014). We have recently reported that G-1 (1(1-(4-(6-bromobenzo(1,3)dioxol-5-yl)-3a,4,5,9b-tetrahydro-3H-cyclopenta(c)quinolin-8-yl)-ethanone)), which selectively activates the third ER, G protein-coupled receptor 30 (GPR30 or GPER) (Bologa *et al*. 2006), inhibited the growth of multiple PC cell lines and PC-3 xenografts, and exerted few or no adverse effects on the animals (Chan *et al*. 2010). These results indicate that G-1, by targeting GPR30, might offer a new treatment option for PC.

GPR30 is structurally unrelated to the classical ERs (ESR1 and ESR1). It is a seven-transmembrane-domain receptor localized at the cell surface (Bologa *et al*. 2006, Funakoshi *et al*. 2006), endoplasmic reticulum (Thomas *et al*. 2005, Prossnitz *et al*. 2007, Otto *et al*. 2008), perinuclear compartment (Cheng *et al*. 2011), and nucleus (Madeo & Maggiolini 2010). The successful development of a highly selective non-steroidal agonist, G-1, for GPR30, provides a tool for studying the action of GPR30 independent of the actions mediated by ESR1 and ESR2 (Bologa *et al*. 2006, Blasko *et al*. 2009). Activation of GPR30 was found to play opposite roles in the regulation of the growth of various normal and neoplastic tissues, promoting growth of breast, endometrium, and ovarian tissues (Filardo *et al*. 2000, Vivacqua *et al*. 2006, Albanito *et al*. 2007, Pandey *et al*. 2009), but inhibiting growth of thymocytes, urothelial cells, vascular smooth muscle cells, and ER-positive breast cancer cells (Albanito *et al*. 2007). The dual action of GPR30 could be related in part to its differential activation of downstream mediators, including EGFR, PI3K, Erk1/2, cAMP, and intracellular Ca^{2+} (reviewed in Maggiolini & Picard (2010) and Prossnitz & Barton (2011)). We demonstrated that in PC cells, the activation of GPR30 by G-1 leads to growth inhibition via an ERK/p21-mediated cell cycle arrest at the G2 phase (Chan *et al*. 2010). In addition, we found that G-1 inhibited the growth of PC-3 xenografts that lack the androgen receptor (AR). Still unknown are the mode of action of G-1 *in vivo* and the potential link between its efficacy and androgen status in PC.

This study evaluated the efficacy of G-1 in inhibiting the growth of LNCaP xenografts during the androgen-sensitive (AS) or the castration-resistant (CR) phase. In this study, we report that G-1 inhibited the growth of the xenograft in castrated (low testosterone) animals but not in intact, androgen-supported animals (high testosterone). The G-1-induced growth inhibition in the CR xenograft was associated with massive necrosis, neutrophil infiltration, upregulation of a set of cell-mediated immune response genes, and enhanced expression of *GPR30* (*GPER1*). Results obtained from cell-based experiments revealed that *GPR30* is repressed by androgen,

http://erc.endocrinology-journals.org
DOI: 10.1530/ERC-14-0402

Published by Bioscientifica Ltd.

whereas immunohistochemical results indicated a larger proportion of human CRPC metastases than primary PC express high GPR30 level. Collectively, these results provide support for targeting GPR30 with G-1 as a possible new approach for the treatment of CRPC.

Materials and methods

Human specimens

Human tissue microarrays were obtained from Massachusetts General Hospital (primary PC) and the University of Washington (metastatic CRPC). Samples were de-identified; only those with complete clinical information, follow-up data, and good tissue quality were included. The primary PC cohort comprised one specimen each from 232 patients with PC (i.e. 232 specimens) taken at prostatectomy (Leung *et al.* 2010). The metastatic CRPC cohort comprised patients who participated in the Rapid Autopsy Program during the period 1999–2006; it consisted of 123 CRPC specimens, including 75 bone (spine, ribs, pelvis, sternum, ischium, iliac, and sacrum), 29 lymph node, 14 liver, and five lung metastasis tissues from 24 patients. The use of the specimens was reviewed and approved by the Institutional Review Board committees of the respective universities.

Cell culture and siRNA experiments

Human PC cell lines LNCaP and PC-3 were obtained from the American Type Culture Collection (ATCC, Manassas, VA, USA) and passaged for less than 3 months after resuscitation. Both LNCaP and PC-3 were retro-authenticated by ATCC with short tandem repeat profiling (March 13, 2013) and confirmed to be the original cell line. LNCaP cells were maintained in RPMI-1640 medium (Invitrogen) supplemented with 10% FBS; sodium pyruvate, 1 mmol/l; L-glutamine, 2 mmol/l; and D-glucose, 1.25 g/l. PC-3 cells were maintained in F-12K medium (ATCC) supplemented with 10% FBS. Cells were cultured at 37 °C in an atmosphere of 5% CO_2. For androgen treatment (R1881 and dihydrotestosterone (DHT)), LNCaP (2.5×10^5) and PC-3 (2×10^5) cells were seeded in phenol-red-free RPMI-1640 (with supplements) and F-12K media, respectively, supplemented with 10% charcoal-stripped FBS. For drug treatment, drugs were added daily for 4 days, and the medium was changed every 2 days. For siRNA-AR (siAR) transfection, cells were replenished with 1.6 ml of fresh medium and 400 µl of siAR-DharmaFECT mixture (50 nM Stealth RNAi siAR, Invitrogen; DharmaFECT3 for LNCaP and DharmaFECT2 for PC-3 cells, Dharmacon, Lafayette, CO, USA) the following day. At day 3, cells were recovered with the respective medium containing 10% charcoal-stripped FBS, and drugs were added daily for 4 days. Transfection was repeated on day 2 of drug treatment. At the end of the experiments, cells were collected for RNA extraction. For the transfection-negative control, cells were treated with DharmaFECT and siRNA-non-targeting (siNT, Dharmacon).

Chromatin immunoprecipitation assay

Chromatin immunoprecipitation (ChIP)-sequencing and ChIP were carried out as described previously using an antibody to AR (ab74272, Abcam, Cambridge, MA, USA; Decker *et al.* 2012). The site-specific qPCR primers for the AR-binding site at the *GPER1* (*GPR30*) locus were as follows: forward, 5′-CTGGGACAACGTGAGCAGTAAG-3′ and, reverse, 5′-CCAACTACTTTACCAGCCAGCA-3′. The primers for prostate-specific antigen (PSA (*KLK3*)) enhancer and control regions have been described previously (Zheng *et al.* 2013).

Microarray experiment and analysis

RNA was extracted from LNCaP xenografts with TRIzol Reagent (Invitrogen); RNA extracts with integrity numbers of less than 8 (four animals in each group), as measured by Agilent 2100 Bioanalyzer (Agilent, Santa Clara, CA, USA), were used for microarray analysis. The detailed microarray study is available in the Supplementary Methods, see section on supplementary data given at the end of this article. The data are accessible through the NCBI Gene Expression Omnibus Series accession number: GSE54974.

Xenograft study

In the first set of experiments, *GPR30* mRNA expression was compared in tumors grown before and after the castration of mice. Male athymic nude mice (4–6 weeks old, 20–25 g, Taconic, Hudson, NY, USA) each received a subcutaneous implant of a 2 cm-long silastic capsule containing ~15 mg testosterone (Sigma), while the animals were under general anesthesia using isoflurane. After 2 days, LNCaP cells (5×10^6 cells) in 150 µl of Matrigel (BD Biosciences, Franklin Lakes, NJ, USA) were injected subcutaneously into the flanks of mice, and the tumors that developed were measured twice weekly (Chan *et al.* 2010). When the tumors reached 150–300 mm^3, mice were divided into two groups: intact and castrated animals. Tumors growing in the intact mice are referred

http://erc.endocrinology-journals.org
DOI: 10.1530/ERC-14-0402

Published by Bioscientifica Ltd.

as AS tumors. For the castrated group, the silastic capsules were removed and mice were surgically castrated under general anesthesia using isoflurane. Tumors regressed and then regrew after castration (approximately 3 weeks post-castration); these tumors are referred as CR. AS or CR tumors at approximately 1000 mm^3 were collected to determine the expression of *GPR30* mRNA.

In the second set of experiments, the therapeutic efficacy of G-1 on AS and CR tumors was evaluated and compared. LNCaP xenografts were developed as described in the first set of experiments. Both AS and CR tumors were enrolled when tumors reach approximately 300–400 mm^3 in size. Mice received subcutaneous injections of a vehicle (95% PBS, 2.5% DMSO, and 2.5% ethanol; v/v) or G-1 (4 mg/kg) daily for 16 days. Tumors and body weight were measured twice weekly. Mice were killed and weighed after removal of the xenografts. The protocol for animal use was approved by the Institutional Animal Care Committee at the University of Cincinnati.

Serum enzyme assays

Serum obtained from mice was assayed for creatine kinase (CK), lactate dehydrogenase (LDH), alanine transaminase (ALT), and aspartate transaminase (AST) using IDTox enzyme assay kits (ID Labs, London, ON, Canada) following the manufacturer's protocols.

Quantitative real-time PCR

Total RNA was treated with RNase-free DNase (Qiagen) and reverse-transcribed (Chan *et al.* 2010). Real-time PCR was carried out as described previously (Chan *et al.* 2010). Species-specific primer sequences are presented in Supplementary Table S1, see section on supplementary data given at the end of this article. PCRs with SYBR GreenER PCR Master-Mix (Invitrogen) were monitored using the 7900HT Fast Real-time PCR System (Applied Biosystems). Individual mRNA levels were normalized to glyceraldehyde-3-phosphate dehydrogenase (*GAPDH*).

Histopathology and immunohistochemistry analyses

Formalin-fixed xenograft samples were processed for hematoxylin and eosin (H&E) staining and subjected to histological examination for necrosis and inflammation; the thickness of the tumor capsule was determined by the surgical pathologist (J W). Analysis of paraffin-embedded human PC and LNCaP xenograft sections by immunohistochemistry (IHC) was performed as described previously (Leav *et al.* 2001). Antibodies and quantification of necrosis and markers are described in the Supplementary Methods and Table S2, see section on supplementary data given at the end of this article.

For clinical specimens, GPR30 expression was graded independently by two investigators (H-M L and J W) in a blinded manner. Signal intensity (0–3) and percentage of signal coverage (0–100) of each section were scored, and the product of the intensity and coverage was represented as an *H*-score (0–300) (Huang *et al.* 2005). For the metastatic CRPC cohort, *H*-scores were an average of duplicated cores in a specified metastatic site of each patient. In all cases of bone metastases, two to three sites were acquired per patient and an average *H*-score was calculated. The distribution of the *H*-score showed bi-modal or multi-modal properties in the clinical data: 45% of the specimens showed *H*-scores of less than 100, approximately 32% of the specimens showed *H*-scores of 100–199 and 23% of the specimens amassed *H*-scores of 200–300. In this study, we used a dichotomous variable of *H*-score group (i.e. *H*-score of 100 or more versus less than 100) in the analysis to reduce possible bias due to the distribution of the original *H*-score and to improve the statistical power. In order to assess the sensitivity of using different definitions to the *H*-score variables, the same analysis was repeated after replacing the dichotomous variable with a three-level category variable (i.e. *H*-score 0–99 versus 100–199 versus 200–300) as well as the original *H*-score. Those results were found to be consistent with the results of the main analysis using the dichotomous variable presented in this study.

Statistical analyses

Numerical dependent variables were analyzed by one-way ANOVA and the *post hoc* Bonferroni tests to compare means if more than two groups were involved. *t*-tests were used if means of two groups were compared. Categorical dependent variables were compared among groups using χ^2 tests. All differences were considered significant when $P<0.05$.

Results

G-1 inhibits growth and induces necrosis in CR tumors with no apparent toxicity to the host

We compared the inhibitory effect of G-1 on AS or CR tumors growing in intact or castrated (low testosterone) mice respectively. Administration of G-1 significantly

http://erc.endocrinology-journals.org
DOI: 10.1530/ERC-14-0402

Published by Bioscientifica Ltd.

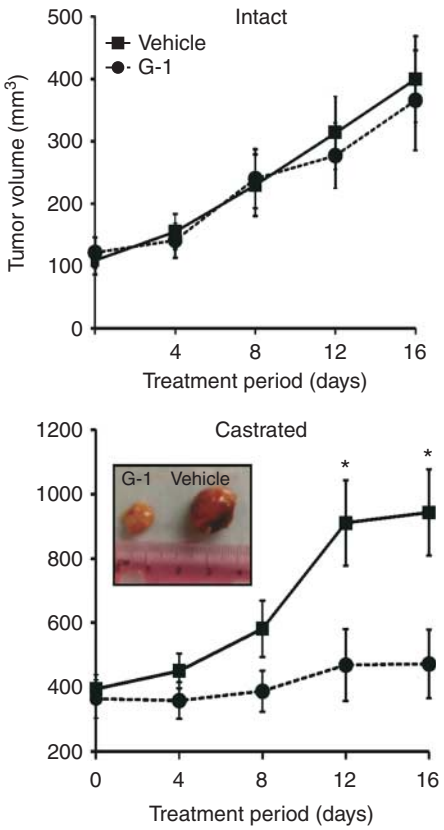

Figure 1
G-1 inhibited growth and induced necrosis in the castration-resistant tumors. G-1 inhibited growth of the CR tumor (bottom panel) but not the androgen-sensitive tumors (top panel). When LNCaP xenografts grew to 150 mm^3, mice were divided into two groups: intact and castrated. Intact animals received subcutaneous injections of a vehicle (2.5% DMSO and 5% ethanol) or G-1 (4 mg/kg) daily for 16 days. For the castrated group, mice were castrated and, when the tumor re-emerged, they were treated with a vehicle or G-1 daily for 16 days. Error bars represent mean ± S.E.M., $n=6$–8/group, $^*P<0.05$.

inhibited the growth of CR tumors after 16 days of treatment ($P<0.05$, Fig. 1). Similar results were obtained in CR tumors including C4-2 and PC-3 (Supplementary Figure S3, see section on supplementary data given at the end of this article). Massive necrosis and inflammation were observed only in the G-1-treated LNCaP CR tumors (in seven out of eight mice). Inflammation was attended by considerable neutrophil infiltration of the necrotic area as well as of the healthy area of these tumors (Fig. 2A). This intratumoral neutrophil infiltration was not observed in either vehicle-treated CR tumors or vehicle/G-1-treated AS tumors that displayed only ischemic necrotic foci with no inflammation/neutrophils (Fig. 2A). We did not examine T cells in this study because nude mice are deficient in these cells (Pelleitier & Montplaisir 1975). B cells and macrophages were found exclusively in the intratumoral stroma and the tumor capsule, respectively, in all treatment groups (Supplementary Figure S1). Notably, G-1-induced necrosis occupied an average of 65% of the tumor volume ($P=0.0003$, Fig. 2B). Furthermore, G-1 significantly reduced the intratumoral microvessel density in CR tumors but not in AS tumors (Fig. 2C, left panel). No significant alteration in microvessel density was observed in the tumor capsule with G-1 treatment (Fig. 2C, right panel). In the viable area of the tumors, cell proliferation (Ki67 staining) remained relatively constant in the four treatment groups except for an increase of 10–20% when compared with vehicle-treated counterparts in Ki67-staining cells in G-1-treated CR tumors (Fig. 2D, left panel). G-1 induced a slight but significant increase in apoptosis (cleaved caspase-3 staining) in the CR tumors (Fig. 2D, right panel).

Our previous work had demonstrated that G-1 did not have general toxicity (on the basis of body weight and tissue histology) in the animals (Chan *et al.* 2010). In this study, we further report that G-1 did not induce any changes in body weight or cause functional damage to the heart or the liver in mice after 16 days of treatment with G-1, as indicated by the levels of injury biomarkers in the serum (CK and LDH for heart injuries; AST and ALT for liver injuries, Fig. 2E).

G-1 induced specific changes in gene expression exclusively in CR tumors

Global transcriptome profiling was performed on vehicle/G-1-treated AS and CR tumors (four groups of tumors, $n=4$). Overall, the profiling results identified 2446 differentially expressed genes among the four treatment groups (false discovery rate (FDR) <0.1, $P<0.01$, $n=4$ per group). Unbiased hierarchical clustering analysis showed no significant differences in gene expression between the vehicle-treated and the G-1-treated AS tumors (Fig. 3, left side of heat map). However, this analysis identified two clusters of genes (a total of 1082) that were altered by G-1 exclusively in the CR tumors (Fig. 3, right side of heat map). Subsequent gene shaving using two additional criteria – $P<0.01$ and a difference of at least 1.5-fold between G-1-treated and vehicle-treated CR tumors – yielded a final set of 99 genes (Fig. 3A, gray panel). Ingenuity Pathway Analysis (IPA) of the 99 genes showed enrichment of the top biological pathway 'antigen presentation, cell-to-cell signaling and interaction, and inflammatory response', followed by 'genetic disorder, neurological disease, and skeletal and muscular disorders'. Furthermore, the top canonical

http://erc.endocrinology-journals.org
DOI: 10.1530/ERC-14-0402

Published by Bioscientifica Ltd.

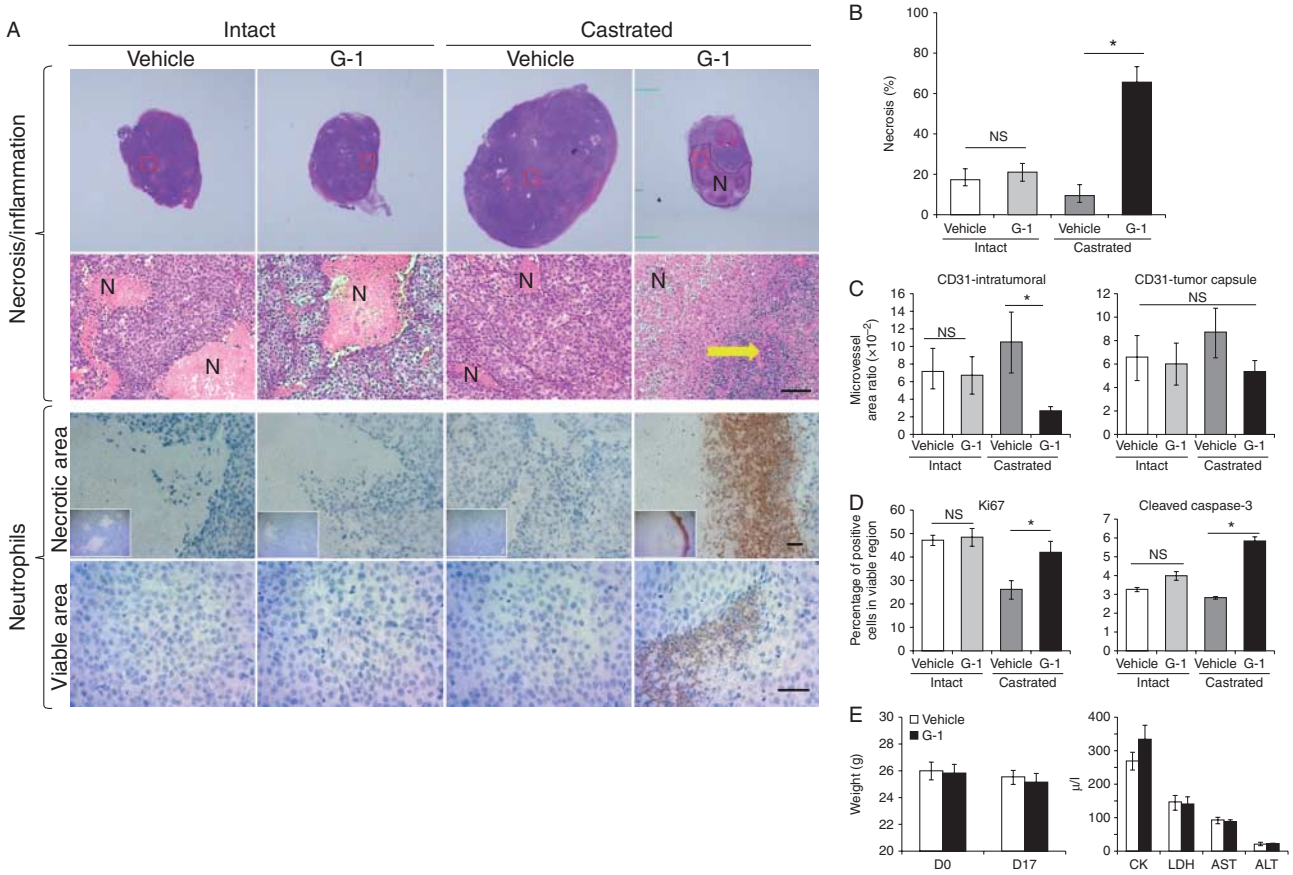

Figure 2

G-1 induced massive necrosis and neutrophil infiltration in the CR tumors. (A) G-1 triggered massive necrosis in CR tumors. Tumor sections were stained with H&E, and the necrotic area was quantified as described in the Supplementary Methods. (B) G-1 induced significant necrosis associated with massive inflammation, which in turn was associated with neutrophil infiltration, both surrounding the necrotic area and within the viable area, in CR tumors only. The yellow arrow represents massive inflammation. Magnification: 20× (H&E, upper panel), 200× (H&E, lower panel), 100× (neutrophil IHC, upper panel), and 200× (neutrophil IHC, lower panel). Scale bars represent 50 μm in all micrographs. (C) G-1 reduced the microvessel area ratio in the intratumoral stromal region but not in the tumor capsule. Microvessel area ratio is calculated as the ratio of the microvessel area to the intratumoral stromal area or the capsule area. (D) Ki67 and cleaved caspase-3 staining of tumor cells was used to determine proliferation and apoptosis respectively. (E) G-1 did not induce toxicity in castrated mice as determined by the absence of changes in body weight (left panel) and in serum assays of organ damage marker enzymes (right panel). Error bars represent mean ± S.E.M., $n=6$–8/group, $^*P<0.05$; NS, not significant; H&E, hematoxylin and eosin; IHC, immunohistochemistry.

pathway identified in this specific set of G-1-associated genes is 'communication between innate and adaptive immune cells' (Supplementary Table S3, see section on supplementary data given at the end of this article).

To focus on identifying molecular mediators of G-1-induced inflammation/neutrophil infiltration, we selected a set of genes from the 99-gene panel for confirmation based on a literature search showing their relatedness to cell-mediated immune responses. Quantitative real-time PCR analyses ($n=6$ per group) validated the upregulation of the expression of these genes in G-1-treated CR tumors but not in G-1-treated AS tumors when compared with their respective vehicle-treated controls. These include four chemokine genes *CP*, *IL8* (*CXCL8*), *CCL2*, and *CXCL12*; three interferon-induced antiviral genes *IFIT2*, *IFIT3*, *IFIT4*; and *SOD2*, an important oxidative stress response gene (Fig. 3B). As human interleukin 8 (IL8) is a strong chemo-attractant for both human and mouse neutrophils (Geiser *et al.* 1993, Schaider *et al.* 2003), we analyzed murine neutrophil-related cytokine genes using quantitative real-time PCR. Expression of murine genes involved in neutrophil movement, accumulation, adhesion, activation, and phagocytic respiratory burst, including *Il1b*, *Il6*, *Il18*, *Tnfa* (*Tnf*), *Cxcl12*, *Cxcl1*, *Cxcl3*, *S100a8*, *S100a9*, and *Cd14* (Cacalano *et al.* 1994, Leung *et al.* 2001, Ryckman *et al.* 2003, Harokopakis &

Published by Bioscientifica Ltd.

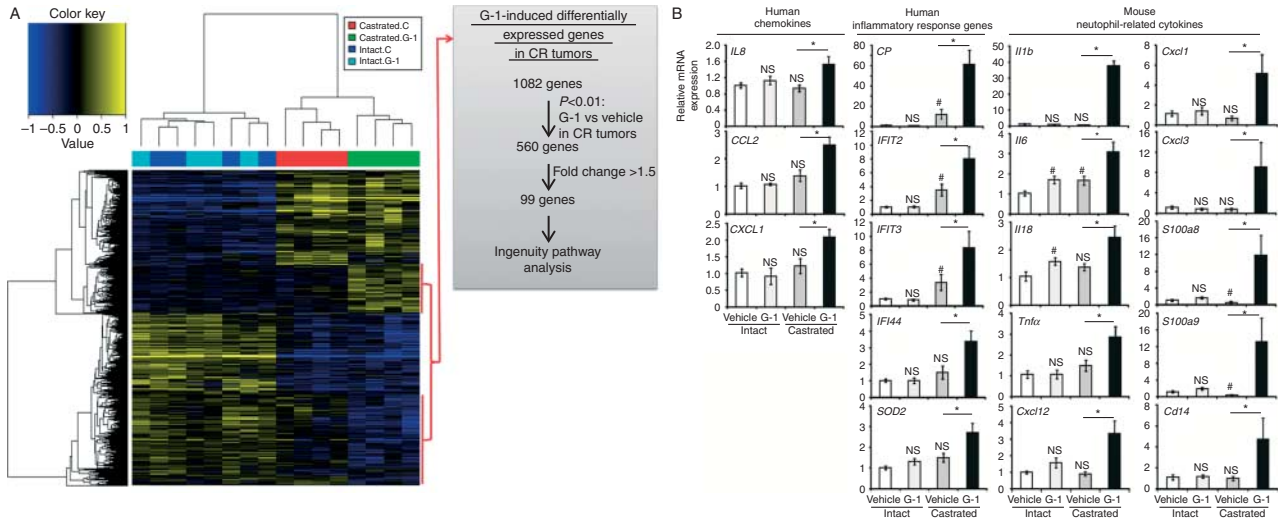

Figure 3

G-1 induced unique changes in gene expression in castrated animals. (A) Heat map of hierarchically clustered differential gene expression in intact or castrated animals treated with a vehicle or G-1 blue, down-regulated; yellow, upregulated; $n=4$ per group. A scheme for gene selection for Ingenuity Pathway Analysis is shown. (B) Quantitative real-time PCR analyses of the G-1-induced human and mouse genes in intact and castrated animals. Data were normalized to the levels of housekeeping genes: human-specific *GAPDH* (for human genes) or *ActB* (for mouse genes). Error bars represent mean ± S.E.M., $n=6$. $^{\#}P<0.05$ compared with intact-vehicle treatment and $^{*}P<0.05$ compared with castrated-vehicle treatment. NS, not significant.

Hajishengallis 2005, Eash *et al*. 2010), was elevated by 1.8- to 50.9-fold in G-1-treated vs vehicle-treated CR tumors (Fig. 3B). Interestingly, the expression of human *IL1B* was not altered in CR tumors with G-1 treatment.

Androgen represses *GPR30* expression via AR, and castration increases *GPR30* expression

In an attempt to explain why G-1 inhibited growth only in an androgen-deprived environment, we determined the effect of androgen on *GPR30* expression. Androgen is the principal hormone regulating prostate function. Treatment of LNCaP cell cultures with R1881 (a synthetic androgen) or DHT (the physiologically active androgen) reduced the expression of *GPR30* mRNA; the effects of these androgens were abolished by cotreatment with bicalutamide, an AR antagonist, or by transduction of a siRNA against AR (Fig. 4A and B, upper panels). These responses were not observed in the AR-negative PC-3 cells (Fig. 4A and B, bottom panels). These results indicate that androgen represses *GPR30* expression via mechanisms involving the AR. Furthermore, ChIP-sequencing analyses of LNCaP cells revealed a strong AR-binding site approximately 3.5 kb downstream of the 3′ end of the *GPR30* (*GPER1*) gene after androgen stimulation (Supplementary Figure S2, see section on supplementary data given at the end of this article, upper panel). This AR-binding site on *GPR30* was further validated by an independent site-specific ChIP–qPCR analysis (Supplementary Figure S2, lower panel).

In the LNCaP xenograft model, expression of *GPR30* mRNA was significantly higher (approximately eightfold) in CR tumors grown in castrated mice than in AS tumors grown in intact mice (Fig. 4C). Expression of *AR* mRNA in CR tumors was increased by 1.8- to 4.6-fold when compared with that in AS tumors (data not shown). These results are in concordance with those from cell-based studies, indicating that GPR30 expression is repressed by androgen via AR-mediated signaling.

GPR30 expression is higher in metastatic CRPC than in primary PC

We reasoned that GPR30 in CRPC metastases needs to be expressed at significant levels before we can consider it as a new therapeutic target for CRPC. Hence, we used IHC to assess the level of GPR30 expression in specimens obtained from two cohorts of patients. The first cohort included only primary cancers from specimens obtained at prostatectomy ($n=232$) and the second comprised CRPC metastases ($n=123$). We found that 80% of the metastatic CRPC specimens expressed high levels of GPR30, with an

http://erc.endocrinology-journals.org
DOI: 10.1530/ERC-14-0402

Published by Bioscientifica Ltd.

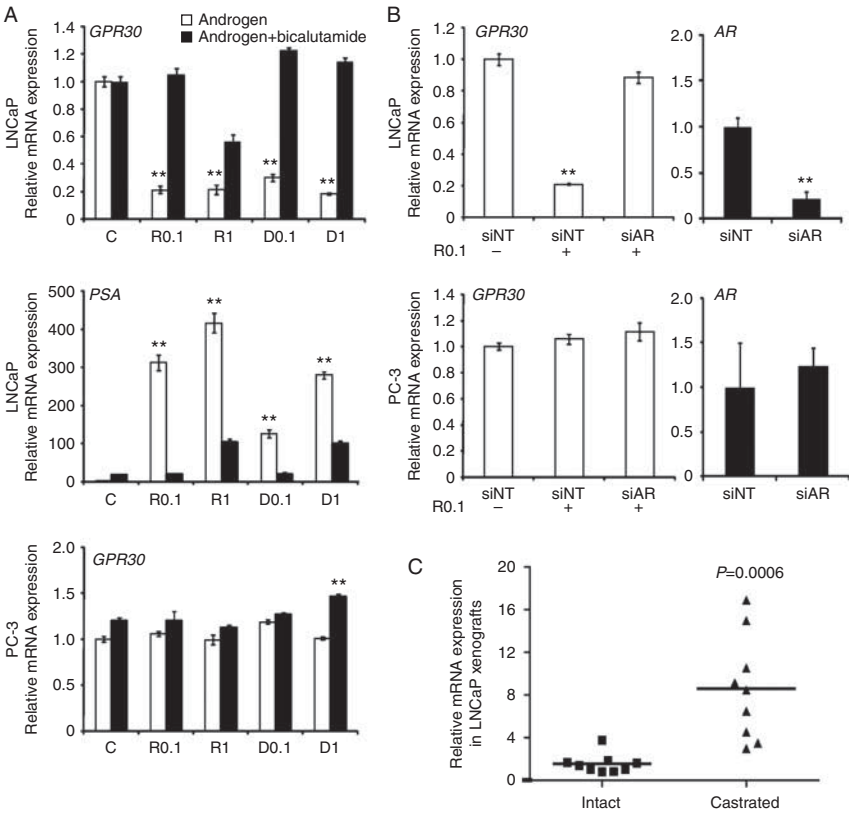

Figure 4

Androgen suppressed GPR30 expression via AR. (A) Androgen (white bars, 0.1 and 1 nM) suppressed GPR30 expression, and suppression was reversed by bicalutamide (black bars) in AR-positive LNCaP cells but not in AR-negative PC-3 cells. Cells were treated with androgen in the presence or absence of bicalutamide for 4 days. Prostate-specific antigen (PSA) was a positive control for the androgen-stimulated AR response gene. (B) siAR abolished the androgen-suppressed GPR30 expression in LNCaP cells. Error bars represent mean ± S.D. of three independent experiments, $^{**}P<0.01$. (C) Castration upregulated GPR30 expression *in vivo*. RNA was extracted, and GPR30 expression of the LNCaP xenograft in intact mice (AS tumor, $n=9$) was compared with that after castration of mice (CR tumor, $n=9$). Relative mRNA expression was compared with that of intact mouse no. 1. AR, androgen receptor; D, dihydroxytestosterone; PSA, prostate-specific antigen; R, R1881; siNT, siRNA-non-targeting; siAR, siRNA-AR.

H-score of 100 or more when compared with 54% of primary PC specimens with an *H*-score of 100 or more ($P=0.001$) (Fig. 5).

GPR30 staining in PC was not correlated with age, the Gleason score of primary cancer, final PSA level, type of androgen deprivation therapy (ADT), or duration of ADT (Supplementary Table S4, see section on supplementary data given at the end of this article). Interestingly, no difference in the *H*-scores of GPR30 was observed among the 75 bone metastases obtained from different locations (*H*-score approximately 162–165; pelvis/sternum/ischium/iliac/sacrum versus rib/limb versus spine; Supplementary Table S5).

Discussion

In this study, we determined that G-1, a GPR30 agonist, inhibited the growth of CR tumors but not during their preceding AS growth phase, with no detectable toxicity to the host. The G-1-induced growth inhibitory response was manifested as massive necrosis attended by marked neutrophil infiltration in the affected tumors, associated with the activation of gene pathways involved in innate antitumor immunity. We also demonstrated that androgen suppressed GPR30 expression in an AR-dependent manner and that castration markedly upregulated its expression. Clinically, we observed an elevated prevalence of high levels of GPR30 in CRPC metastases when compared with that in primary PC. Taken together, these findings provide evidence for the effective preclinical targeting of GPR30 with G-1 for CRPC.

In this study, we aimed to examine the activation of GPR30 by G-1 in both an androgen-supported (intact) and an androgen-deprived (castrated) environment *in vivo*. We had previously demonstrated that G-1 inhibited growth in cell culture experiments and a hormone-independent PC-3

http://erc.endocrinology-journals.org
DOI: 10.1530/ERC-14-0402

Published by Bioscientifica Ltd.

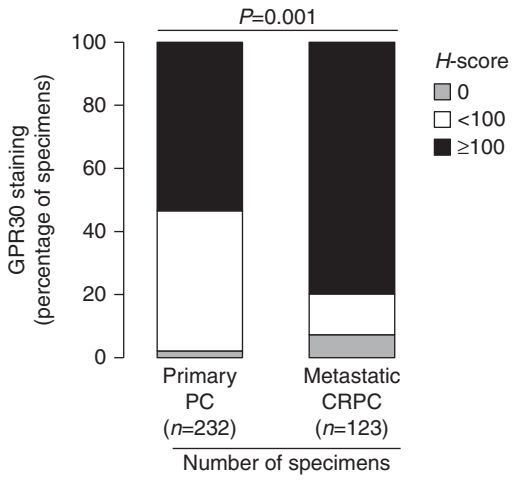

Figure 5
GPR30 staining in primary PC and CRPC metastases. A high level of GPR30 was detected in a larger proportion of metastatic CRPC specimens when compared with primary PC specimens.

xenograft in castrated hosts (Chan *et al*. 2010). This study further demonstrated the efficacy of G-1 in the LNCaP xenograft model, which recapitulates the natural history of PC progression from AS to CR. We found that, in the LNCaP xenograft model, G-1 inhibited the growth of CR tumors but not AS tumors, indicating that the androgen deprivation may favor the anti-tumor action of G-1.

Histological examinations have indicated that G-1 induced massive tumor necrosis in the castrated mice and invasion of the viable region of G1-treated tumors by numerous tumor-infiltrating neutrophils (TINs). At the molecular level, upregulation of chemokine and inflammatory response genes, including *CP*, *IL8*, *CCL2*, *CXCL12*, and *IFIT*s, were uncovered by transcriptome profiling and confirmed by qPCR. Thus, one hypothesis is that chemokines secreted by viable CRPC cells and/or additional tumor tissue remodeling factors stimulated by G-1 may direct the migration of neutrophils (illustrated in Fig. 6). Neutrophils have been implicated in tumor progression and antitumor response. Mild infiltration of neutrophils stimulates proliferation and metastasis in cancer (Gregory & Houghton 2011). However, high levels of TINs induce a destructive oncolytic response (Fu *et al*. 2011) and are associated with cytotoxicity and tumor regression (Di Carlo *et al*. 2001). Neutrophils produce cytotoxic mediators, including reactive oxygen species, proteases, membrane-perforating agents, and soluble cell-kill mediators (Di Carlo *et al*. 2001). Moderate or extensive

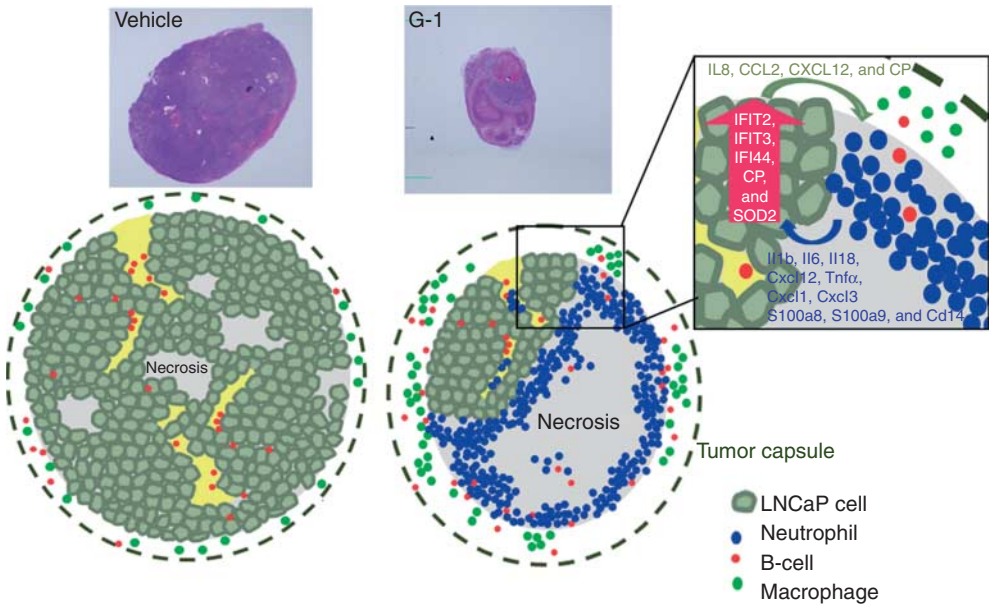

Figure 6
A schematic diagram showing G-1-induced innate antitumor response in castration-resistant LNCaP prostate cancer *in vivo*. For LNCaP xenografts in vehicle- or G-1-treated intact animals or vehicle-treated castrated animals, focal ischemic necrosis was detected in the tumor. However, in G-1-treated castrated animals, massive necrosis and neutrophil infiltration were detected in the necrotic area as well as within the viable area of the tumor. (Box) In human xenografts, the levels of expression of human-specific chemokine and inflammatory response genes were increased; in the mouse stroma, the levels of expression of a panel of murine-specific neutrophil-related cytokine genes were elevated. In both intact and castrated animals, macrophages resided in the tumor capsule and B cells localized to the intratumoral stroma of the LNCaP xenograft.

http://erc.endocrinology-journals.org
DOI: 10.1530/ERC-14-0402

Published by Bioscientifica Ltd.

levels of TINs are associated with reduced mortality in gastric cancer (Caruso *et al*. 2002), indicating that neutrophils are active in immunosurveillance against cancer. Key TIN-associated cell-kill mediators, including IL1β and tumour necrosis factor alpha (TNFα) (Di Carlo *et al*. 2001), were detected in the G-1-induced tumor necrosis. Previous results have indicated that transgenic expression of IL8 and TNFα in tumor cells elicited prominent neutrophil-mediated antitumor activity (Hirose *et al*. 1995, Musiani *et al*. 1996). In addition, ceruloplasmin (CP) produced by the CR tumor cells attracts neutrophils and enhances phagocytosis of neutrophils (Saenko *et al*. 1994). In contrast to the systemic upregulation of cytokines, which may pose a health hazard to immunocompromised patients with cancer, local and specific recruitment of neutrophils may provide a new approach to the targeted treatment of cancer (Hirose *et al*. 1995, Fu *et al*. 2011).

GPR30 expression has been reported to be upregulated by various growth factors, HIF1α, and progestin (Ahola *et al*. 2002, Albanito *et al*. 2008, Recchia *et al*. 2011, De Marco *et al*. 2013). However, only one report described a decrease in GPR30 expression after estrogen treatment in the human internal mammary artery (Haas *et al*. 2007). This estrogen-induced suppression of GPR30 was not detected in neurons (Jacobi *et al*. 2007), indicating that the regulation of GPR30 expression is cell-context-specific. In this study, we demonstrated for the first time that androgen, the principal hormone in the prostate, inhibited GPR30 expression that was dependent on AR. Interest has started to focus on the crosstalk between AR and ER signaling in PC (Yang *et al*. 2012, Claessens & Tilley 2014, Nelson *et al*. 2014). The goal of current treatments of CRPC is to maximally suppress androgen signaling, which may in turn remove the androgen suppression of GPR30 expression, resulting in a high level of GPR30 in late-stage CRPC. In this study, we provided convincing evidence that, in both a preclinical model and in human specimens, reduced androgen levels in CRPC enhanced GPR30 expression when compared with hormone-naïve PC. The wide expression and high levels of GPR30 may highlight an unprecedented opportunity to target this protein in clinical metastases of CRPC.

Existing therapies for CRPC offer limited gains in survival and trigger adverse effects; thus, attention has begun to focus on the sequence of application of these treatments (Higano & Crawford 2011). The current LNCaP model represents a subtype of CRPC in which G-1 induced intra-tumoral neutrophil infiltration associated with tumor necrosis. Similarly, we reasoned that a subset of patients harboring CRPC may benefit from G-1 therapy if it is delivered before the patients receive chemotherapy, which can compromise neutrophil production. In light of the most recent CRPC that failed second-generation ADT (i.e. abiraterone acetate and MDV3100), whether or not the expression of GPR30 or the population of patients expressing high levels of GPR30 is increased upon resistance is a clinically interesting question with respect to the further exploration of GPR30 as a novel targeted therapy for late-stage CRPC. Importantly, in all the animal studies reported to date, G-1 did not induce adverse effects (Blasko *et al*. 2009, Dennis *et al*. 2009, Chan *et al*. 2010, Gao *et al*. 2011). G-1 toxicity to the functions of vital organs including heart and liver has been further proven to be undetectable in this study. One major concern regarding estrogen-related treatment in PC is the increase in the risk of venous thromboembolism (reviewed in Cox & Crawford (1995)). Although G-1 is a specific GPR30 agonist that has been shown not to bind ERα at a concentration up to 10 μM (Bologa *et al*. 2006), definitive evidence for the absence of estrogen-mediated coagulopathy *in vivo* is required.

Our findings, taken together, indicated that G-1 effectively inhibited preclinical CRPC growth with a low risk of toxicity; underscoring that G-1 or other GPR30-specific agonists might serve as novel anticancer agents for CRPC that expresses GPR30. The upregulation of GPR30 expression after androgen ablation and the recruitment of neutrophils to the CR tumors are both indicative of a potentially important therapeutic window for G-1/GPR30-targeted therapy preferably under the conditions of a low or ultra-low androgen levels in CRPC before chemotherapy.

Supplementary data

This is linked to the online version of the paper at http://dx.doi.org/10.1530/ERC-14-0402.

Declaration of interest

The authors declare that there is no conflict of interest that could be perceived as prejudicing the impartiality of the research reported.

Funding

This work was supported by Veteran Affairs (Merit Award I01BX000675 to S-M Ho), the National Institutes of Health (grant numbers P30ES006096, U01ES019480, and U01ES020988 to S-M Ho and P50CA097186 Pacific Northwest SPORE Career Development Award to H-M Lam), and the Prostate Cancer Foundation (Young Investigator Award to H-M Lam).

Published by Bioscientifica Ltd.

Acknowledgements

The authors thank the Genomics, Epigenomics and Sequencing Core at the University of Cincinnati for Affymetrix microarray experiments, Ms Dan Song for her support during the immunohistochemistry study, Dr Yuet-Kin Leung for critical reading of the manuscript, and Ms Nancy K Voynow for her professional editing of this manuscript.

References

Ahola TM, Purmonen S, Pennanen P, Zhuang YH, Tuohimaa P & Ylikomi T 2002 Progestin upregulates G-protein-coupled receptor 30 in breast cancer cells. *European Journal of Biochemistry* **269** 2485–2490. (doi:10.1046/j.1432-1033.2002.02912.x)

Albanito L, Madeo A, Lappano R, Vivacqua A, Rago V, Carpino A, Oprea TI, Prossnitz ER, Musti AM, Ando S *et al.* 2007 G protein-coupled receptor 30 (GPR30) mediates gene expression changes and growth response to 17β-estradiol and selective GPR30 ligand G-1 in ovarian cancer cells. *Cancer Research* **67** 1859–1866. (doi:10.1158/0008-5472.CAN-06-2909)

Albanito L, Sisci D, Aquila S, Brunelli E, Vivacqua A, Madeo A, Lappano R, Pandey DP, Picard D, Mauro L *et al.* 2008 Epidermal growth factor induces G protein-coupled receptor 30 expression in estrogen receptor-negative breast cancer cells. *Endocrinology* **149** 3799–3808. (doi:10.1210/en.2008-0117)

Blasko E, Haskell CA, Leung S, Gualtieri G, Halks-Miller M, Mahmoudi M, Dennis MK, Prossnitz ER, Karpus WJ & Horuk R 2009 Beneficial role of the GPR30 agonist G-1 in an animal model of multiple sclerosis. *Journal of Neuroimmunology* **214** 67–77. (doi:10.1016/j.jneuroim.2009.06.023)

Bologa CG, Revankar CM, Young SM, Edwards BS, Arterburn JB, Kiselyov AS, Parker MA, Tkachenko SE, Savchuck NP, Sklar LA *et al.* 2006 Virtual and biomolecular screening converge on a selective agonist for GPR30. *Nature Chemical Biology* **2** 207–212. (doi:10.1038/nchembio775)

de Bono JS, Oudard S, Ozguroglu M, Hansen S, Machiels JP, Kocak I, Gravis G, Bodrogi I, Mackenzie MJ, Shen L *et al.* 2010 Prednisone plus cabazitaxel or mitoxantrone for metastatic castration-resistant prostate cancer progressing after docetaxel treatment: a randomised open-label trial. *Lancet* **376** 1147–1154. (doi:10.1016/S0140-6736(10)61389-X)

de Bono JS, Logothetis CJ, Molina A, Fizazi K, North S, Chu L, Chi KN, Jones RJ, Goodman OB Jr, Saad F *et al.* 2011 Abiraterone and increased survival in metastatic prostate cancer. *New England Journal of Medicine* **364** 1995–2005. (doi:10.1056/NEJMoa1014618)

Cacalano G, Lee J, Kikly K, Ryan AM, Pitts-Meek S, Hultgren B, Wood WI & Moore MW 1994 Neutrophil and B cell expansion in mice that lack the murine IL-8 receptor homolog. *Science* **265** 682–684. (doi:10.1126/science.8036519)

Caruso RA, Bellocco R, Pagano M, Bertoli G, Rigoli L & Inferrera C 2002 Prognostic value of intratumoral neutrophils in advanced gastric carcinoma in a high-risk area in northern Italy. *Modern Pathology* **15** 831–837. (doi:10.1097/01.MP.0000020391.98998.6B)

Chan QK, Lam HM, Ng CF, Lee AY, Chan ES, Ng HK, Ho SM & Lau KM 2010 Activation of GPR30 inhibits the growth of prostate cancer cells through sustained activation of Erk1/2, c-jun/c-fos-dependent upregulation of p21, and induction of G_2 cell-cycle arrest. *Cell Death and Differentiation* **17** 1511–1523. (doi:10.1038/cdd.2010.20)

Cheng SB, Graeber CT, Quinn JA & Filardo EJ 2011 Retrograde transport of the transmembrane estrogen receptor, G-protein-coupled-receptor-30 (GPR30/GPER) from the plasma membrane towards the nucleus. *Steroids* **76** 892–896. (doi:10.1016/j.steroids.2011.02.018)

Claessens F & Tilley W 2014 Androgen signaling and steroid receptor crosstalk in endocrine cancers. *Endocrine-Related Cancer* **21** E3–E5. (doi:10.1530/ERC-14-0274)

Cox RL & Crawford ED 1995 Estrogens in the treatment of prostate cancer. *Journal of Urology* **154** 1991–1998. (doi:10.1016/S0022-5347(01)66670-9)

Decker KF, Zheng D, He Y, Bowman T, Edwards JR & Jia L 2012 Persistent androgen receptor-mediated transcription in castration-resistant prostate cancer under androgen-deprived conditions. *Nucleic Acids Research* **40** 10765–10779. (doi:10.1093/nar/gks888)

De Marco P, Bartella V, Vivacqua A, Lappano R, Santolla MF, Morcavallo A, Pezzi V, Belfiore A & Maggiolini M 2013 Insulin-like growth factor-I regulates GPER expression and function in cancer cells. *Oncogene* **32** 678–688. (doi:10.1038/onc.2012.97)

Dennis MK, Burai R, Ramesh C, Petrie WK, Alcon SN, Nayak TK, Bologa CG, Leitao A, Brailoiu E, Deliu E *et al.* 2009 *In vivo* effects of a GPR30 antagonist. *Nature Chemical Biology* **5** 421–427. (doi:10.1038/nchembio.168)

Di Carlo E, Forni G, Lollini P, Colombo MP, Modesti A & Musiani P 2001 The intriguing role of polymorphonuclear neutrophils in antitumor reactions. *Blood* **97** 339–345. (doi:10.1182/blood.V97.2.339)

Eash KJ, Greenbaum AM, Gopalan PK & Link DC 2010 CXCR2 and CXCR4 antagonistically regulate neutrophil trafficking from murine bone marrow. *Journal of Clinical Investigation* **120** 2423–2431. (doi:10.1172/JCI41649)

Filardo EJ, Quinn JA, Bland KI & Frackelton AR Jr 2000 Estrogen-induced activation of Erk-1 and Erk-2 requires the G protein-coupled receptor homolog, GPR30, and occurs via *trans*-activation of the epidermal growth factor receptor through release of HB-EGF. *Molecular Endocrinology* **14** 1649–1660. (doi:10.1210/mend.14.10.0532)

Fu X, Tao L, Rivera A, Xu H & Zhang X 2011 Virotherapy induces massive infiltration of neutrophils in a subset of tumors defined by a strong endogenous interferon response activity. *Cancer Gene Therapy* **18** 785–794. (doi:10.1038/cgt.2011.46)

Funakoshi T, Yanai A, Shinoda K, Kawano MM & Mizukami Y 2006 G protein-coupled receptor 30 is an estrogen receptor in the plasma membrane. *Biochemical and Biophysical Research Communications* **346** 904–910. (doi:10.1016/j.bbrc.2006.05.191)

Gao F, Ma X, Ostmann AB & Das SK 2011 GPR30 activation opposes estrogen-dependent uterine growth via inhibition of stromal ERK1/2 and estrogen receptor alpha (ERα) phosphorylation signals. *Endocrinology* **152** 1434–1447. (doi:10.1210/en.2010-1368)

Geiser T, Dewald B, Ehrengruber MU, Clark-Lewis I & Baggiolini M 1993 The interleukin-8-related chemotactic cytokines GROα, GROβ, and GROγ activate human neutrophil and basophil leukocytes. *Journal of Biological Chemistry* **268** 15419–15424.

Gregory AD & Houghton AM 2011 Tumor-associated neutrophils: new targets for cancer therapy. *Cancer Research* **71** 2411–2416. (doi:10.1158/0008-5472.CAN-10-2583)

Haas E, Meyer MR, Schurr U, Bhattacharya I, Minotti R, Nguyen HH, Heigl A, Lachat M, Genoni M & Barton M 2007 Differential effects of 17β-estradiol on function and expression of estrogen receptor α, estrogen receptor β, and GPR30 in arteries and veins of patients with atherosclerosis. *Hypertension* **49** 1358–1363. (doi:10.1161/HYPERTENSIONAHA.107.089995)

Harokopakis E & Hajishengallis G 2005 Integrin activation by bacterial fimbriae through a pathway involving CD14, Toll-like receptor 2, and phosphatidylinositol-3-kinase. *European Journal of Immunology* **35** 1201–1210. (doi:10.1002/eji.200425883)

Higano CS & Crawford ED 2011 New and emerging agents for the treatment of castration-resistant prostate cancer. *Urologic Oncology* **29** S1–S8. (doi:10.1016/j.urolonc.2011.08.013)

Higano CS, Schellhammer PF, Small EJ, Burch PA, Nemunaitis J, Yuh L, Provost N & Frohlich MW 2009 Integrated data from 2 randomized, double-blind, placebo-controlled, phase 3 trials of active cellular immunotherapy with sipuleucel-T in advanced prostate cancer. *Cancer* **115** 3670–3679. (doi:10.1002/cncr.24429)

Hirose K, Hakozaki M, Nyunoya Y, Kobayashi Y, Matsushita K, Takenouchi T, Mikata A, Mukaida N & Matsushima K 1995 Chemokine gene transfection into tumour cells reduced tumorigenicity in nude mice in association with neutrophilic infiltration. *British Journal of Cancer* **72** 708–714. (doi:10.1038/bjc.1995.398)

Published by Bioscientifica Ltd.

Ho SM, Lee MT, Lam HM & Leung YK 2011 Estrogens and prostate cancer: etiology, mediators, prevention, and management. *Endocrinology and Metabolism Clinics of North America* **40** 591–614. (doi:10.1016/j.ecl.2011.05.002)

Huang HJ, Neven P, Drijkoningen M, Paridaens R, Wildiers H, Van Limbergen E, Berteloot P, Amant F, Vergote I & Christiaens MR 2005 Association between tumour characteristics and HER-2/neu by immunohistochemistry in 1362 women with primary operable breast cancer. *Journal of Clinical Pathology* **58** 611–616. (doi:10.1136/jcp.2004.022772)

Huggins C & Hodges CV 2002 Studies on prostatic cancer: I. The effect of castration, of estrogen and of androgen injection on serum phosphatases in metastatic carcinoma of the prostate. 1941. *Journal of Urology* **168** 9–12. (doi:10.1016/S0022-5347(05)64820-3)

Jacobi JS, Martin C, Nava G, Jeziorski MC, Clapp C & Martinez de la EG 2007 17-β-estradiol directly regulates the expression of adrenergic receptors and kisspeptin/GPR54 system in GT1–7 GnRH neurons. *Neuroendocrinology* **86** 260–269. (doi:10.1159/000107770)

Kantoff PW, Higano CS, Shore ND, Berger ER, Small EJ, Penson DF, Redfern CH, Ferrari AC, Dreicer R, Sims RB *et al*. 2010 Sipuleucel-T immunotherapy for castration-resistant prostate cancer. *New England Journal of Medicine* **363** 411–422. (doi:10.1056/NEJMoa1001294)

Langley RE, Cafferty FH, Alhasso AA, Rosen SD, Sundaram SK, Freeman SC, Pollock P, Jinks RC, Godsland IF, Kockelbergh R *et al*. 2013 Cardiovascular outcomes in patients with locally advanced and metastatic prostate cancer treated with luteinising-hormone-releasing-hormone agonists or transdermal oestrogen: the randomised, phase 2 MRC PATCH trial (PR09). *Lancet Oncology* **14** 306–316. (doi:10.1016/S1470-2045(13)70025-1)

Leav I, Lau KM, Adams JY, McNeal JE, Taplin ME, Wang J, Singh H & Ho SM 2001 Comparative studies of the estrogen receptors β and α and the androgen receptor in normal human prostate glands, dysplasia, and in primary and metastatic carcinoma. *American Journal of Pathology* **159** 79–92. (doi:10.1016/S0002-9440(10)61676-8)

Leung BP, Culshaw S, Gracie JA, Hunter D, Canetti CA, Campbell C, Cunha F, Liew FY & McInnes IB 2001 A role for IL-18 in neutrophil activation. *Journal of Immunology* **167** 2879–2886. (doi:10.4049/jimmunol.167.5.2879)

Leung YK, Lam HM, Wu S, Song D, Levin L, Cheng L, Wu CL & Ho SM 2010 Estrogen receptor β2 and β5 are associated with poor prognosis in prostate cancer, and promote cancer cell migration and invasion. *Endocrine-Related Cancer* **17** 675–689. (doi:10.1677/ERC-09-0294)

Madeo A & Maggiolini M 2010 Nuclear alternate estrogen receptor GPR30 mediates 17β-estradiol-induced gene expression and migration in breast cancer-associated fibroblasts. *Cancer Research* **70** 6036–6046. (doi:10.1158/0008-5472.CAN-10-0408)

Maggiolini M & Picard D 2010 The unfolding stories of GPR30, a new membrane-bound estrogen receptor. *Journal of Endocrinology* **204** 105–114. (doi:10.1677/JOE-09-0242)

Musiani P, Allione A, Modica A, Lollini PL, Giovarelli M, Cavallo F, Belardelli F, Forni G & Modesti A 1996 Role of neutrophils and lymphocytes in inhibition of a mouse mammary adenocarcinoma engineered to release IL-2, IL-4, IL-7, IL-10, IFN-α, IFN-γ, and TNF-α. *Laboratory Investigation* **74** 146–157.

Nelson AW, Tilley WD, Neal DE & Carroll JS 2014 Estrogen receptor beta in prostate cancer: friend or foe? *Endocrine-Related Cancer* **21** T219–T234. (doi:10.1530/ERC-13-0508)

Norman G, Dean ME, Langley RE, Hodges ZC, Ritchie G, Parmar MK, Sydes MR, Abel P & Eastwood AJ 2008 Parenteral oestrogen in the treatment of prostate cancer: a systematic review. *British Journal of Cancer* **98** 697–707. (doi:10.1038/sj.bjc.6604230)

Oh WK 2002 The evolving role of estrogen therapy in prostate cancer. *Clinical Prostate Cancer* **1** 81–89. (doi:10.3816/CGC.2002.n.009)

Otto C, Rohde-Schulz B, Schwarz G, Fuchs I, Klewer M, Brittain D, Langer G, Bader B, Prelle K, Nubbemeyer R *et al*. 2008 G protein-coupled receptor 30 localizes to the endoplasmic reticulum and is not activated by estradiol. *Endocrinology* **149** 4846–4856. (doi:10.1210/en.2008-0269)

Pandey DP, Lappano R, Albanito L, Madeo A, Maggiolini M & Picard D 2009 Estrogenic GPR30 signalling induces proliferation and migration of breast cancer cells through CTGF. *EMBO Journal* **28** 523–532. (doi:10.1038/emboj.2008.304)

Pelleitier M & Montplaisir S 1975 The nude mouse: a model of deficient T-cell function. *Methods and Achievements in Experimental Pathology* **7** 149–166.

Prossnitz ER & Barton M 2011 The G-protein-coupled estrogen receptor GPER in health and disease. *Nature Reviews. Endocrinology* **7** 715–726. (doi:10.1038/nrendo.2011.122)

Prossnitz ER, Arterburn JB & Sklar LA 2007 GPR30: a G protein-coupled receptor for estrogen. *Molecular and Cellular Endocrinology* **265** 138–142. (doi:10.1016/j.mce.2006.12.010)

Recchia AG, De Francesco EM, Vivacqua A, Sisci D, Panno ML, Ando S & Maggiolini M 2011 The G protein-coupled receptor 30 is up-regulated by hypoxia-inducible factor-1α (HIF-1α) in breast cancer cells and cardiomyocytes. *Journal of Biological Chemistry* **286** 10773–10782. (doi:10.1074/jbc.M110.172247)

Ryckman C, Vandal K, Rouleau P, Talbot M & Tessier PA 2003 Proinflammatory activities of S100: proteins S100A8, S100A9, and S100A8/A9 induce neutrophil chemotaxis and adhesion. *Journal of Immunology* **170** 3233–3242. (doi:10.4049/jimmunol.170.6.3233)

Saenko EL, Skorobogat'ko OV, Tarasenko P, Romashko V, Zhuravetz L, Zadorozhnaya L, Senjuk OF & Yaropolov AI 1994 Modulatory effects of ceruloplasmin on lymphocytes, neutrophils and monocytes of patients with altered immune status. *Immunological Investigations* **23** 99–114. (doi:10.3109/08820139409087792)

Schaider H, Oka M, Bogenrieder T, Nesbit M, Satyamoorthy K, Berking C, Matsushima K & Herlyn M 2003 Differential response of primary and metastatic melanomas to neutrophils attracted by IL-8. *International Journal of Cancer* **103** 335–343. (doi:10.1002/ijc.10775)

Schellhammer P 2012 Life after failure of traditional androgen deprivation therapy. *Urologic Oncology* **30** S10–S14. (doi:10.1016/j.urolonc.2012.01.009)

Tannock IF, de Wit R, Berry WR, Horti J, Pluzanska A, Chi KN, Oudard S, Theodore C, James ND, Turesson I *et al*. 2004 Docetaxel plus prednisone or mitoxantrone plus prednisone for advanced prostate cancer. *New England Journal of Medicine* **351** 1502–1512. (doi:10.1056/NEJMoa040720)

Thomas P, Pang Y, Filardo EJ & Dong J 2005 Identity of an estrogen membrane receptor coupled to a G protein in human breast cancer cells. *Endocrinology* **146** 624–632. (doi:10.1210/en.2004-1064)

Vivacqua A, Bonofiglio D, Recchia AG, Musti AM, Picard D, Ando S & Maggiolini M 2006 The G protein-coupled receptor GPR30 mediates the proliferative effects induced by 17β-estradiol and hydroxytamoxifen in endometrial cancer cells. *Molecular Endocrinology* **20** 631–646. (doi:10.1210/me.2005-0280)

Yang L, Ravindranathan P, Ramanan M, Kapur P, Hammes SR, Hsieh JT & Raj GV 2012 Central role for PELP1 in nonandrogenic activation of the androgen receptor in prostate cancer. *Molecular Endocrinology* **26** 550–561. (doi:10.1210/me.2011-1101)

Zheng D, Decker KF, Zhou T, Chen J, Qi Z, Jacobs K, Weilbaecher KN, Corey E, Long F & Jia L 2013 Role of WNT7B-induced noncanonical pathway in advanced prostate cancer. *Molecular Cancer Research* **11** 482–493. (doi:10.1158/1541-7786.MCR-12-0520)

Received in final form 30 September 2014
Accepted 6 October 2014
Made available online as an Accepted Preprint
6 October 2014

Published by Bioscientifica Ltd.

PLOS ONE

RESEARCH ARTICLE

Cellular Adhesion Promotes Prostate Cancer Cells Escape from Dormancy

Nazanin Ruppender[1], Sandy Larson[1], Bryce Lakely[1], Lori Kollath[1], Lisha Brown[1], Ilsa Coleman[2], Roger Coleman[2], Holly Nguyen[1], Peter S. Nelson[2,3], Eva Corey[1], Linda A. Snyder[4], Robert L. Vessella[5,1], Colm Morrissey[1], Hung-Ming Lam[1]*

1 Department of Urology, University of Washington, Seattle, Washington, United States of America, **2** Divison of Human Biology, Fred Hutchinson Cancer Research Center, Seattle, Washington, United States of America, **3** Department of Medicine, University of Washington, Seattle, Washington, United States of America, **4** Janssen Research and Development, LLC, Spring House, Pennsylvania, United States of America, **5** Department of Veterans Affairs Medical Center, Seattle, Washington, United States of America

* minglam@u.washington.edu

Citation: Ruppender N, Larson S, Lakely B, Kollath L, Brown L, Coleman I, et al. (2015) Cellular Adhesion Promotes Prostate Cancer Cells Escape from Dormancy. PLoS ONE 10(6): e0130565. doi:10.1371/journal.pone.0130565

Editor: Lucia R. Languino, Thomas Jefferson University, UNITED STATES

Received: February 11, 2015

Accepted: May 21, 2015

Published: June 19, 2015

Data Availability Statement: All gene expression files are available from the GEO database (accession number GSE64262)

Funding: This work was supported by Janssen Research and Development LLC (http://www.janssenrnd.com), and PO1 CA85859 from the National Institutes of Health (http://grants.nih.gov/grants/funding/ac_search_results.htm?text_curr = p01).

Competing Interests: The authors have declared that no competing interests exist.

Abstract

Dissemination of prostate cancer (PCa) cells to the bone marrow is an early event in the disease process. In some patients, disseminated tumor cells (DTC) proliferate to form active metastases after a prolonged period of undetectable disease known as tumor dormancy. Identifying mechanisms of PCa dormancy and reactivation remain a challenge partly due to the lack of *in vitro* models. Here, we characterized *in vitro* PCa dormancy-reactivation by inducing cells from three patient-derived xenograft (PDX) lines to proliferate through tumor cell contact with each other and with bone marrow stroma. Proliferating PCa cells demonstrated tumor cell-cell contact and integrin clustering by immunofluorescence. Global gene expression analyses on proliferating cells cultured on bone marrow stroma revealed a downregulation of TGFB2 in all of the three proliferating PCa PDX lines when compared to their non-proliferating counterparts. Furthermore, constitutive activation of myosin light chain kinase (MLCK), a downstream effector of integrin-beta1 and TGF-beta2, in non-proliferating cells promoted cell proliferation. This cell proliferation was associated with an upregulation of CDK6 and a downregulation of E2F4. Taken together, our data provide the first clinically relevant *in vitro* model to support cellular adhesion and downregulation of TGFB2 as a potential mechanism by which PCa cells may escape from dormancy. Targeting the TGF-beta2-associated mechanism could provide novel opportunities to prevent lethal PCa metastasis.

Introduction

The dissemination of prostate cancer (PCa) cells to the bone marrow is an early event in the PCa disease process [1, 2]. In many cases, these disseminated tumor cells (DTC) proliferate to form active metastases after a prolonged period of undetectable disease following prostatectomy. This latency period is often referred to as tumor dormancy. To date, dormancy remains

a significant clinical challenge, as PCa patients presented with bone metastases ultimately stop responding to second line therapies and eventually succumb to the disease. Thus, it has become paramount to identify mechanisms of tumor dormancy in an effort to prevent PCa recurrence.

A dormant tumor cell does not actively proliferate, yet has the potential to multiply given the right external cues. By this definition, multiple scenarios could potentially induce dormancy, including unfavorable tumor microenvironment, nutrient starvation, the inherent nature of the DTC, or epigenetic changes caused by the microenvironment [2, 3]. However, not all instances of indolent PCa necessarily constitute dormancy. A patient may simply have slow-growing tumor cells residing at the metastatic site at the time of initial treatment and experience recurrence shortly thereafter. Others may never experience recurrence, while a subset of patients experience recurrence only after extended periods. To date, the mechanisms of dormancy remain largely unknown. However, the urokinase-like plasminogen activator (uPA) and its associated receptor (uPAR) have been implicated in the regulation of dormancy in various cancers. Specifically, high levels of uPA and uPAR induce dormancy escape by upregulating ERK/p38 ratio within cancer cells [4, 5]. This high uPAR expression was associated with the activation of $\alpha_v\beta_1$ integrin, resulting in tumor growth [4–7]. In a separate study, uPA-regulated migration of tumor cells was activated by the myosin light chain kinase (MLCK) [8] which phosphorylation was induced by ERK [9]. MLCK is a known regulator of contractility, motility, and adhesion [10, 11], however the role of MLCK in PCa dormancy escape remains unknown.

Matrix and intercellular adhesions has been implicated in tumor dormancy regulation. Studies showed that integrin-mediated cellular adhesion to the extracellular matrix activates MAPKs [12–14] which regulates tumor growth [15–19]. In PCa, upregulation of β_1 integrin promotes the growth and invasion of cells [3, 20], and interactions between tumor and stroma may be attributable to the escape of dormant cells from radiotherapy [21]. Recent studies examining human PCa cell lines on mouse bone marrow stroma have identified important factors in the mouse hematopoietic niche that regulate dormancy [22, 23].

We here characterized the dormancy and growth of three PCa patient-derived xenografts (PDXs) established from metastases obtained at rapid autopsy or surgery on human bone marrow microenvironment *in vitro*. These PDXs (LuCaP 86.2, 92, and 93) displayed *in vitro* quiescence in typical cell culture conditions which may represent dormancy and we aimed to identify the role of cell-cell adhesion in the release of PCa from dormancy in a human bone marrow context. We determined that tumor cell-cell contact on bone marrow stroma is necessary for LuCaP PDX cells to proliferate *in vitro* and was associated with a universal downregulation of TGFB2. Furthermore, LuCaP PDXs dormancy reactivation could be recapitulated by constitutively activating MLCK and cyclin-dependent kinase 6 (CDK6).

Materials and Methods

Dissociation, isolation, and culture of LuCaP PDX *in vitro*

Bone marrow stromal cells (BMSC) that were isolated from a patient with PCa bone metastases (BM2508) were seeded at 50,000 cells/cm^2 overnight. The following day, BM2508 cells were treated with 10 μg/mL mitomycin C (Sigma, St Louis, MO) for 1 hour. LuCaP PDXs that were routinely passaged *in vivo* as described previously [21] were excised and dissociated using the Miltenyi human tumor dissociation kit (Miltenyi Biotec Inc., San Diego, CA; #130-95-929) and enriched by positive selection using magnetic microbeads against human epithelial antigen EpCAM/CD326 (Miltenyi Biotec Inc.; #130-061-101) according to the manufacturer's instructions. LuCaP PDX cells were then seeded on top of the BM2508 cells at either 50,000 cells/cm^2 (G; growing/proliferating) or 50 cells/cm^2 (NG; not growing/dormant). At day 8, the LuCaP

PDX cells were differentially trypsinized and enriched by positive and negative selection with magnetic beads, fluorescently labeled for EpCAM/CD326 and individually plucked with a micromanipulator as described previously [24]. Furthermore, to ensure that NG cells were dormant instead of senescent, a β-galactosidase assay (Pierce Biotechnology, Inc., Waltham, MA; #75707) was performed on all NG LuCaP PDX cells according to manufacturer's instructions. All procedures involving human subjects were approved by the Institutional Review Board of the University of Washington Medical Center and all subjects signed informed consent. The animal study was specifically approved by the University of Washington Institutional Animal Care and Use Committee and all animal procedures were performed in compliance with the NIH guidelines.

Immunofluorescent staining

The LuCaP PDX cells were dissociated, selected and plated as described above on glass coverslips conjugated with lysine. At day 8, cells were fixed with ice-cold methanol, blocked with 5% horse-goat-chicken serum and stained for EpCAM and Ki67 or $_1$ integrin using a FITC-conjugated mouse monoclonal anti-human Ber-EP4 antibody (DAKO, Carpinteria, CA; F086001), and a rabbit polyclonal anti-human Ki-67 antibody (Santa Cruz Biotechnology, Dallas, TX; SC-15402) or a rabbit polyclonal anti-human ITGB1 antibody (Santa Cruz Biotechnology; SC-9970) in conjunction with a goat anti-rabbit Alexa-Fluor 546 conjugated secondary antibody (Life Technologies, Carlsbad, CA; A-11035). Coverslips were then mounted with ProLong Gold antifade reagent containing DAPI (Life Technologies; P-36931).

Cell count and WST-1 assays

C4-2B (a gift from Dr. Leland Chung; [25]) and dissociated LuCaP PDX cells (LuCaP 86.2, 92, 93, 96, 141; [26–28]) were plated in RPMI-1640 or MEM (Life Technologies) respectively supplemented with 10% fetal bovine serum (FBS). Cells were seeded either sparsely (50 cells/cm^2) or densely (50,000 cells/cm^2) on a confluent monolayer of BMSC (50,000 cells/cm^2) that was pretreated with 10 μg/ml mitomycin C. For C4-2B cells seeded sparsely on BMSC, after 1 and 8 days, cells were stained for EpCAM, Ki67, and DAPI as described above. Only EpCAM+-epithelial cells (representing C4-2B cells because BMSC are EpCAM-) were counted in the whole chamber under a fluorescent microscope using 200× magnification. For C4-2B cells seeding without BMSC, WST-1 assay (Roche Diagnostics Corporation, Indianapolis, IN) was carried out according to the manufacturer's instructions. Absorbance was read on a microplate reader at 450 nm, and the background absorbance (media only) was subtracted from all readings. For LuCaP PDX cells, after 3, 7, and 14 days on BMSC, cells were trypsinized, stained for EpCAM and Ki67 as described above, and resuspended in 50 μl of ProLong Gold antifade reagent containing DAPI. Two-aliquots of 10 μl of stained cells were counted and EpCAM + epithelial cells (i.e. LuCaP PDX cells) were recorded.

Flow cytometric analysis

C4-2B cells were cultured overnight in RPMI-1640 medium supplemented with 10% FBS and then treated with DMSO or ML-7 (10μM) for 24h and 48h. The treated cells were trypsinized, fixed, stained with 10 μg/μL DAPI (4',6-diamidino-2-phenylindole, Life Technologies)/1% NP-40 /10% DMSO, and lysed using 25G syringe. At least 10,000 stained cells were analyzed using BD LSR II Flow Cytometer System (BD Biosciences, San Jose, CA) and cell cycle was analyzed by MultiCycle (De Novo Software, Glendale, CA)

Viral transduction and drug treatments of LuCaP PDX cells *in vitro*

LuCaP PDXs were dissociated and selected as described above and plated at 50,000 cells/cm^2 without stromal cells. The following day, cells were transduced at an MOI (multiplicity of infection) of 10 with one of the following: an adenoviral vector that either contained an activated form of myosin light chain kinase (A-tMK, a gift from Drs. Zuzana Strakova, Jody Martin, and Primal de Lanerolle**,** [29]), an empty vector, or a lentiviral vector that contained either cDNA for CDK6 or GFP (Applied Biological Materials, pLentiIII-EF1α). Cells were transduced in MEM supplemented with 10% FBS and 8 μg/mL polybrene (Santa Cruz Biotechnology). Cells were either immunofluorescently stained as described above or trypsinized for RNA extraction. To determine whether MLCK activity is necessary for PCa proliferation, C4-2B cells, which readily proliferate *in vitro*, were plated at 50,000 cells/cm^2 in RPMI medium (Life Technologies) supplemented with 10% FBS. The cells were then either treated with 10 μM ML-7 (Sigma; I2764) or DMSO control for 24 hours.

RNA extraction and amplification

For 10-cell transcriptomic study, 10 individually isolated cells per xenograft line were lysed and amplified cDNA was generated from the total RNA using the NuGEN Ovation RNA Amplification System as described previously [24, 30]. The cDNA was arrayed on Agilent 44K whole human genome expression oligonucleotide microarrays (Agilent Technologies, Inc.). For other *in vitro* experiments, RNA was isolated using the RNEasy mini kit (Qiagen Inc., Valencia, CA). One microgram of RNA was reverse transcribed using the Qiagen RT^2 first strand kit, followed by PCR array or RT-qPCR analysis.

Labeling and hybridization of amplified material to whole human genome expression oligonucleotide microarrays

Amplified cDNA from each sample was labeled using the BioPrime Total Genomic Labeling System (Life Technologies, Grand Island, NY) and microarray was performed according to previous procedures [24, 30] with slight modifications. Briefly, hybridization probes were prepared by combining 4 μg of Alexa Fluor 3-labeled sample with 400 ng Alexa Fluor 5-labeled reference. The probes were denatured at 95°C and hybridized at 63°C on Agilent Human 4x44K microarrays (Agilent Technologies, Inc., Santa Clara, CA), washed, and fluorescent array images were collected using the Agilent DNA microarray scanner. The data were loess normalized within arrays and quantile normalized between arrays in R using the Limma Bioconductor package. Data were filtered to remove probes with mean signal intensities below 300. The Statistical Analysis of Microarray (SAM) program (http://www-stat.stanford.edu/~tibs/SAM/) [31] was used to analyze expression differences between groups using unpaired, two-sample t-tests and controlled for multiple testing by estimating q-values using the false discovery rate (FDR) method. Microarray data are deposited in the Gene Expression Omnibus database under the accession number GSE64262.

Gene expression analyses

To determine whether differential transcription observed in NG (not growing/dormant) versus G (growing/proliferating) groups were enriched for genes within canonical pathways and Gene Ontology gene sets, the t-test results were subjected to Gene Set Enrichment Analysis (GSEA) using preranked mode with permutation testing of the gene sets to adjust for multiple hypothesis testing, generating an FDR. Unsupervised, hierarchical clustering of the most differentially expressed was performed between NG and G groups based on SAM score (SAM score >2 and

$p \leq 0.05$, a total of 238 genes) using Cluster 3.0 (bonsai.hgc.jp/~mdehoon/software/cluster/software.htm) and Java TreeView (http://jtreeview.sourceforge.net/).

Ingenuity Pathway Analysis

The 238 differentially expressed genes between NG and G groups were imported into Ingenuity Pathway Analysis (IPA, Ingenuity Systems; https://www.ingenuity.com) to identify molecular and cellular functions and upstream regulators involved in cell proliferation or dormancy as previously described [30].

Quantitative real-time PCR

For PCR array, 25ng of cDNA was used for human cell-cycle PCR array (Qiagen Inc., PAHS-020Z) according to manufacturer's instructions. For qPCR analysis, 2ng (G and NG 10-cell study) or 10ng (lentiviral transduction studies) of cDNA was used for the Platinum SYBR Green qPCR SuperMix-UDG system (Life Technologies, 11733–038) in conjunction with the following primers: CDK6: (F) 5'AGGCTGCTGTTTTCTCTCCA3', (R) 5'CCACACTGCTTCT TGGGTCT3'; E2F4: (F) 5'TGATGTGCCTGTTCTCAACC3', (R) 5'GAGTCCTGTTCC CCTGCTCT3'.; RPS15: (F) 5'TCCGGCAAGATGGCAGAAGTAG3', (R) 5'CCACGCCGCGG TAGGT3'; CDC42: (F) 5'GTCACAGTTATGATTGGTGGAGA3', (R) 5' TCAGCGGTCGTA ATCTGTCA3'; FN1: (F) 5'AAGAGGCAGGCTCAGCAAAT3', (R) 5' GTCATAACAACCG GGCTTGC3'; TGFB2: (F) 5'TCTTCCCCTCCGAAAATGCC3', (R) 5' TCTCCATTGCT GAGACGTCAA3'.

Results

PDX cells require cell-cell contact to proliferate *in vitro*

The PCa xenografts we have established from metastases obtained at rapid autopsy or surgery do not proliferate *in vitro* after dissociation under standard monoculture conditions [32]. Of the five LuCaP PCa PDX lines we studied, none of them displayed measurable β-galactosidase activity (data not shown), suggesting these cells are dormant rather than senescent. As dormant cells by definition retain the potential to proliferate, we sought to determine whether these xenografts could be "activated" *in vitro*. We developed an *in vitro* model recapitulating the PCa cells in contact with BMSC and allowed the LuCaP PDX cells seeded either sparsely without tumor-tumor cell contact (NG, not growing, 50 cells/cm^2) or densely where cells were in direct contact with each other (G, growing, 50,000 cells/cm^2; Fig 1A). We here reported that when LuCaP 86.2, 96, and 141 were seeded densely on a monolayer of BMSC, they showed an increase in cell number after 14 days, whereas the cells that were seeded sparsely failed to proliferate (Fig 1B and data not shown). In contrast, C4-2B cells seeded sparsely on BMSC showed an increase in cell number after 7 days (S1 Fig). To visually detect the association between tumor cell-cell contact and proliferation, we expanded the study to five LuCaP lines for immunofluorescent detection. After 14 days in culture, no positive Ki67 staining was detected in NG cells that were sparsely seeded without tumor cell-cell contact (Fig 1C, upper panel). Consistent with the trypan blue exclusion assay, positive Ki67 staining was observed in G cells that were densely seeded and displayed cell-cell contact, suggesting that tumor cell-cell contact was associated with cell proliferation (Fig 1C, lower panel).

β1 Integrin activity associates with LuCaP PDX cell proliferation *in vitro*

When direct cell-cell contact occurs, integrins were reported to be activated resulting in cell cycle progression and cell proliferation [33]. We therefore examined in LuCaP PDX cells

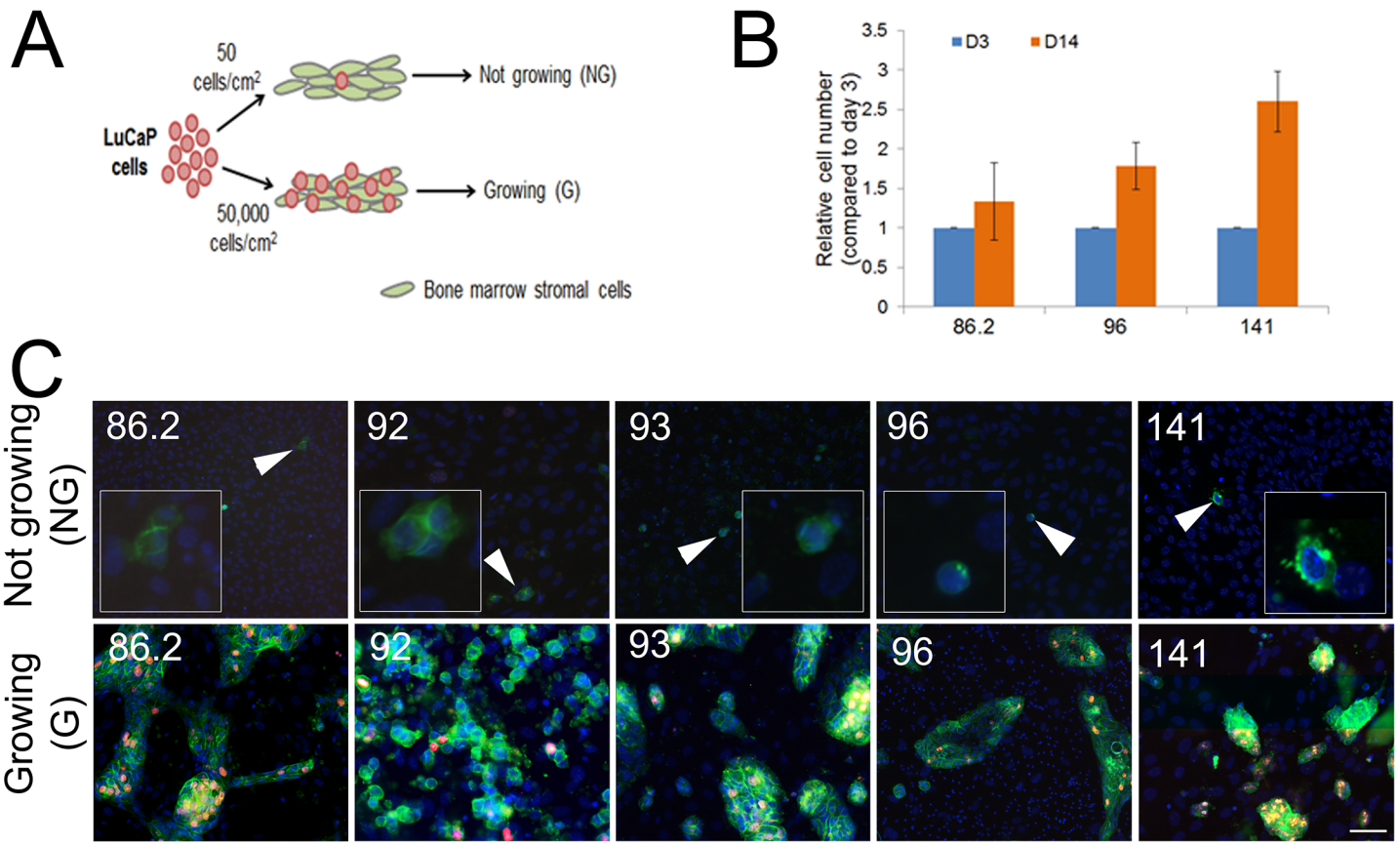

Fig 1. LuCaP PCa PDX cells grow on a monolayer of bone marrow stromal cells (BMSC) when seeded densely. A) A scheme showing the *in vitro* culture condition for not growing (NG) and growing (G) LuCaP PDX cells on BMSC. LuCaP cells were seeded sparsely at 50 cells/cm^2 or densely at 50,000 cells/cm^2 on a confluent layer of BMSC (50,000 cells/cm^2) pretreated with 10 μg/mL mitomycin C to inhibit BMSC cell division. B) LuCaP cells seeded densely on BMSC were quantified by positive EpCAM staining on day 3, 7, and 14 post-seeding. C) LuCaP cells (86.2, 92, 93, 96, and 141) were seeded sparsely (upper panel; NG) or densely (lower panel; G) on BMSC. After 14 days, cells were fixed with ice-cold methanol and fluorescently stained with Ki67 to assess proliferation. Green, EpCAM; Red, Ki67; Blue, DAPI. White arrow: sparsely seeded cells showing negative Ki67 staining after 14 days. Magnification: 200x. Scale bar: 50 μm. Experiments were repeated 2–3 times and graphs showing mean ± SEM or representative pictures were shown.

doi:10.1371/journal.pone.0130565.g001

whether β_1 integrin clustering was activated in response to cell-cell contact. In LuCaP 86.2, 92, and 93, when seeded densely on a monolayer of BMSC, the proliferating G cells showed clustering of β_1 integrin, whereas the non-proliferating NG cells seeded sparsely did not display clustering of β_1 integrin (Fig 2).

Gene expression analysis revealed downregulation of TGFB2 in proliferating cells

Next, we conducted microarray gene expression analysis to delineate the mechanisms underlying the activation of β_1 integrin and cell proliferation. A total of 238 genes (SAM score $\geq$2 or $\leq$-2, $p<0.05$) were differentially expressed between dormant/not growing (NG) and proliferating/growing (G) cells in LuCaP 86.2, 92, and 93 (Fig 3A). We observed that cellular movement was the top molecular and cellular function altered (Fig 3B, $p<0.05$) and a decreased activation was predicted (Fig 3C, z-score -2.4) in G when compared to NG cells. Interestingly, Ingenuity Pathway Analysis identified a top regulator effector network for those genes involved in the decreased activation on cellular movement and demonstrated that endothelin 1 (EDN1) was the common upstream regulator for the downregulation of CDC42, FN1, and FOSL1, which

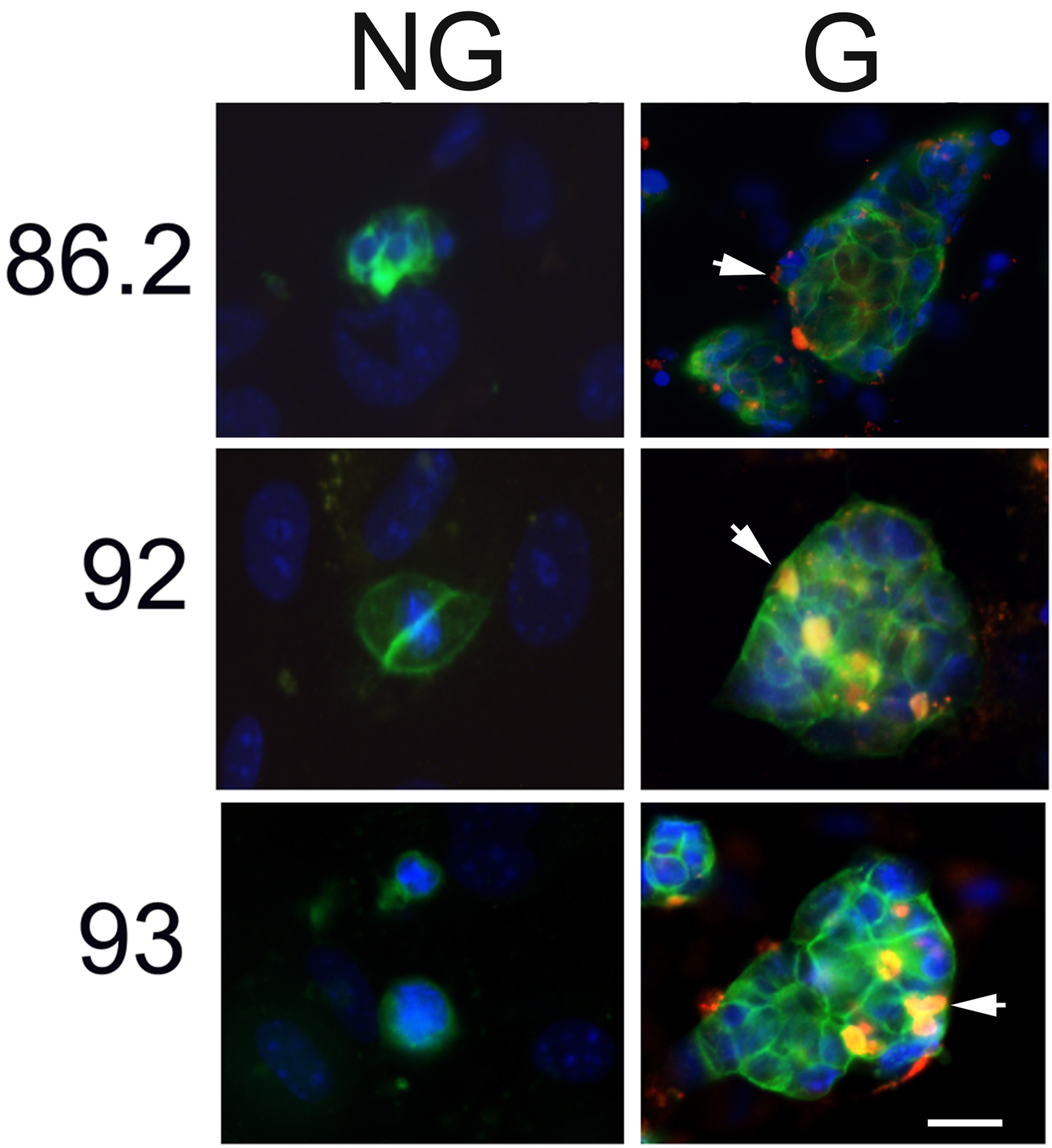

Fig 2. β_1 integrin clusters were observed in LuCaP PDX cells proliferating *in vitro*. LuCaP 86.2, 92, and 93 were dissociated and cultured on a confluent monolayer of BMSC. β_1 integrin immunofluorescent staining revealed integrin clustering (red clusters and highlighted by the white arrow) in densely seeded cells that were growing (G). This clustering was not detected in sparsely seeded, nonproliferative cells (not growing, NG). Green, EpCAM; Red, β1 integrin; Blue, DAPI. Magnification: 200x. Scale bar: 20 μm.

doi:10.1371/journal.pone.0130565.g002

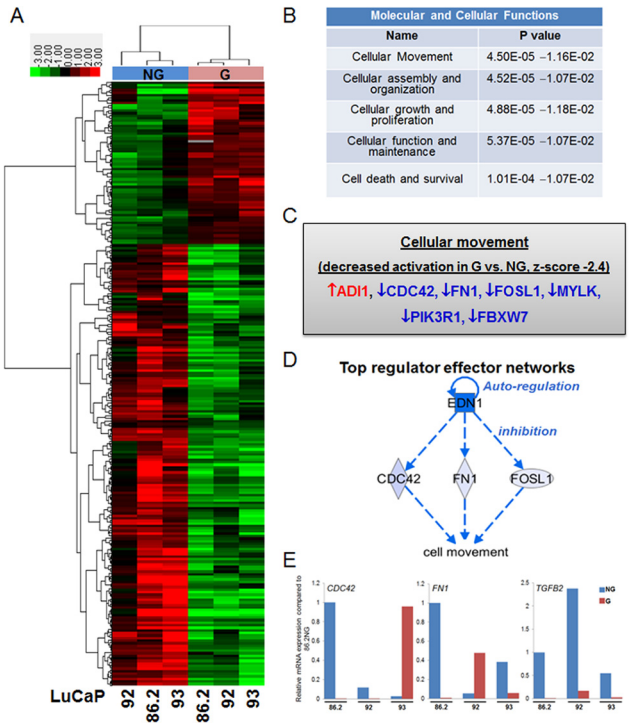

Fig 3. Genes associated with cellular movement were downregulated in proliferating LuCaP cells. A) Heat map of hierarchically clustered differential gene expression in NG and G LuCaP PDX cells. Green, downregulated; red, upregulated. B) Ingenuity pathway analysis showing cellular movement was the top molecular and cellular function altered between NG and G cells. C) List of eight genes that were involved in the decreased activation of cellular movement in G when compared to NG cells. D) EDN1 was predicted to be the top regulator that affected the cell movement via downregulation of FN1, CDC42, and FOSL1. E) Quantitative real-time PCR showed a downregulation of FN1, CDC42 and TGFb2 in growing LuCaP lines. Data were normalized to the levels of housekeeping gene RPS15. NG: not growing; G: growing.

doi:10.1371/journal.pone.0130565.g003

resulted in decreased cell movement (Fig 3C and 3D). Despite EDN1 being identified as the top common upstream regulator for decreased cellular movement in G when compared to NG cells, microarray expression analysis showed that it was not significantly altered in G when compared to NG cells (1.2 fold upregulation in G cells with a SAM score 0.2, data not shown). Since *FOSL1* has a very low endogenous level, therefore we focused on validating *CDC42* and *FN1* using real-time qPCR and found that both genes were downregulated in G cells in two of the three LuCaP PDX lines tested (Fig 3E). Furthermore, TGFβ2 is a known downstream effector of β_1 integrin and upregulation of *TGFB2* expression has been reported to be associated with migration and cancer dormancy [34, 35], we examined and found that *TGFB2* expression was consistently downregulated in G when compared to NG cells in all three LuCaP PDX lines by real-time qPCR (Fig 3E). In clinically derived DTC isolated from the bone marrow, we validated that *FN1* ($p<0.01$, from gene expression dataset GSE48995, [26]) and *TGFB2* [35] were upregulated in patients with no evidence of disease when compared to patients with active PCa metastasis, whereas no significant gene expression change for *CDC42* ($p = 0.67$) was detected between the two groups of DTC (data not shown).

Activation of MLCK promoted PCa PDX cells proliferation via CDK6 in the absence of BMSC

Myosin light chain kinase (MLCK) is a common effector for β_1 integrin, CDC42 and TGFβ2 and its activation has been implicated in cell proliferation [36–38]. To determine if activation of MLCK is involved in LuCaP PDX cell proliferation, we virally transduced a constitutively active form of MLCK (A-tMK) in LuCaP PDX cells. A-tMK transduction in LuCaP 86.2, 92, and 93 cells that normally do not proliferate resulted in cell clustering and positive Ki-67 expression, whereas cells transduced with an empty vector did not show cell clustering or positive Ki67 staining (Fig 4A). Gene expression analysis focusing on cell cycle regulators demonstrated that A-tMK-transduced LuCaP cells expressed an upregulated level of cyclin-dependent kinase 6 (CDK6, 3 to 22 fold) and a concurrent downregulated level of E2F transcription factor 4 (E2F4, 4 to 6 fold; Fig 4B).

To validate the involvement of MLCK activation in cell proliferation, we inhibited MLCK in C4-2B cells that readily proliferate *in vitro* in an attempt to inhibit cell proliferation. Upon MLCK inhibition by the MLCK inhibitor ML-7, C4-2B cell proliferation was reduced as evidenced by the loss of Ki67 staining (Fig 4C), the decrease in WST-1 absorbance (Fig 4D), and the arrest of cells in the G1 phase (S2 Fig). In addition, the decrease in cell proliferation was accompanied by a 4.9-fold downregulation in CDK6 mRNA expression in C4-2B cells treated with ML-7 ($p = 0.007$). The expression of E2F4, however, did not show a significant upregulation in C4-2B cells (Fig 4E). Collectively, the data suggested that activation of MLCK played a role in stimulating cell proliferation which is associated with an upregulation of CDK6.

Overexpression of CDK6 facilitates the proliferation of LuCaP xenografts *in vitro*

To validate upregulation of CDK6 promoted LuCaP PDX cell proliferation, we infected LuCaP 86.2, 92, and 93 cells with lentivirus containing constitutively active CDK6 vector and examined the proliferation. LuCaP 86.2, 92, and 93 cells normally did not proliferate in the absence of BMSC, however ectopic expression of CDK6 promoted cell proliferation as evidenced by the positive Ki67 staining (Fig 5).

Discussion

PCa cells may remain quiescent/dormant for years and proliferate to form active metastases at distant sites. Little is known to date about the mechanisms underlying the induction and release from dormancy in PCa cells that reside in the bone marrow. Major reasons include the lack of patient specimens and relevant human *in vitro* and *in vivo* models. We previously reported a potential dormancy signature associated with DTC isolated from PCa patients with no evidence of disease [30]. Here, instead of using immortalized PCa cell lines that readily proliferate *in vitro*, we used clinically relevant PDX cells to examine the mechanism underlying direct cell-cell interaction to restore cell proliferation. We characterized three LuCaP PCa PDXs residing on the human bone marrow stroma, which displayed quiescent/dormant and proliferating phenotypes depending on the cell seeding density. Our results showed that tumor cell-cell contact induced cell proliferation which may represent dormancy escape via activation of β_1 integrin associated with universal downregulation of TGFB2 signaling and upregulation of MLCK activation/CDK6 in PCa PDXs.

Recent studies in other solid tumors, such as in the head, neck, and breast, have implicated elements of the cytoskeletal migration and adhesion machinery in the activation of indolent tumor cells [4–7, 38–41]. β_1 Integrin is critical for the initiation of tumorigenesis and the

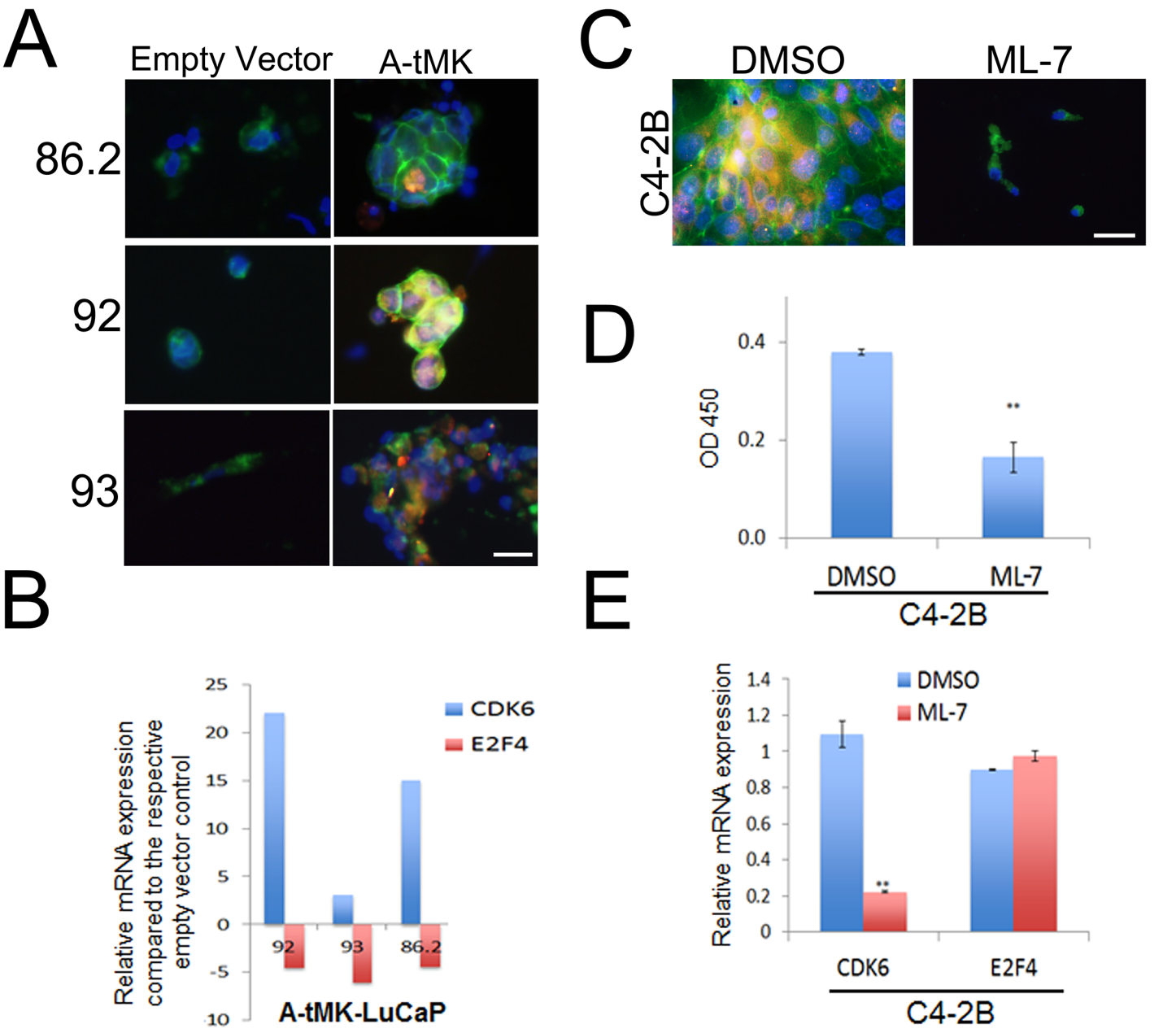

Fig 4. Constitutive activation of MLCK promotes proliferation of LuCaP PDX cells via upregulation of CDK6. A) LuCaP cells were infected with lentivirus containing A-tMK (constitutively activate MLCK) showed positive Ki67 staining, whereas cells transduced with an empty vector did not. B) In LuCaP 86.2, 92, and 93, ectopic expression of A-tMK induced an upregulation of CDK6 and a concurrent downregulation of E2F4 when compared to that of the empty vector-transduced cells. Inhibition of MLCK with the MLCK inhibitor ML-7 suppressed proliferation by C) abolishing Ki67 expression, D) decreasing cell viability assessed by WST-1 assay and E) downregulating CDK6 expression. E2F4 expression was not altered by the ML-7. Green, EpCAM; Red, Ki67; Blue, DAPI. Magnification: 200x. Scale bar: 20 μm. **p< 0.01 as compared to the DMSO control. CDK6: cyclin-dependent kinase 6; E2F4: E2F transcription factor 4.

doi:10.1371/journal.pone.0130565.g004

maintenance of the proliferative capacity of tumors [33, 41]. In PCa, we found that cell-cell contact, both between tumor cells and with an underlying stroma, was associated with the activation of β_1 integrin and was essential to facilitate the growth of quiescent PCa xenograft cells *in vitro*. While cell-cell contact has to our knowledge not been directly reported as a requirement for dormancy release, several mechanisms associated with the migration and adhesion of

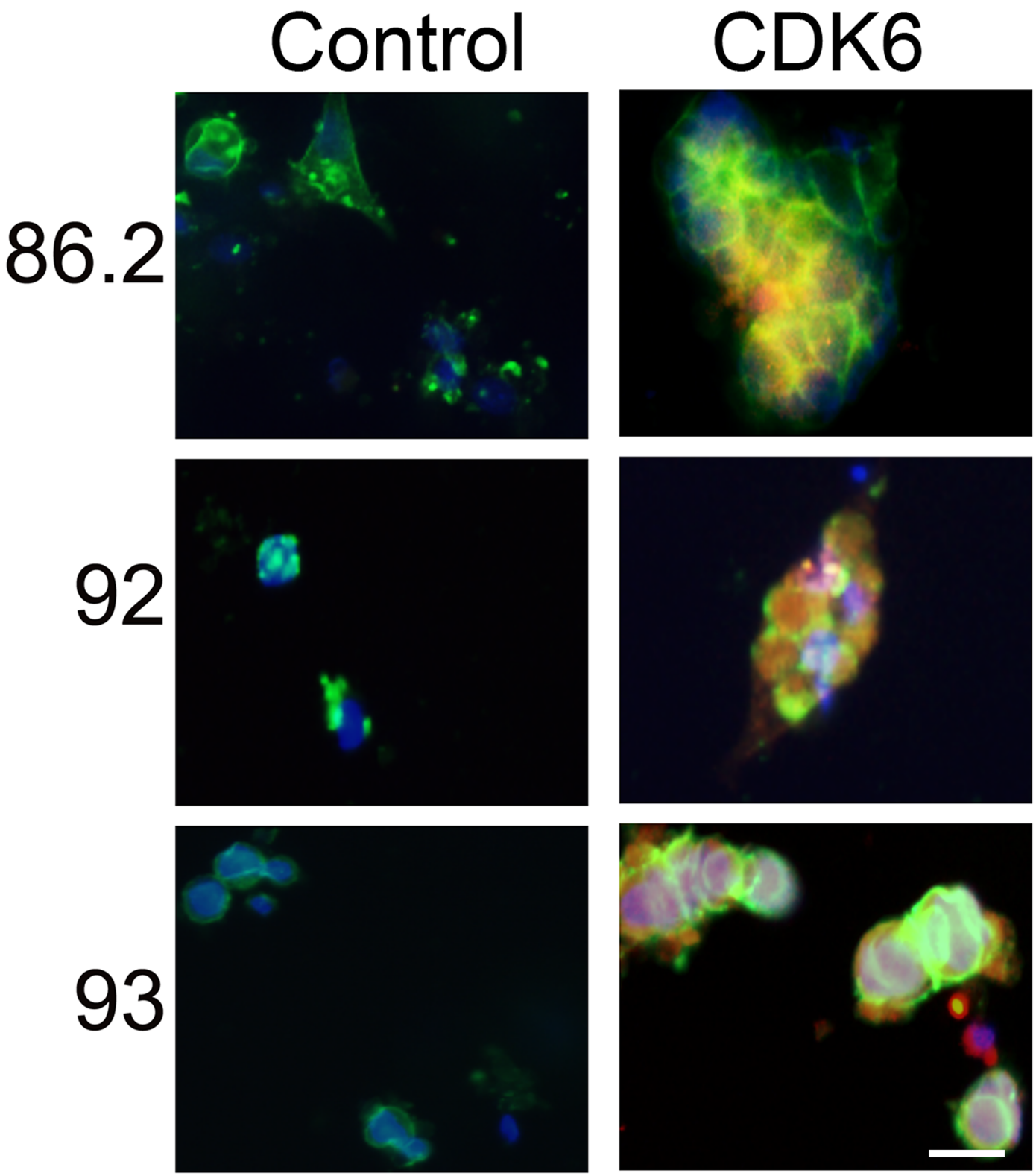

Fig 5. CDK6 overexpression induced proliferation of LuCaP PDX cells *in vitro*. LuCaP 86.2, 92 and 93 cells were lentivirally transduced to overexpress CDK6 and cultured *in vitro* to assess proliferation. Positive Ki67 indicated that CDK6 overexpression facilitated proliferation in these cells. Green, EpCAM; Red, Ki67; Blue, DAPI. Magnification: 200x. Scale bar: 20 μm.

doi:10.1371/journal.pone.0130565.g005

tumor cells have been implicated in this process. Specifically, activation of $\alpha_5\beta_1$ integrin has been shown to release human squamous carcinoma and breast cancer cells from dormancy [6, 7, 39, 41], and activation of α_5 β_1 integrin induce cell adhesion and migration [42, 43] as well as proliferation on extracellular matrix [44]. Thus, it is not surprising that given an opportunity to come into contact within the bone marrow microenvironment, these normally quiescent LuCaP PDX cells begin to proliferate *in vitro*.

Activation of β_1 integrin has been shown to induce the downregulation of TGF β2 and Cdc42 [45, 46]. Global gene expression analysis on the reactivated cells versus dormant cells highlighted a decrease in TGF β2 signaling in proliferating PCa PDX cells which was consistent with the observation that TGF β2 induced dormancy of malignant DTC in head and neck squamous cell carcinoma [47]. This is in concordance with the data from clinically derived DTC that *TGFB2* expression is higher in PCa patients with no evidence of disease when compared to patients with advanced disease [35]. Furthermore, Cdc42 was implicated in activation of p38 and growth arrest in cancers [7] and was downregulated in proliferating PCa PDX cells in the current study. Of note, MLCK is a well-known downstream effector of adhesion- and motility-mediated mechanisms including β_1 integrin [9, 10, 38, 40], and its activation has been linked to cell survival [40]. In our study, the downregulation of CDC42 and TGFB2 pointed to a possible activation of MLCK leading to cell proliferation. Indeed, introduction of constitutively active MLCK alone was adequate to induce proliferation in LuCaP PDX cells that normally retain dormant *in vitro*. Conversely, C4-2B cells, which readily proliferate *in vitro*, were growth suppressed upon treatment with the MLCK inhibition ML-7. These data correlated well with a previous study by Barkan and colleagues that demonstrated quiescence *in vitro* and inhibition of metastatic outgrowth of various breast cancer cell lines upon inhibition of MLCK [38].

In the current study, activation of MLCK resulted in an upregulation of CDK6 in all three LuCaP PDX lines. CDK 6 associates with cyclin D1 to transition cells through the G1 phase of the cell cycle [48] and is regulated by the androgen receptor (AR) [49]. Instead of acting as a primary regulator, AR may act as an enhancer for CDK6 expression because *CDK6* upregulation upon MLCK activation was 5–7 fold higher in the AR-positive LuCaP 92 and LuCaP 86.2 cells compared to the upregulation in AR-negative neuroendocrine LuCaP 93 cells [26, 27]. On the other hand, E2F4 is known to act in conjunction with Smad3 as a cofactor for TGF transcription [50], which has been shown to induce apoptosis in PCa [51, 52]. Furthermore, E2F4 has been demonstrated to enforce G2 arrest in C4-2B cells in response to genotoxic stress [53]. We observed a downregulation of the E2F4 in proliferating LuCaP PDXs expressing activated MLCK, suggesting that the downregulation in E2F4 may be allowing LuCaP PDX cells to progress through the cell cycle and escape quiescence/dormancy (Fig 6).

Collectively, we presented the first *in vitro* model demonstrating non-proliferating PCa PDX cells resumed proliferation on human bone marrow stromal microenvironment. These models provide evidence to support that direct cell-cell interaction promotes cell proliferation partly via β_1 integrin activation. A clinically interesting but not yet addressed question is whether or not a patient showing an increased number of DTC (i.e. increased chance of DTC contact with each other) will result in an increased rate of tumor cell proliferation and hence metastatic outgrowth. Maintaining disseminated PCa cells in a dormant, indolent state is an attractive clinical prospect as is inducing active PCa cells to become dormant. However, such treatments require an intimate understanding of PCa dormancy mechanisms. While confirmatory *in vivo* studies are required to conclusively determine a dormancy release mechanism in PCa, these findings represent an important and encouraging first step in the identification of such a mechanism for this heterogeneous disease.

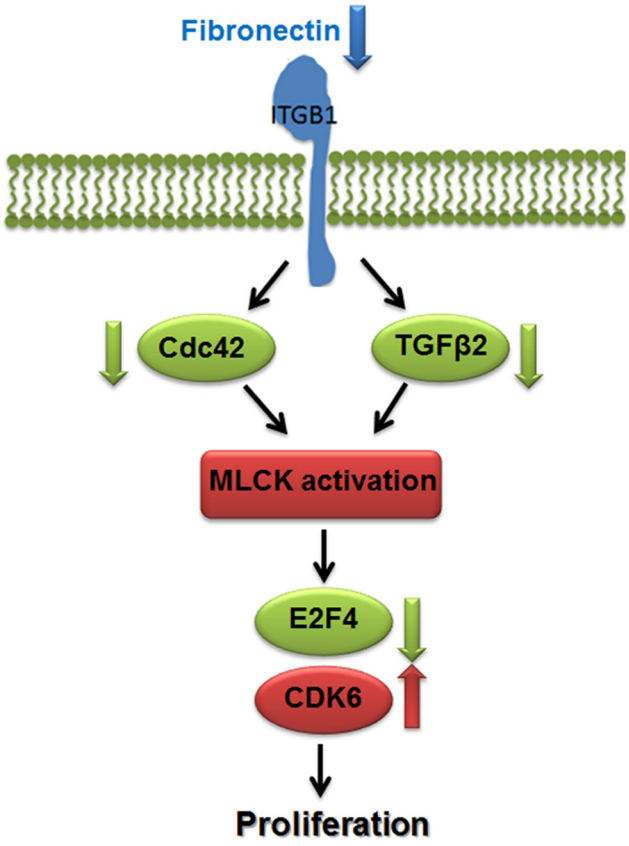

Fig 6. Potential mechanism for PCa release from quiescence/dormancy. Decreased fibronectin activation on β_1 integrin downregulates TGF β2 and Cdc42 resulting in activation of MLCK. This activity leads to the deactivation of growth suppressor like E2F4 and activation of cell cycle regulator CDK6, promoting cell proliferation.

doi:10.1371/journal.pone.0130565.g006

Supporting Information

S1 Fig. C4-2B cells grow on a monolayer of bone marrow stromal cells (BMSC) when seeded sparsely. A) C4-2B cells were seeded sparsely (50 cells/cm^2) on BMSC, cells were fixed with ice-cold methanol and fluorescently stained for Ki67 to assess proliferation. Green, EpCAM; Red, Ki67, Blue, DAPI. Magnification: 200x. Scale bar: 50 μm. B) EpCAM-positive cells were counted on day 1 and day 7. Data are presented as mean±S.D of two independent experiments. $^{**}p<0.01$ when compared to day 1.
(PDF)

S2 Fig. Cell cycle analysis of ML-7 treatment on C4-2B cells. A) A representative histogram of DAPI-stained C4-2B cells treated with either DMSO or ML-7 (10μM) for 24h or 48h. Cell cycle was analyzed by flow cytometry. B) Percentage of cells in G1, S, and G2/M phase of C4-2B cells treated with DMSO or ML-7. Data are presented as mean±S.D of two independent experiments. $^{*}p<0.05$ when compared to the DMSO control.
(PDF)

Acknowledgments

The material is also the result of work supported by resources from the VA Puget Sound Heath Care System, Seattle, Washington (R.L.V. is a research career scientist). H.M.L. is a recipient of the Young Investigator Award from the Prostate Cancer Foundation, the Career Development Award from the Pacific Northwest Prostate Cancer SPORE (P50 CA097186) and an Idea Development Award from the Department of Defense (W81XWH-14-1-0271). We would like to thank Dr. Julio Aguirre-Ghiso for his advice, Dr. Leland Chung for the C4-2B cells, Ms. Donna Prunkard for the flow cytometry analyses, and Drs. Zuzana Strakova, Jody Martin, and Primal de Lanerolle for the A-tMK construct.

Author Contributions

Conceived and designed the experiments: NR LAS RLV CM HML. Performed the experiments: NR SL BL LK LB IC RC. Analyzed the data: NR IC LB CM HML. Contributed reagents/materials/analysis tools: PSN EC HN LAS RLV CM HML. Wrote the paper: NR SL BL LK IC RC PSN EC LAS RLV CM HML.

References

1. Morgan TM, Lange PH, Porter MP, Lin DW, Ellis WJ, Gallaher IS, et al. (2009) Disseminated tumor cells in prostate cancer patients after radical prostatectomy and without evidence of disease predicts biochemical recurrence. Clin Cancer Res 15(2): 677–683. doi: 10.1158/1078-0432.CCR-08-1754 PMID: 19147774
2. Lam HM, Vessella RL, Morrissey C (2014) The role of the microenvironment-dormant prostate disseminated tumor cells in the bone marrow. Drug Discov Today Technol 11: 41–47. doi: 10.1016/j.ddtec.2014.02.002 PMID: 24847652
3. Ruppender NS, Morrissey C, Lange PH, Vessella RL (2013) Dormancy in solid tumors: implications for prostate cancer. Cancer Metastasis Rev 2013; 32(3–4): 501–509. doi: 10.1007/s10555-013-9445-5 PMID: 23907184
4. Aguirre Ghiso JA, Kovalski K, Ossowski L (1999) Tumor dormancy induced by downregulation of urokinase receptor in human carcinoma involves integrin and MAPK signaling. J Cell Biol 147(1): 89–104. PMID: 10508858
5. Allgayer H, Aguirre-Ghiso JA (2008) The urokinase receptor (u-PAR)—a link between tumor cell dormancy and minimal residual disease in bone marrow? APMIS 116(7–8): 602–614. doi: 10.1111/j.1600-0463.2008.01230.x PMID: 19133014
6. Aguirre-Ghiso JA, Liu D, Mignatti A, Kovalski K, Ossowski L. (2001) Urokinase receptor and fibronectin regulate the ERK(MAPK) to p38(MAPK) activity ratios that determine carcinoma cell proliferation or dormancy in vivo. Mol Biol Cell 12(4): 863–879. PMID: 11294892
7. Aguirre-Ghiso JA, Estrada Y, Liu D, Ossowski L. ERK(MAPK) activity as a determinant of tumor growth and dormancy; regulation by p38(SAPK). Cancer Res 2003; 63(7): 1684–1695. PMID: 12670923
8. Nguyen DH, Catling AD, Webb DJ, Sankovic M, Walker LA, Somlyo AV, et al. (1999) Myosin light chain kinase functions downstream of Ras/ERK to promote migration of urokinase-type plasminogen activator-stimulated cells in an integrin-selective manner. J Cell Biol 146(1): 149–164. PMID: 10402467
9. Klemke RL, Cai S, Giannini AL, Gallagher PJ, de LP, Cheresh DA. (1997) Regulation of cell motility by mitogen-activated protein kinase. J Cell Biol 137(2): 481–492. PMID: 9128257
10. Huang C, Jacobson K, Schaller MD. (2004) MAP kinases and cell migration. J Cell Sci 117(Pt 20): 4619–4628. PMID: 15371522
11. Chen P, Xie H, Sekar MC, Gupta K, Wells A. (1994) Epidermal growth factor receptor-mediated cell motility: phospholipase C activity is required, but mitogen-activated protein kinase activity is not sufficient for induced cell movement. J Cell Biol 127(3): 847–857. PMID: 7962064
12. Schlaepfer DD, Hanks SK, Hunter T, van der Geer P. (1994) Integrin-mediated signal transduction linked to Ras pathway by GRB2 binding to focal adhesion kinase. Nature 372(6508): 786–791. PMID: 7997267
13. Zhu X, Assoian RK. (1995) Integrin-dependent activation of MAP kinase: a link to shape-dependent cell proliferation. Mol Biol Cell 6(3): 273–282. PMID: 7612963

14. Weigelt B, Lo AT, Park CC, Gray JW, Bissell MJ. (2010) HER2 signaling pathway activation and response of breast cancer cells to HER2-targeting agents is dependent strongly on the 3D microenvironment. Breast Cancer Res Treat 122(1): 35–43. doi: 10.1007/s10549-009-0502-2 PMID: 19701706

15. Howe GA, Addison CL. (2012) beta1 integrin: an emerging player in the modulation of tumorigenesis and response to therapy. Cell Adh Migr 6(2): 71–77. doi: 10.4161/cam.20077 PMID: 22568952

16. Morazzani M, de Carvalho DD, Kovacic H, Smida-Rezgui S, Briand C, Penel C. (2004) Monolayer versus aggregate balance in survival process for EGF-induced apoptosis in A431 carcinoma cells: Implication of ROS-P38 MAPK-integrin alpha2beta1 pathway. Int J Cancer 110(6): 788–799. PMID: 15170659

17. Pickl M, Ries CH. (2009) Comparison of 3D and 2D tumor models reveals enhanced HER2 activation in 3D associated with an increased response to trastuzumab. Oncogene 28(3): 461–468. doi: 10.1038/onc.2008.394 PMID: 18978815

18. Wang F, Weaver VM, Petersen OW, Larabell CA, Dedhar S, Briand P, et al. (1998) Reciprocal interactions between beta1-integrin and epidermal growth factor receptor in three-dimensional basement membrane breast cultures: a different perspective in epithelial biology. Proc Natl Acad Sci U S A 95 (25): 14821–14826. PMID: 9843973

19. Windus LC, Kiss DL, Glover T, Avery VM. (2012) In vivo biomarker expression patterns are preserved in 3D cultures of Prostate Cancer. Exp Cell Res 318(19): 2507–2519. doi: 10.1016/j.yexcr.2012.07.013 PMID: 22841689

20. Josson S, Sharp S, Sung SY, Johnstone PA, Aneja R, Wang R, et al. (2010) Tumor-Stromal Interactions Influence Radiation Sensitivity in Epithelial- versus Mesenchymal-Like Prostate Cancer Cells. J Oncol 2010.

21. Kumar A, White TA, MacKenzie AP, Clegg N, Lee C, Dumpit RF, et al. (2011) Exome sequencing identifies a spectrum of mutation frequencies in advanced and lethal prostate cancers. Proc Natl Acad Sci U S A 108(41): 17087–17092. doi: 10.1073/pnas.1108745108 PMID: 21949389

22. Kim JK, Jung Y, Wang J, Joseph J, Mishra A, Hill EE, et al. (2013) TBK1 regulates prostate cancer dormancy through mTOR inhibition. Neoplasia 15(9): 1064–1074. PMID: 24027431

23. Taichman RS, Patel LR, Bedenis R, Wang J, Weidner S, Schumann T, et al. (2013) GAS6 receptor status is associated with dormancy and bone metastatic tumor formation. PLoS One 8(4): e61873. doi: 10.1371/journal.pone.0061873 PMID: 23637920

24. Welty CJ, Coleman I, Coleman R, Lakely B, Xia J, Chen S, et al. (2013) Single cell transcriptomic analysis of prostate cancer cells. BMC Mol Biol 14: 6–16. doi: 10.1186/1471-2199-14-6 PMID: 23414343

25. Thalmann GN, Anezinis PE, Chang SM, Zhau HE, Kim EE, Hopwood VL, et al. (1994) Androgen-independent cancer progression and bone metastasis in the LNCaP model of human prostate cancer. Cancer Res 54(10): 2577–2581. PMID: 8168083

26. Perner S, Demichelis F, Beroukhim R, Schmidt FH, Mosquera JM, Setlur S, et al. (2006) TMPRSS2: ERG fusion-associated deletions provide insight into the heterogeneity of prostate cancer. Cancer Res 66(17): 8337–8341. PMID: 16951139

27. Zhang X, Morrissey C, Sun S, Ketchandji M, Nelson PS, True LD, et al. (2011) Androgen receptor variants occur frequently in castration resistant prostate cancer metastases. PLoS One 6(11): e27970. doi: 10.1371/journal.pone.0027970 PMID: 22114732

28. Nguyen HM, Corey E. (2011) Methodology to investigate androgen-sensitive and castration-resistant human prostate cancer xenografts in preclinical setting. Methods Mol Biol 776: 295–312. doi: 10.1007/978-1-61779-243-4_17 PMID: 21796533

29. Ihnatovych I, Hu W, Martin JL, Fazleabas AT, de LP, Strakova Z. (2007) Increased phosphorylation of myosin light chain prevents in vitro decidualization. Endocrinology 148(7): 3176–3184. PMID: 17412815

30. Chery L, Lam HM, Coleman I, Lakely B, Coleman R, Larson S, et al. (2014) Characterization of single disseminated prostate cancer cells reveals tumor cell heterogeneity and identifies dormancy associated pathways. Oncotarget 5(20): 9939–9951. PMID: 25301725

31. Tusher VG, Tibshirani R, Chu G. (2001) Significance analysis of microarrays applied to the ionizing radiation response. Proc Natl Acad Sci U S A 98(9): 5116–5121. PMID: 11309499

32. Young SR, Saar M, Santos J, Nguyen HM, Vessella RL, Peehl DM. (2013) Establishment and serial passage of cell cultures derived from LuCaP xenografts. Prostate 73(12): 1251–1262. doi: 10.1002/pros.22610 PMID: 23740600

33. Giancotti FG, Ruoslahti E. (1999) Integrin signaling. Science 285(5430): 1028–1032. PMID: 10446041

34. Gao J, Zhu Y, Nilsson M, Sundfeldt K. (2014) TGF-beta isoforms induce EMT independent migration of ovarian cancer cells. Cancer Cell Int 14(1): 72. doi: 10.1186/s12935-014-0072-1 PMID: 25278811

35. Sosa MS, Parikh F, Maia AG, Estrada Y, Bosch A, Bragado P, et al. (2015) NR2F1 controls tumor cell dormancy via SOX9 and RAR β driven quiescence programs. Nat Commun. 6: 6170–6184. doi: 10.1038/ncomms7170 PMID: 25636082

36. Schiller HB, Hermann MR, Polleux J, Vignaud T, Zanivan S, Friedel CC, et al. (2013) beta1- and alphav-class integrins cooperate to regulate myosin II during rigidity sensing of fibronectin-based microenvironments. Nat Cell Biol 15(6): 625–636. doi: 10.1038/ncb2747 PMID: 23708002

37. Sinpitaksakul SN, Pimkhaokham A, Sanchavanakit N, Pavasant P. (2008) TGF-beta1 induced MMP-9 expression in HNSCC cell lines via Smad/MLCK pathway. Biochem Biophys Res Commun 371(4): 713–718. doi: 10.1016/j.bbrc.2008.04.128 PMID: 18457660

38. Barkan D, Kleinman H, Simmons JL, Asmussen H, Kamaraju AK, Hoenorhoff MJ, et al. (2008) Inhibition of metastatic outgrowth from single dormant tumor cells by targeting the cytoskeleton. Cancer Res 68(15): 6241–6250. doi: 10.1158/0008-5472.CAN-07-6849 PMID: 18676848

39. Aguirre Ghiso JA. (2002) Inhibition of FAK signaling activated by urokinase receptor induces dormancy in human carcinoma cells in vivo. Oncogene 21(16): 2513–2524. PMID: 11971186

40. Street CA, Bryan BA. (2011) Rho kinase proteins—pleiotropic modulators of cell survival and apoptosis. Anticancer Res 31(11): 3645–3657. PMID: 22110183

41. White DE, Kurpios NA, Zuo D, Hassell JA, Blaess S, Mueller U, et al. (2004) Targeted disruption of beta1-integrin in a transgenic mouse model of human breast cancer reveals an essential role in mammary tumor induction. Cancer Cell 6(2): 159–170. PMID: 15324699

42. Goodman SL, Picard M. (2012) Integrins as therapeutic targets. Trends Pharmacol Sci 33(7): 405–412. doi: 10.1016/j.tips.2012.04.002 PMID: 22633092

43. Zhao X, Guan JL. (2011) Focal adhesion kinase and its signaling pathways in cell migration and angiogenesis. Adv Drug Deliv Rev 63(8): 610–615. doi: 10.1016/j.addr.2010.11.001 PMID: 21118706

44. Keely PJ. (2011) Mechanisms by which the extracellular matrix and integrin signaling act to regulate the switch between tumor suppression and tumor promotion. J Mammary Gland Biol Neoplasia 16(3): 205–219. doi: 10.1007/s10911-011-9226-0 PMID: 21822945

45. Cox EA, Sastry SK, Huttenlocher A. (2001) Integrin-mediated adhesion regulates cell polarity and membrane protrusion through the Rho family of GTPases. Mol Biol Cell 12(2): 265–277. PMID: 11179414

46. Worthington JJ, Klementowicz JE, Travis MA. (2011) TGFbeta: a sleeping giant awoken by integrins. Trends Biochem Sci 36(1): 47–54. doi: 10.1016/j.tibs.2010.08.002 PMID: 20870411

47. Bragado P, Estrada Y, Parikh F, Krause S, Capobianco C, Farina HG, et al. (2013) TGF-beta2 dictates disseminated tumour cell fate in target organs through TGF-beta-RIII and p38alpha/beta signalling. Nat Cell Biol 15(11): 1351–1361. doi: 10.1038/ncb2861 PMID: 24161934

48. Peters G. (1994) The D-type cyclins and their role in tumorigenesis. J Cell Sci Suppl 18: 89–96. PMID: 7883799

49. Lim JT, Mansukhani M, Weinstein IB. (2005) Cyclin-dependent kinase 6 associates with the androgen receptor and enhances its transcriptional activity in prostate cancer cells. Proc Natl Acad Sci U S A 102 (14): 5156–5161. PMID: 15790678

50. Chen CR, Kang Y, Siegel PM, Massague J (2002) E2F4/5 and p107 as Smad cofactors linking the TGFbeta receptor to c-myc repression. Cell 110(1): 19–32. PMID: 12150994

51. Yang J, Song K, Krebs TL, Jackson MW, Danielpour D (2008) Rb/E2F4 and Smad2/3 link survivin to TGF-beta-induced apoptosis and tumor progression. Oncogene 27(40): 5326–5338. doi: 10.1038/onc.2008.165 PMID: 18504435

52. Song K, Wang H, Krebs TL, Wang B, Kelley TJ, Danielpour D (2010) DHT selectively reverses Smad3-mediated/TGF-beta-induced responses through transcriptional down-regulation of Smad3 in prostate epithelial cells. Mol Endocrinol 24(10): 2019–2029. doi: 10.1210/me.2010-0165 PMID: 20739403

53. Crosby ME, Jacobberger J, Gupta D, Macklis RM, Almasan A (2007) E2F4 regulates a stable G2 arrest response to genotoxic stress in prostate carcinoma. Oncogene 26(13): 1897–1909. PMID: 17043659

Published OnlineFirst December 19, 2016; DOI: 10.1158/1078-0432.CCR-16-2054

Cancer Therapy: Preclinical

Clinical Cancer Research

Characterization of an Abiraterone Ultraresponsive Phenotype in Castration-Resistant Prostate Cancer Patient-Derived Xenografts

Hung-Ming Lam[1,2], Ryan McMullin[3], Holly M. Nguyen[1], Ilsa Coleman[4], Michael Gormley[5], Roman Gulati[4], Lisha G. Brown[1], Sarah K. Holt[1], Weimin Li[5], Deborah S. Ricci[6], Karin Verstraeten[7], Shibu Thomas[5], Elahe A. Mostaghel[4,8], Peter S. Nelson[4,8], Robert L. Vessella[1,9], and Eva Corey[1]

Abstract

Purpose: To identify the molecular signature associated with abiraterone acetate (AA) response and mechanisms underlying AA resistance in castration-resistant prostate cancer patient-derived xenografts (PDXs).

Experimental Design: SCID mice bearing LuCaP 136CR, 77CR, 96CR, and 35CR PDXs were treated with AA. Tumor volume and prostate-specific antigen were monitored, and tumors were harvested 7 days after treatment or at end of study for gene expression and immunohistochemical studies.

Results: Three phenotypic groups were observed based on AA response. An ultraresponsive phenotype was identified in LuCaP 136CR with significant inhibition of tumor progression and increased survival, intermediate responders LuCaP 77CR and LuCaP 96CR with a modest tumor inhibition and survival benefit, and LuCaP 35CR with minimal tumor inhibition and no survival benefit upon AA treatment. We identified a molecular signature of secreted proteins associated with the AA ultraresponsive phenotype. Upon resistance, AA ultraresponder LuCaP 136CR displayed reduced androgen receptor (AR) signaling and sustainably low nuclear glucocorticoid receptor (nGR) localization, accompanied by steroid metabolism alteration and epithelial–mesenchymal transition phenotype enrichment with increased expression of NF-κB–regulated genes; intermediate and minimal responders maintained sustained AR signaling and increased tumoral nGR localization.

Conclusions: We identified a molecular signature of secreted proteins associated with AA ultraresponsiveness and sustained AR/GR signaling upon AA resistance in intermediate or minimal responders. These data will inform development of noninvasive biomarkers predicting AA response and suggest that further inhibition along the AR/GR signaling axis may be effective only in AA-resistant patients who are intermediate or minimal responders. These findings require verification in prospective clinical trials. *Clin Cancer Res; 23(9); 2301–12. ©2016 AACR.*

Introduction

Androgen-deprivation therapy (ADT) has been the mainstay therapy for patients with advanced prostate cancer (1). Abiraterone acetate (AA), the prodrug of abiraterone, is a specific CYP17A1 inhibitor that blocks androgen biosynthesis, resulting in effective reduction of serum and intratumoral androgens (2–4). AA was the first second-generation ADT shown to improve survival in patients with metastatic castration-resistant prostate cancer (mCRPC) (5–9). Although dramatic decline in prostate-specific antigen (PSA) was achieved in some patients, others exhibited a subtle PSA response or *de novo* resistance, and disease progression is universal (1, 5, 9).

Predictive biomarkers that distinguish ultraresponders from intermediate or minimal responders to AA are critically needed. Early attempts using circulating tumor cells (CTCs) showed that TMPRSS2-ERG fusion did not predict the response to AA in patients with CRPC (10). However, Antonarakis and colleagues recently showed that patients with CRPC with positive androgen receptor transcript variant (ARv7) in their pretreatment CTC did not demonstrate PSA decline, and 68% of a small cohort of patients with negative ARv7 demonstrated >50% PSA decline

[1]Department of Urology, University of Washington, Seattle, Washington. [2]State Key Laboratory of Quality Research in Chinese Medicine, Macau Institute for Applied Research in Medicine and Health, Macau University of Science and Technology, Macau (SAR), China. [3]LabConnect, Seattle, Washington. [4]Fred Hutchinson Cancer Research Center, Seattle, Washington. [5]Janssen Research and Development, Spring House, Pennsylvania. [6]Janssen Research and Development, Raritan, New Jersey. [7]Janssen Research and Development, Beerse, Belgium. [8]Department of Medicine, University of Washington, Seattle, Washington. [9]Department of Veterans Affairs Medical Center, Seattle, Washington.

Note: Supplementary data for this article are available at Clinical Cancer Research Online (http://clincancerres.aacrjournals.org/).

Current address for R. McMullin: Janssen Research and Development, Spring House, Pennsylvania.

H.-M. Lam and R. McMullin share first authorship.

Corresponding Author: Eva Corey, University of Washington, Mailstop 356510, Seattle, WA 98195. Phone: 206-543-1461; Fax: 206-543-1146; E-mail: ecorey@u.washington.edu

doi: 10.1158/1078-0432.CCR-16-2054

Published OnlineFirst December 19, 2016; DOI: 10.1158/1078-0432.CCR-16-2054

Translational Relevance

Abiraterone acetate (AA) improves survival in patients with metastatic castration-resistant prostate cancer (mCRPC); however, not all tumors respond, and responding tumors eventually develop resistance. Currently, there is no information available regarding how to stratify patients for durable AA therapy, and the mechanisms underlying AA resistance are diverse. We used patient-derived xenograft models that recapitulated the diverse clinical response of CRPC to AA and identified a molecular signature of secreted proteins associated with the AA ultraresponsive phenotype. The signature will provide the much-needed information on noninvasive biomarker development to select AA-responsive patients. Upon resistance, our results suggested reduced androgen receptor (AR) signaling and sustainably low nuclear glucocorticoid receptor (nGR) localization in the AA ultraresponders. In contrast, sustained AR signaling and increased nGR localization were observed in the intermediate and minimal responders. Further inhibition along the AR/GR signaling axis may be effective in AA-resistant patients who are intermediate or minimal responders.

after receiving AA (11), suggesting that the detection of positive ARv7 in CTCs may predict AA sensitivity.

De novo and acquired resistance to AA is emerging clinically, and there are preclinical and clinical efforts to investigate the mechanisms of resistance. In preclinical studies, resistance to AA was associated with an induction of full-length AR, ARv7, and CYP17A1 (12). In clinical studies, the presence of ARv7 in CTCs was associated with resistance to AA and shorter overall survival (11). In addition, acquired resistance to AA has been associated with the emergence of AR mutations that have been reported in up to 20% of patients who progressed (13–15). Recently, upregulation of glucocorticoid receptor (GR) has been shown to be a possible bypass mechanism to ADT, and patients with CRPC with positive GR in their bone marrow biopsies were less likely to have a durable response to enzalutamide, another second-generation ADT (16).

Currently, there is little information about biomarkers to identify patients who will durably respond to AA, and the mechanisms of resistance are diverse. In the present study, we evaluated the AA response in a panel of LuCaP CRPC patient-derived xenografts (PDX) that displayed differential responsiveness to AA and identified a molecular signature associated with AA ultraresponsiveness. We also provided evidence to support diverse resistance mechanisms upon AA treatment. This study highlights potential noninvasive biomarkers that may be used to select patients for durable AA therapy, and potential targeting of the epithelial–mesenchymal transition (EMT)/nuclear factor κB (NF-κB) pathway in AA ultraresponsive or AR/GR pathways in AA intermediate- or minimally responsive CRPC.

Materials and Methods

Prostate cancer PDX models

Animal procedures were carried out in accordance with NIH guidelines and upon University of Washington Institutional Animal Care and Use Committee approval. Four different LuCaP human CRPC PDXs (LuCaP 136CR, LuCaP 77CR, LuCaP 96CR, and LuCaP 35CR) were used. All four PDXs express wild-type AR but exhibit differential expression of PSA, PTEN, and ERG (corresponding patient information is summarized in Supplementary Table S1). Two additional PDX models (LuCaP 70CR and LuCaP 86.2CR) were used for survival analysis upon AA treatment and assessment of gene signature.

Intact male CB-17 SCID mice (aged ∼6 weeks; Charles River Laboratories) were implanted subcutaneously with tumor bits of LuCaP 136 or LuCaP 77. Mice were castrated when tumor volume was $\geq$100 mm^3. When tumor regrew to 1.5-fold the original volume, tumors were referred to as LuCaP 136CR or LuCaP 77CR (Fig. 1). LuCaP 96CR and LuCaP 35CR are castration-resistant PDXs that are propagated in castrated male mice. Castrated male CB-17 SCID mice were implanted subcutaneously with LuCaP 96CR or LuCaP 35CR tumor bits and enrolled when tumor volume reached $\geq$100 mm^3 (Fig. 1). Upon enrollment, mice were randomized to vehicle (20% HPbCD/0.37N HCl/PBS) or AA treatment groups (0.5 mmol/kg; Janssen Pharmaceutical Companies). Animals were treated by oral gavage on a weekly schedule of 5 days on, 2 days off. Tumor volume and body weight were measured twice weekly, and blood samples were drawn weekly for PSA measurements using AxSym Total PSA Assay (Abbott Laboratories). Five animals in each group were sacrificed 7 days after the initiation of treatment (D7), and the remaining animals were followed and sacrificed when tumors exceeded 1,000 mm^3 (end of study, EOS) or sacrificed if animals became compromised. At sacrifice (D7 or EOS), half of the tumor was harvested for paraffin embedding and half was frozen for subsequent analyses. Treatment schemes for LuCaP 70CR and LuCaP 86.2CR are illustrated in Supplementary Fig. S1.

Intratumoral androgen measurement

Intratumoral androgen levels were measured using mass spectrometry as described previously (17, 18). Vehicle-treated tumors and AA-resistant tumors harvested at EOS were used for these analyses.

Immunohistochemistry

Hematoxylin and eosin staining of paraffin-embedded tissues was used to identify viable tumor cells in the tissues. Two cores (five to eight tumors per group) were punched and placed in tissue microarrays. The tissue microarray slides were stained for AR (F39.4.1, 1:100; BioGenex), GR (D6H2L, 1:100; Cell Signaling Technology), chromogranin A (DAK-A3, 1:100; DAKO), and synaptophysin (D-4, 1:200; Santa Cruz Biotechnology) using standard procedures as described previously (19–21). All evaluations were performed in a blinded fashion, and a quasi-continuous immunohistochemical (IHC) score was calculated by multiplying each intensity level (0 for no stain, 1 for faint stain, and 2 for intense stain) by the corresponding percentage of cells (0–100%) at the corresponding intensity and totaling the results. IHC scores ranged from 0 (no staining in any cell) to 200 (intense staining in 100% of the cells).

RNA extraction

Frozen pieces of tumor were embedded in Optimal Cutting Temperature Compound, and 5-μm sections were stained with hematoxylin and eosin. Areas of viable tumor cells were identified and macro-dissected for RNA extraction using a standard procedure with RNA STAT 60 (Tel-Test). RNA was then purified using an

Published OnlineFirst December 19, 2016; DOI: 10.1158/1078-0432.CCR-16-2054

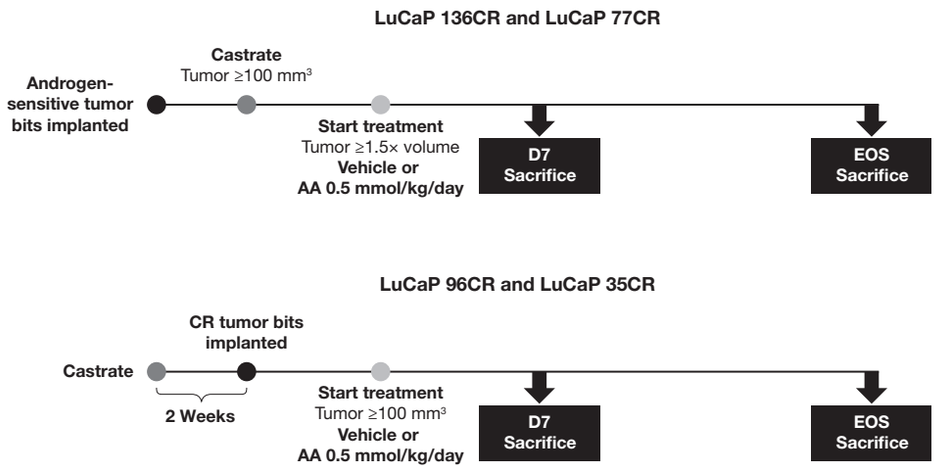

Figure 1.
Treatment scheme for AA on CRPC PDXs. Castration-resistant tumors were developed, and mice were treated orally with either vehicle or AA (0.5 mmol/kg/day). Mice were sacrificed and tumors were harvested on D7 or when tumors reached 1,000 mm^3 (EOS).

RNeasy Mini kit utilizing the optional DNase digestion in solution prior to purification (Qiagen) for subsequent gene expression analyses. RNA integrity number was determined using the Agilent Bioanalyzer system (Agilent).

Gene expression analyses

For Affymetrix microarray analyses, biotin-labeled amplified RNA (aRNA) was synthesized from 200 ng total RNA using the 3′ IVT Express Kit (Affymetrix). The aRNA was purified using Agencourt RNAClean XP beads (Beckman Coulter Inc.) on the BioMek FX Workstation (Beckman Coulter Inc.). Biotin-labeled aRNA was fragmented using the 3′ IVT Express Kit. A total of 4.5 μg fragmented biotin-labeled aRNA was hybridized on an HT Human Genome (HG)-U219 96-array plate. The plate was washed, stained, and scanned with the GeneTitan Instrument. All reagents were from Affymetrix. Gene expression microarray data were normalized to minimize systematic technical variation using robust multichip average (22) and represented in the $\log_2$ scale. Data were filtered to remove probes with mean signal intensities below the 25th percentile of signal intensities for all probes. The Significance Analysis of Microarrays (SAM) program (http://www-stat.stanford.edu/~tibs/SAM/; ref. 23) was used to analyze expression differences between groups using unpaired, two-sample *t* tests, and controlled for multiple testing by estimating *q* values using the false discovery rate method. Gene family was manually curated from Gene Ontology and Uniprot databases. The AR score was determined by the expression of a 21-gene signature and calculated as described previously (24). Microarray data are deposited in the Gene Expression Omnibus database under the accession number GSE85672.

Ingenuity pathway analysis

The differentially expressed genes between vehicle-treated and AA-resistant tumors at the EOS from each of the four LuCaP models were imported into Ingenuity Pathway Analysis (Ingenuity Systems; https://www.ingenuity.com) to identify molecular and cellular functions and regulator effect network involved in AA resistance as previously described (25, 26).

Gene set enrichment analysis

Gene set enrichment analysis (GSEA; ref. 27) was conducted to evaluate enrichment of differential expression patterns in canonical signaling pathways (Reactome; ref. 28) or predefined gene signatures of prostate cancer core gene expression modules representing distinct biological programs (Compendia Bioscience) and annotated signatures associated with EMT, AR activity, GR activity, and AA response.

Quantitative real-time PCR

Total RNA was reverse-transcribed to cDNA, and real-time PCR was carried out as described previously (29). Species-specific primer sequences are presented in Supplementary Table S2. PCR reactions with SYBR GreenER PCR Master-Mix (Invitrogen) were monitored with the 7900HT Fast Real-time PCR System (Applied Biosystems). Individual mRNA levels were normalized to human RPL13a.

AR sequencing

Genomic DNA was extracted using the DNeasy Blood and Tissue Kit (Qiagen) and PCR amplified using primer AR_exon8_c1-589_F: ATTGCGAGAGAGCTGCATCA and AR_exon8_c1-589_R: TGCTTGTTTTTGTTTTGATTTCC. Sanger sequencing was performed using the BigDye Terminator v3.1 Cycle Sequencing Kit (# 4337454, Life Technologies) according to the manufacturer's recommendations. Sequences were aligned to human AR genomic sequence NC_000023.11 and mRNA RefSeq NM_0044 using Sequencher Software (version 5.1, Gene Codes). Mutations were verified using The Androgen Receptor Gene Mutations Database (McGill University).

Statistical analyses

Survival was determined using Kaplan–Meier estimation of time from start of treatment (vehicle or AA) to sacrifice and compared by log-rank (Mantel–Cox) test. Statistical analyses of tumor volume and PSA responses were performed as described previously (19). Briefly, longitudinal tumor measurements and PSA serum levels were log-transformed and modeled using linear mixed models conditional on the treatment group with random effects for each animal. Following standard diagnostic assessment of model fit, we simulated 1,000 datasets from each fitted model, calculated the empirical mean and 95% confidence limits at each time point, and refitted the models to these datasets. The final results represented means and 95% confidence limits of 1,000 bootstrap replicates. In addition, the rate of change in serum PSA and tumor volume upon AA treatment was tested using estimated

Published OnlineFirst December 19, 2016; DOI: 10.1158/1078-0432.CCR-16-2054

fixed effects for each LuCaP line. Student *t* test and Pearson correlation coefficients were used for statistical comparisons between the groups in the intratumoral androgen measurements, gene expression analysis, and IHC analyses. For GSEA, a gene set that displayed FDR <25% is considered significantly enriched.

Results

Heterogeneous AA responses and identification of an AA ultraresponder in LuCaP PDX models

CRPC was developed using four different models of LuCaP PDXs (Fig. 1). AA treatment improved survival and inhibited tumor progression in three of the four models. In mice bearing LuCaP 136CR tumors, survival was substantially improved in AA-treated compared with vehicle-treated mice ($P < 0.001$), and the median survival improved from 6.8 weeks (vehicle) to 21.8 weeks (AA; denoted as AA ultraresponder; 220% gain in survival; Fig. 2A). AA treatment resulted in statistically significant but modest improvement in survival in mice bearing LuCaP 77CR ($P = 0.05$) and LuCaP 96CR ($P = 0.02$)—both denoted as intermediate responders (36%–74% gain in survival; Fig. 2A). AA did not significantly extend survival in mice bearing LuCaP 35CR (12% gain in survival; $P = 0.52$; denoted as minimal responder; Fig. 2A).

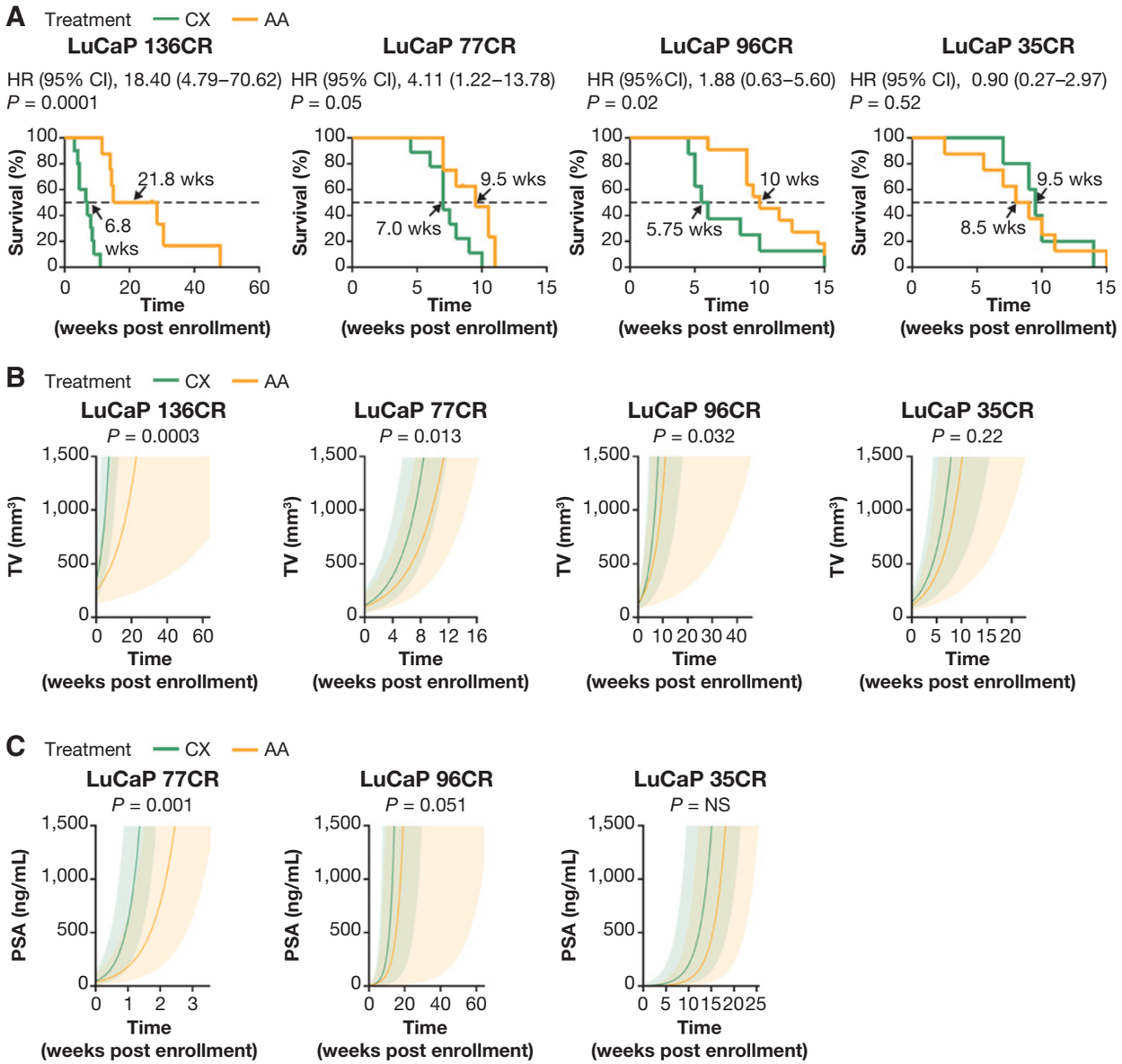

Figure 2.

Ultraresponsiveness to AA in LuCaP 136CR PDX models. **A,** Kaplan–Meier curves showing survival benefits of AA treatment in different LuCaP PDX models. **B,** Linear model analyses of tumor volume. **C,** Serum PSA upon AA treatment. $n = 9$–14 per group.

Published OnlineFirst December 19, 2016; DOI: 10.1158/1078-0432.CCR-16-2054

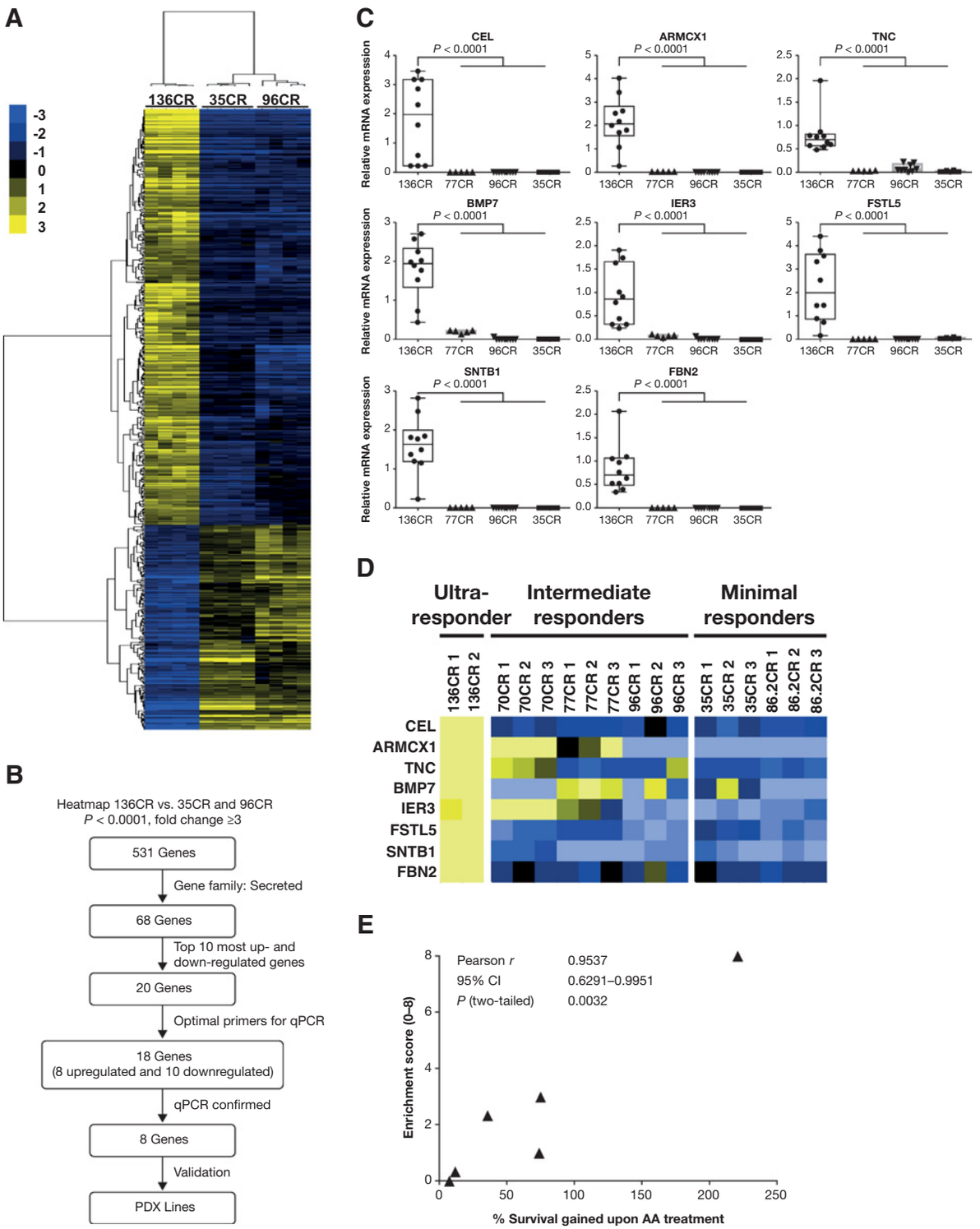

Figure 3.

Gene expression associated with LuCaP 136CR ultraresponsiveness. **A,** Supervised clustering analyses showing 531 differentially expressed genes between LuCaP 136CR and LuCaP 35CR and LuCaP 96CR on D7. Yellow: high gene expression; blue: low gene expression. **B,** Schematic diagram showing gene shaving to identify an eight-gene signature associated with the LuCaP 136CR AA ultraresponsive phenotype. **C,** qPCR confirmation on the eight-gene signature associated with LuCaP 136CR AA ultraresponsive phenotype (D7 and EOS). **D,** Heat map showing the microarray gene expression of the eight-gene signature in multiple LuCaP models. **E,** Correlation between the enrichment of the eight-gene signature associated with AA ultraresponsive phenotype and percentage gained in survival upon AA treatment. Percentage survival gained was calculated based on median survival in AA-treated versus vehicle-treated mice in each xenograft model. Each data point or column represented an individual animal. $P < 0.05$ was considered statistically significant.

Published OnlineFirst December 19, 2016; DOI: 10.1158/1078-0432.CCR-16-2054

Both the AA ultraresponder LuCaP 136CR and intermediate responders LuCaP 77CR and LuCaP 96CR, but not the minimal responder LuCaP 35CR, demonstrated significantly delayed tumor and PSA progression (except for LuCaP 136CR, which has undetectable levels of serum PSA; Fig. 2B and C), followed by both tumor and PSA recurrence. These results suggested the PDX models recapitulated clinical AA response phenotypes comprising ultraresponders with inhibition of tumor progression and a significant extension of survival followed by tumor recurrence, and intermediate and minimal responders with brief or limited AA effect on tumor growth inhibition followed by disease progression.

Gene expression associated with LuCaP 136CR ultraresponsiveness to AA

To identify the gene expression profiles associated with AA ultraresponsiveness, we conducted global transcriptome analyses of the PDX lines. We identified 531 differentially expressed genes between the AA ultraresponder LuCaP 136CR versus the intermediate responder LuCaP 96CR and minimal responder LuCaP 35CR at D7 ($P < 0.0001$, fold change ≥ 3; Fig. 3A). LuCaP 77CR D7 tumors were not included in the global analysis because the specimens were not available, but their EOS tumors were included in the gene expression validation. Of the 156 genes that were successfully mapped into known gene families, 68 (44%) were secreted proteins (Supplementary Fig. S2A). We observed that the differential expression of these 68 secretory proteins in LuCaP 136CR were consistent between early time point (D7; Supplementary Fig. S2B) and EOS (Supplementary Fig. S2C), suggesting the expression of these markers was not dependent on age of mice or tumor size. We then selected the top 10 upregulated and downregulated genes of secreted proteins (total 20 genes) in the AA ultraresponder LuCaP 136CR compared with the intermediate and minimal responders for qPCR validation (Fig. 3B and Supplementary Fig. S3). Primers for 18 genes were available, and qPCR confirmed all of the eight upregulated genes (*CEL*, *ARMCX1*, *TNC*, *BMP7*, *IER3*, *FSTL5*, *SNTB1*, and *FBN2*; Fig. 3C) and 10 downregulated genes (*IL17RB*, *GDF15*, *ST6GAL1*, *SPOCK1*, *MSMB*, *INHBB*, *MINPP1*, *GALS3BP*, *C15orf48*, and *PLA2G2A*; Supplementary Fig. S4). However, the downregulated genes showed more variable expression in the intermediate (LuCaP 77CR, LuCaP 96CR) and minimal (LuCaP 35CR) responders and therefore were not included in the development of a stringent gene signature for AA ultraresponsiveness.

We next validated the highly consistent eight-gene signature that was upregulated in the AA ultraresponder LuCaP 136CR in an independent cohort of six LuCaP models that displayed different responses to AA. As expected, the signature positively correlated with the percentage gained survival on AA ($R = 0.95$, $P = 0.0002$; Fig. 3D and E), supporting the potential of this eight-gene signature in predicting AA ultraresponsiveness.

Mechanisms associated with the acquired resistance of individual AA-responsive phenotypes

To identify response and resistance mechanisms specific to different AA response phenotypes, we conducted global transcriptome analyses on the AA-treated (D7) and AA-resistant (EOS) tumors. Interestingly, upon AA resistance, a distinct set of genes was differentially expressed in each of the four models (vehicle vs. AA, $P < 0.01$, fold change ≥ 2), and there was virtually no overlap of genes between ultraresponders and intermediate/minimal responders or within the intermediate and minimal responders (Fig. 4A and Supplementary Table S5), suggesting that the AA-induced resistance mechanisms are largely diverse. Next, we conducted Ingenuity Pathway Analysis to identify molecular and cellular function involved in the AA resistance in individual models. For both ultraresponder LuCaP 136CR and the intermediate responder LuCaP 77CR, cell growth and proliferation represented 40% to 45% of genes that were associated with AA resistance. In LuCaP 96CR, a majority of AA differentially expressed genes were related to cell morphology (30%), whereas in the minimal responder, AA differentially expressed genes were principally mapped to cell-to-cell signaling (20%) or cellular death and survival (20%; Fig. 4B).

GSEA analysis showed that AA treatment of LuCaP 77CR was negatively associated with signatures of cell growth and androgen-regulated genes upon resistance at EOS (Supplementary Fig. S5). Similarly, AA treatment of LuCaP 96CR was negatively associated with a cell cycle–associated signature that was previously reported to be decreased in a cell line–derived xenograft model of AA resistance (Supplementary Fig. S4; ref. 30). Interestingly, in the AA ultraresponder LuCaP 136CR, we identified steroid metabolism as the top altered regulator effect network upon AA resistance (Fig. 4C), which, together with the high basal expression of the cholesterol esterase *CEL*, implies that alterations in the steroid availability and usage may contribute to the development of AA resistance in this model. Importantly, GSEA analysis showed that AA treatment of LuCaP 136CR was initially negatively associated with signatures of proliferation, cell growth, and a selected AR transcriptional program at D7, and this negative proliferation signature persisted but with fewer genes represented at the leading edge at EOS (Supplementary Fig. S5). Despite the negative association with the specific proliferation markers, LuCaP 136CR acquired AA resistance that was enriched with genes associated with NF-κB transcriptional activity, EMT, extracellular matrix, and prostate basal cells (Supplementary Fig. S5). These results suggest the diversity of resistance mechanisms to AA and specifically indicate potential mechanisms that drive AR-independent resistance in the AA ultraresponsive phenotype.

Low basal AR signaling and a further reduction of androgen signaling upon resistance in the AA ultraresponder LuCaP 136CR

We examined the AR signaling axis to gain insight into its role in AA resistance and tumor progression. Previous reports showed that AA treatment elevated serum levels of progesterone and other upstream steroids that activated mutant AR (e.g., L701H and T878A) leading to AA resistance (14, 31–33). To elucidate whether AR mutation was involved in the differential AA responsiveness observed in our models, we sequenced the ligand-binding domain of AR and detected no mutation in the AA-treated LuCaP PDXs (data not shown), suggesting that the differential AA responsiveness was not due to AR mutation.

We next conducted targeted analysis on intratumoral androgens and androgen signaling pathways in AA-resistant tumors. We used a sensitive liquid chromatography–mass spectrometry method to detect intratumoral androgens that are sensitive to AA inhibition. In the ultraresponder LuCaP 136CR, AA treatment significantly reduced intratumoral levels of testosterone ($P = 0.009$), dihydrotestosterone ($P = 0.04$), androstenedione ($P = 0.03$; Fig. 5A), and androsterone ($P = 0.04$; Supplementary

Published OnlineFirst December 19, 2016; DOI: 10.1158/1078-0432.CCR-16-2054

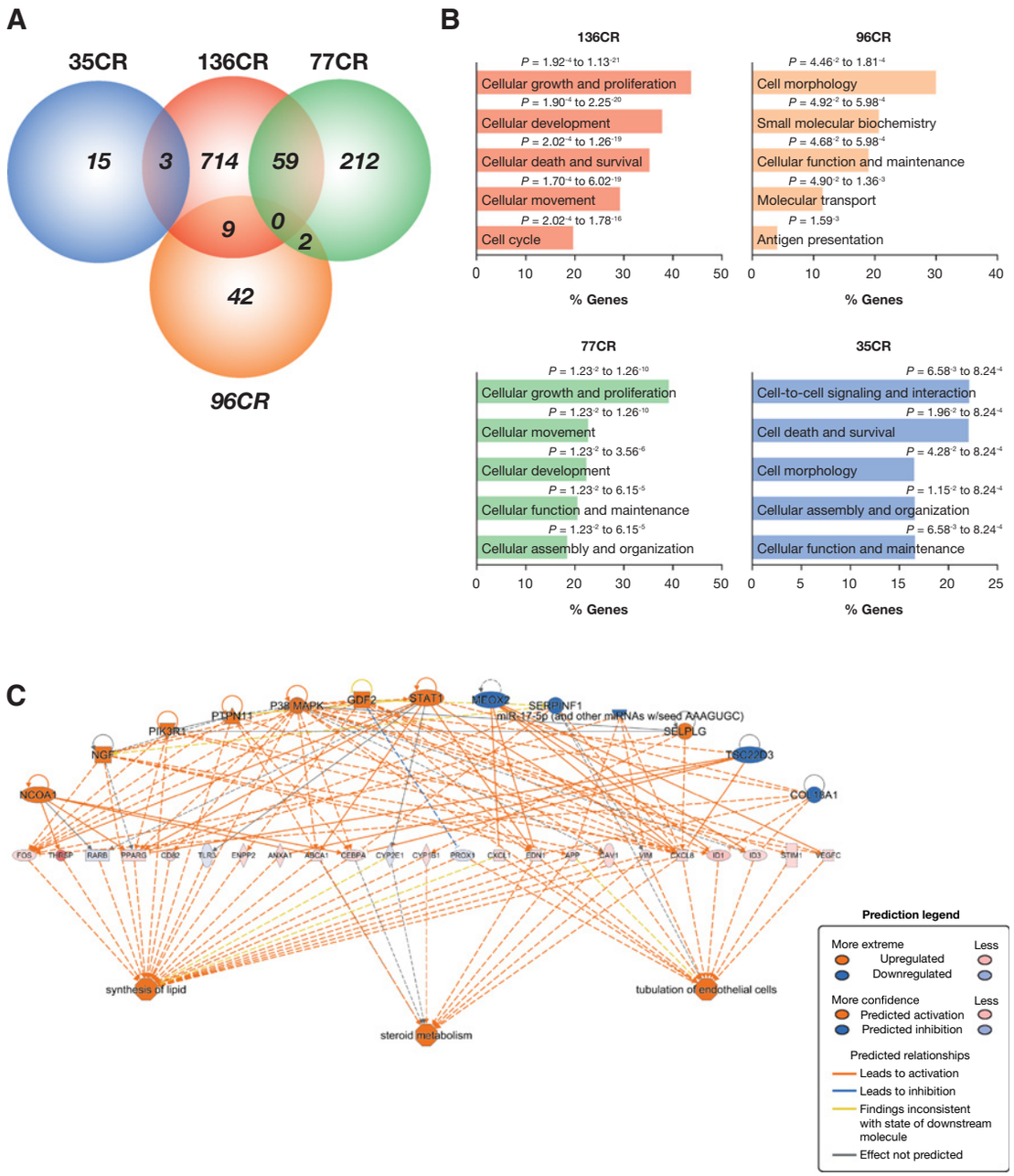

Figure 4.

Biological mechanisms underlying the acquired resistance to AA. **A,** Venn diagrams showing distinct gene alternations by AA upon treatment resistance at EOS among different LuCaP PDXs. **B,** Ingenuity Pathway Analysis identified the molecular and cellular functions associated with AA resistance in different LuCaP PDXs. **C,** Top regulator effect network in AA-resistant tumors in the AA ultraresponder LuCaP 136CR PDXs.

Fig. S6). Interestingly, LuCaP 136CR demonstrated the lowest basal AR signaling among the LuCaP lines tested, depicted by a low AR activity score (Fig. 5B) and a low AR signature score (Fig. 5C). Upon AA resistance, the decrease in intratumoral androgens was accompanied by a general downregulation of steroidogenic enzymes, including *LDLR* ($P = 0.004$), *STARD4* ($P = 0.005$), and *DUSP1* ($P = 0.01$; Supplementary Table S3; ref. 12), a further downregulation of AR activity (Fig. 5B), and a reduced AR signature score (Fig. 5C). These results suggested reduced AR signaling in the AA ultraresponder LuCaP 136CR upon resistance.

In contrast, despite decreasing testosterone in the intermediate responders LuCaP 77CR ($P = 0.03$) and LuCaP 96CR ($P = 0.02$) upon AA treatment, high variability in dihydrotestosterone levels was observed in LuCaP 77CR and a statistically insignificant reduction was observed in LuCaP 96CR ($P = 0.11$; Fig. 5A). Upstream steroids, including pregnenolone ($P = 0.02$) and

Published OnlineFirst December 19, 2016; DOI: 10.1158/1078-0432.CCR-16-2054

dehydroepiandrosterone (DHEA; $P = 0.056$), were increased in the intermediate responder LuCaP 77CR upon AA resistance (Supplementary Fig. S5), whereas progesterone was decreased in the intermediate responder LuCaP 96CR ($P = 0.02$; Supplementary Fig. S6). Consistent with the sustained level of intratumoral androgens, no reduction in the enrichment in AR-responsive genes (Fig. 5B) and AR signature (Fig. 5C) was detected upon AA resistance in the intermediate responders LuCaP 77CR and LuCaP 96CR. Similarly, in the AA minimal responder LuCaP 35CR, AA treatment showed an initial negative association with GSEA signatures of AR- and GR-regulated genes at D7 (Supplementary Fig. S5) and a reduction in our selected AR signature (Fig. 5C). However, the negative association was not observed upon AA resistance at EOS (Supplementary Fig. S5), and the AA-resistant tumor demonstrated a persistent expression of steroidogenic enzymes (Supplementary Table S3), AR-responsive genes (Fig. 5B), and AR signature (Fig. 5C). Due to the limited number of LuCaP 35CR AA-resistant tumors available, statistically significant change in the intratumoral androgens was not observed in these tumors upon AA resistance (Fig. 5A). Collectively, these results pointed to sustained AR signaling in the AA intermediate and minimal responders upon resistance. In all models, we also tested whether the AA-resistant tumors acquired a neuroendocrine phenotype. Our results showed that both neuroendocrine markers (chromogranin A and synaptophysin) were absent or minimally expressed (<0.1% in LuCaP 77CR) in the vehicle-treated tumors, and the expression did not change upon AA resistance (data not shown).

Finally, we questioned whether AR and GR levels in the tumor may contribute to the downregulation of AR signaling in the AA-resistant tumors in the ultraresponder LuCaP 136CR and the sustained AR signaling in the intermediate or minimal responders. In the ultraresponder LuCaP 136CR, the gene expression of AR and ARv7 was increased upon castration (Supplementary Table S4) but remained unchanged upon further androgen ablation by AA (Fig. 5D), and the nuclear AR and GR localization was not altered upon AA resistance (Fig. 5E and F). The nuclear GR level remained low even upon AA resistance in the ultraresponder LuCaP 136CR (Fig. 5F). In the intermediate and minimal responders, increased expression of AR and its variants was observed upon castration in LuCaP 77CR (Supplementary Table S4), but the expression of AR and ARv7 generally remained unchanged upon AA resistance except for LuCaP 96CR (Fig. 5D). Nuclear localization of AR remained high (i.e., H-score > 100) in the intermediate and minimal responders, although a slight decrease in nuclear AR localization for LuCaP 77CR was observed upon AA resistance (Fig. 5D and F). Collectively, these findings suggested active AR signaling in these AA-resistant tumors. Importantly, we observed a high basal level of nuclear GR in the AA minimal responder LuCaP 35CR (Fig. 5F) and a consistent upregulation of both GR gene expression (NR3C1, except for LuCaP 35CR) and nuclear localization for all intermediate and minimal responders (Fig. 5D and F). These GR results may suggest that high basal nuclear GR localization is associated with AA minimal responsiveness, and that an increase in nuclear GR upon AA treatment is associated with rapid, acquired resistance. In summary, upon AA resistance, the ultraresponder LuCaP 136CR displayed lower intratumoral androgens and AR signaling accompanied by sustainably low nuclear GR localization. In contrast, the intermediate and minimal responders demonstrated a slight decrease in intratumoral androgens and sustained AR signaling associated with an increase in nuclear GR localization.

Discussion

AA is effective in a subset of patients, but responding tumors eventually develop resistance. We used PDX models that recapitulated the diverse clinical responses of CRPC to AA and identified heterogeneous response phenotypes, including ultraresponsive, intermediate, and minimal. The ultraresponsive phenotype represents not only AA sensitivity but also durability. We report for the first time that the AA ultraresponsive phenotype is represented by a molecular signature of secreted proteins and biochemical features, including low basal AR signaling and a low basal nuclear GR level, which is insensitive to AA-induced upregulation.

Mechanisms underlying acquired resistance to AA are diverse and have not yet been fully identified. GR was shown to compensate for reduced AR activity through activation of overlapping target genes (34). High GR expression was associated with enzalutamide insensitivity (16), and preliminary results of the COU-AA-203 study demonstrated that high GR may predict low AA sensitivity (35). Our results provided novel information to highlight the role of GR in response to AA: (*a*) a low level of nuclear GR, and sustainably low GR on AA therapy, was predictive of durable AA inhibition; (*b*) low to intermediate levels of GR, despite initial response, and increase in nuclear GR were associated with rapid, acquired resistance to AA; and (*c*) a high basal level of GR was associated with *de novo* resistance/minimal responsiveness. Notably, although we observed a concordant increase in both GR transcript and protein expression levels in some models, discordance was present in others. This result indicates that GR transcripts may not ideally reflect the protein level, especially the nuclear protein level indicative of active GR signaling. Retrospective clinical studies investigating response and resistance patterns have suggested cross-response/resistance between enzalutamide and AA (36–43). However, whether a sustainably low level of GR will lead to a durable response to either AA or enzalutamide in patients, and whether an increase in GR is attributable to rapid AA resistance, requires clinical confirmation.

Copy-number gain of *AR* and *CYP17A1* has been shown to predict shorter progression-free survival with AA treatment (44). Our results supported, at a gene expression level, that the intermediate responders LuCaP 77CR/LuCaP 96CR and the minimal responder LuCaP 35CR demonstrated a higher AR level and enhanced androgen signaling when compared with the ultraresponder LuCaP 136CR. On the other hand, other preliminary studies on gene expression using pretreatment primary prostate cancer samples reported a significant association between proliferation-associated genes, androgen-regulated genes, and CYP17 cofactors with longer radiographic progression-free survival of patients receiving AA (45).

In our studies, the ultraresponsive phenotype demonstrated reduced AR signaling upon AA resistance, indicating an emergence of an AR-independent pathway to sustain survival. Upon AA resistance, the ultraresponders presented an enrichment of genes associated with EMT, prostate basal-type cells, and NF-κB activity. This is consistent with a previous report showing an association between EMT induction and the emergence of prostate cancer stem-like cells (CSC)–like phenotype following androgen

Published OnlineFirst December 19, 2016; DOI: 10.1158/1078-0432.CCR-16-2054

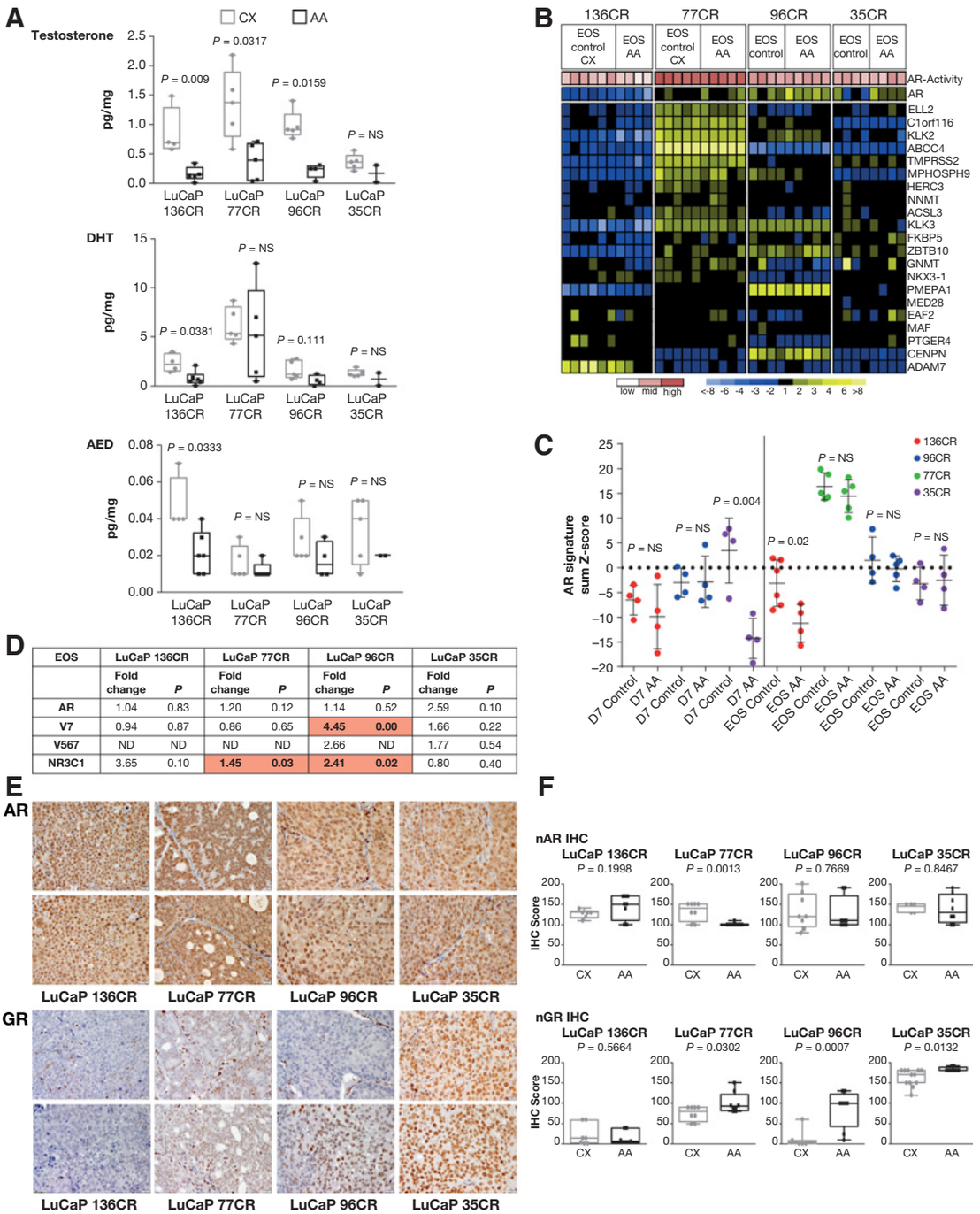

EOS	LuCaP 136CR		LuCaP 77CR		LuCaP 96CR		LuCaP 35CR	
	Fold change	P	Fold change	P	Fold change	P	Fold change	P
AR	1.04	0.83	1.20	0.12	1.14	0.52	2.59	0.10
V7	0.94	0.87	0.86	0.65	**4.45**	**0.00**	1.66	0.22
V567	ND	ND	ND	ND	2.66	ND	1.77	0.54
NR3C1	3.65	0.10	**1.45**	**0.03**	**2.41**	**0.02**	0.80	0.40

Figure 5.

Reduction of androgen signaling upon treatment resistance in the AA ultraresponsive phenotype. **A,** Levels of intratumoral androgens in control and AA-resistant CRPC PDXs measured by mass spectrometry. $n = 2$–6 per group. **B,** Heat map showing the low AR activity (top row, pink squares) and low expression of genes involved in androgen signaling in LuCaP 136CR ($n = 4$–6 per group), and **(C)** their respective AR signature score in LuCaP PDXs ($n = 4$–6 per group). **D,** qPCR analysis in vehicle versus AA-resistant tumors at EOS ($n = 4$–6 per group). **E,** Representative IHC pictures of AR and GR, and **(F)** their respective H-score in control and AA-resistant PDXs ($n = 6$–12 per group). Scale bar, 50 μm. Magnification, ×200. Each data point or column (heat map) represented an individual animal. $P < 0.05$ was considered statistically significant.

Published OnlineFirst December 19, 2016; DOI: 10.1158/1078-0432.CCR-16-2054

deprivation (46). In addition, activation of the NF-κB pathway is involved in the induction and maintenance of EMT (47, 48) and CSC-like characteristics in prostate cancer (49–51). These characteristics are concordant with the results of a preclinical study identifying a progenitor-like cell population with increased NF-κB activity upon resistance to androgen depletion (52) and reduced AR signaling upon increased NF-κB activity in prostate cancer (53). A recent report on NF-κB as a potential resistance mechanism for enzalutamide independent of ARv7 may provide another cross-resistance mechanism for AA (54).

In view of the heterogeneity of patients' responses to AA therapy, identification of biomarkers of responses has important implications for treatment selection in the context of precision oncology. The preclinical eight-gene molecular signature of secreted proteins associated with AA durable response that we identified can potentially be developed into a fast, noninvasive test to predict AA response. However, our results at this point are limited to the preclinical setting and by the number of PDX models representing each response phenotype. Validation in prospective clinical studies is needed to support translational value of this signature.

Collectively, the diverse resistant phenotypes associated with differential AA responses highlighted the need for a tailored next line of therapy. The resistance in the AA ultraresponsive phenotype was represented by low intratumoral androgens and AR signaling accompanied by a sustainably low nuclear GR localization, and alteration in gene expression associated with NF-κB activity and a EMT/basal cell phenotype. In contrast, resistance in the intermediate and minimally responding phenotypes demonstrated sustained AR signaling and increased nuclear GR localization. Novel treatments may be explored to target NF-κB activity with a rationale to prevent or revert an EMT basal cell phenotype in the ultraresponders and to target sustained AR/GR signaling in the intermediate or minimal responders upon AA resistance.

Disclosure of Potential Conflicts of Interest

W. Li holds ownership interest (including patents) in Johnson & Johnson. D.S. Ricci ownership interest (including patents) in Janssen. P.S. Nelson is a consultant/advisory board member for Astellas and Janssen. E. Corey reports receiving commercial research grants from Janssen Research & Development. No potential conflicts of interest were disclosed by the other authors.

Authors' Contributions

Conception and design: H.-M. Lam, R. McMullin, M. Gormley, W. Li, D.S. Ricci, S. Thomas, R.L. Vessella, E. Corey

Development of methodology: H.-M. Lam, H. M. Nguyen, L.G. Brown, K. Verstraeten, E.A. Mostaghel, E. Corey

Acquisition of data (provided animals, acquired and managed patients, provided facilities, etc.): H.-M. Lam, R. McMullin, K. Verstraeten, H.M. Nguyen, L.G. Brown

Analysis and interpretation of data (e.g., statistical analysis, biostatistics, computational analysis): H.-M. Lam, R. McMullin, I. Coleman, M. Gormley, R. Gulati, S.K. Holt, W. Li, E.A. Mostaghel, E. Corey

Writing, review, and/or revision of the manuscript: H.-M. Lam, R. McMullin, H.M. Nguyen, I. Coleman, M. Gormley, R. Gulati, L.G. Brown, S.K. Holt, W. Li, D.S. Ricci, K. Verstraeten, S. Thomas, E.A. Mostaghel, P.S. Nelson, R.L. Vessella, E. Corey

Administrative, technical, or material support (i.e., reporting or organizing data, constructing databases): H.-M. Lam, R. McMullin, W. Li, P.S. Nelson, E. Corey

Study supervision: H.-M. Lam, R. McMullin, W. Li, D.S. Ricci, S. Thomas, E. Corey

Acknowledgments

Editorial assistance was provided by Ira Mills, PhD, of PAREXEL and funded by Janssen Global Services, LLC. We thank Bryce Lakely and Daniel Sondheim for their excellent technical assistance.

Grant Support

The work was supported by The Richard M. Lucas Foundation, the Prostate Cancer Foundation, SU2C-AACR-DT0712, an NIH PO1 CA163227, an NIH R21 CA194798 and the PNW Prostate Cancer SPORE NIH P50 CA097186. HML is a recipient of the Young Investigator Award from the Prostate Cancer Foundation, an Idea Development Award from the Department of Defense (W81XWH-14-1-0271), and an FHCRC/UW Cancer Consortium New Investigator Grant of an NIH P30 CA015704. Janssen Research & Development provided funding support for some of the molecular analyses reported herein.

The costs of publication of this article were defrayed in part by the payment of page charges. This article must therefore be hereby marked *advertisement* in accordance with 18 U.S.C. Section 1734 solely to indicate this fact.

Received August 15, 2016; revised November 9, 2016; accepted December 8, 2016; published OnlineFirst December 19, 2016.

References

1. Crawford ED. Understanding the epidemiology, natural history, and key pathways involved in prostate cancer. Urology 2009;73: S4–10.
2. Attard G, Belldegrun AS, de Bono JS. Selective blockade of androgenic steroid synthesis by novel lyase inhibitors as a therapeutic strategy for treating metastatic prostate cancer. BJU Int 2005;96:1241–6.
3. Barrie SE, Potter GA, Goddard PM, Haynes BP, Dowsett M, Jarman M. Pharmacology of novel steroidal inhibitors of cytochrome P450(17) alpha (17 alpha-hydroxylase/C17-20 lyase). J Steroid Biochem Mol Biol 1994; 50:267–73.
4. O'Donnell A, Judson I, Dowsett M, Raynaud F, Dearnaley D, Mason M, et al. Hormonal impact of the 17alpha-hydroxylase/C(17,20)-lyase inhibitor abiraterone acetate (CB7630) in patients with prostate cancer. Br J Cancer 2004;90:2317–25.
5. de Bono JS, Logothetis CJ, Molina A, Fizazi K, North S, Chu L, et al. Abiraterone and increased survival in metastatic prostate cancer. N Engl J Med 2011;364:1995–2005.
6. Fizazi K, Scher HI, Molina A, Logothetis CJ, Chi KN, Jones RJ, et al. Abiraterone acetate for treatment of metastatic castration-resistant prostate cancer: Final overall survival analysis of the COU-AA-301 randomised, double-blind, placebo-controlled phase 3 study. Lancet Oncol 2012;13:983–92.
7. Ryan CJ, Smith MR, de Bono JS, Molina A, Logothetis CJ, de Souza P, et al. Abiraterone in metastatic prostate cancer without previous chemotherapy. N Engl J Med 2013;368:138–48.
8. Rathkopf DE, Smith MR, de Bono JS, Logothetis CJ, Shore ND, de Souza P, et al. Updated interim efficacy analysis and long-term safety of abiraterone acetate in metastatic castration-resistant prostate cancer patients without prior chemotherapy (COU-AA-302). Eur Urol 2014; 66:815–25.
9. Ryan CJ, Smith MR, Fizazi K, Saad F, Mulders PF, Sternberg CN, et al. Abiraterone acetate plus prednisone versus placebo plus prednisone in chemotherapy-naive men with metastatic castration-resistant prostate cancer (COU-AA-302): Final overall survival analysis of a randomised, double-blind, placebo-controlled phase 3 study. Lancet Oncol 2015; 16:152–60.
10. Danila DC, Anand A, Sung CC, Heller G, Leversha MA, Cao L, et al. TMPRSS2-ERG status in circulating tumor cells as a predictive biomarker of sensitivity in castration-resistant prostate cancer patients treated with abiraterone acetate. Eur Urol 2011;60:897–904.

11. Antonarakis ES, Lu C, Wang H, Luber B, Nakazawa M, Roeser JC, et al. AR-V7 and resistance to enzalutamide and abiraterone in prostate cancer. N Engl J Med 2014;371:1028–38.
12. Mostaghel EA, Marck BT, Plymate SR, Vessella RL, Balk S, Matsumoto AM, et al. Resistance to CYP17A1 inhibition with abiraterone in castration-resistant prostate cancer: Induction of steroidogenesis and androgen receptor splice variants. Clin Cancer Res 2011;17:5913–25.
13. Carreira S, Romanel A, Goodall J, Grist E, Ferraldeschi R, Miranda S, et al. Tumor clone dynamics in lethal prostate cancer. Sci Transl Med 2014; 6:254ra125.
14. Chen EJ, Sowalsky AG, Gao S, Cai C, Voznesensky O, Schaefer R, et al. Abiraterone treatment in castration-resistant prostate cancer selects for progesterone responsive mutant androgen receptors. Clin Cancer Res 2015;21:1273–80.
15. Romanel A, Gasi TD, Conteduca V, Jayaram A, Casiraghi N, Wetterskog D, et al. Plasma AR and abiraterone-resistant prostate cancer. Sci Transl Med 2015;7:312re10.
16. Arora VK, Schenkein E, Murali R, Subudhi SK, Wongvipat J, Balbas MD, et al. Glucocorticoid receptor confers resistance to antiandrogens by bypassing androgen receptor blockade. Cell 2013;155:1309–22.
17. Montgomery B, Nelson PS, Vessella R, Kalhorn T, Hess D, Corey E. Estradiol suppresses tissue androgens and prostate cancer growth in castration resistant prostate cancer. BMC Cancer 2010;10:244.
18. Montgomery RB, Mostaghel EA, Vessella R, Hess DL, Kalhorn TF, Higano CS, et al. Maintenance of intratumoral androgens in metastatic prostate cancer: A mechanism for castration-resistant tumor growth. Cancer Res 2008;68:4447–54.
19. Nguyen HM, Ruppender N, Zhang X, Brown LG, Gross TS, Morrissey C, et al. Cabozantinib inhibits growth of androgen-sensitive and castration-resistant prostate cancer and affects bone remodeling. PLoS One 2013;8: e78881.
20. Morrissey C, Brown LG, Pitts TE, Vessella RL, Corey E. Bone morphogenetic protein 7 is expressed in prostate cancer metastases and its effects on prostate tumor cells depend on cell phenotype and the tumor microenvironment. Neoplasia 2010;12:192–205.
21. Pfitzenmaier J, Quinn JE, Odman AM, Zhang J, Keller ET, Vessella RL, et al. Characterization of C4-2 prostate cancer bone metastases and their response to castration. J Bone Miner Res 2003;18:1882–8.
22. Irizarry RA, Hobbs B, Collin F, Beazer-Barclay YD, Antonellis KJ, Scherf U, et al. Exploration, normalization, and summaries of high density oligonucleotide array probe level data. Biostatistics 2003;4:249–64.
23. Tusher VG, Tibshirani R, Chu G. Significance analysis of microarrays applied to the ionizing radiation response. Proc Natl Acad Sci U S A 2001;98:5116–21.
24. Hieronymus H, Lamb J, Ross KN, Peng XP, Clement C, Rodina A, et al. Gene expression signature-based chemical genomic prediction identifies a novel class of HSP90 pathway modulators. Cancer Cell 2006;10:321–30.
25. Lam HM, Ho SM, Chen J, Medvedovic M, Tam NN. Bisphenol A disrupts HNF4alpha-regulated gene networks linking to prostate preneoplasia and immune disruption in noble rats. Endocrinology 2016;157:207–19.
26. Ruppender N, Larson S, Lakely B, Kollath L, Brown L, Coleman I, et al. Cellular adhesion promotes prostate cancer cells escape from dormancy. PLoS One 2015;10:e0130565.
27. Subramanian A, Tamayo P, Mootha VK, Mukherjee S, Ebert BL, Gillette MA, et al. Gene set enrichment analysis: A knowledge-based approach for interpreting genome-wide expression profiles. Proc Natl Acad Sci U S A 2005;102:15545–50.
28. Kanehisa M, Goto S. KEGG: Kyoto encyclopedia of genes and genomes. Nucleic Acids Res 2000;28:27–30.
29. Chan QK, Lam HM, Ng CF, Lee AY, Chan ES, Ng HK, et al. Activation of GPR30 inhibits the growth of prostate cancer cells through sustained activation of Erk1/2, c-jun/c-fos-dependent upregulation of p21, and induction of G(2) cell-cycle arrest. Cell Death Differ 2010; 17:1511–23.
30. Yu Z, Chen S, Sowalsky AG, Voznesensky OS, Mostaghel EA, Nelson PS, et al. Rapid induction of androgen receptor splice variants by androgen deprivation in prostate cancer. Clin Cancer Res 2014;20:1590–600.
31. Cai C, Balk SP. Intratumoral androgen biosynthesis in prostate cancer pathogenesis and response to therapy. Endocr Relat Cancer 2011;18:R175–82.
32. Zhao XY, Malloy PJ, Krishnan AV, Swami S, Navone NM, Peehl DM, et al. Glucocorticoids can promote androgen-independent growth of prostate cancer cells through a mutated androgen receptor. Nat Med 2000;6:703–6.
33. Cai C, Chen S, Ng P, Bubley GJ, Nelson PS, Mostaghel EA, et al. Intratumoral de novo steroid synthesis activates androgen receptor in castration-resistant prostate cancer and is upregulated by treatment with CYP17A1 inhibitors. Cancer Res 2011;71:6503–13.
34. Sahu B, Laakso M, Pihlajamaa P, Ovaska K, Sinielnikov I, Hautaniemi S, et al. FoxA1 specifies unique androgen and glucocorticoid receptor binding events in prostate cancer cells. Cancer Res 2013;73:1570–80.
35. Efstathiou E, Li W, Gormley M, McMullin R, Ricci DS, Davis JW, et al. Biological heterogeneity in localized high-risk prostate cancer (LHRPC) from a study of neoadjuvant abiraterone acetate plus leuprolide acetate (LHRHa) versus LHRHa. J Clin Oncol 2015;33:(supp: abstract 5005).
36. Loriot Y, Bianchini D, Ileana E, Sandhu S, Patrikidou A, Pezaro C, et al. Antitumour activity of abiraterone acetate against metastatic castration-resistant prostate cancer progressing after docetaxel and enzalutamide (MDV3100). Ann Oncol 2013;24:1807–12.
37. Noonan KL, North S, Bitting RL, Armstrong AJ, Ellard SL, Chi KN. Clinical activity of abiraterone acetate in patients with metastatic castration-resistant prostate cancer progressing after enzalutamide. Ann Oncol 2013; 24:1802–7.
38. Schrader AJ, Boegemann M, Ohlmann CH, Schnoeller TJ, Krabbe LM, Hajili T, et al. Enzalutamide in castration-resistant prostate cancer patients progressing after docetaxel and abiraterone. Eur Urol 2014;65:30–6.
39. Badrising S, van der Noort V, van Oort IM, van den Berg HP, Los M, Hamberg P, et al. Clinical activity and tolerability of enzalutamide (MDV3100) in patients with metastatic, castration-resistant prostate cancer who progress after docetaxel and abiraterone treatment. Cancer 2014; 120:968–75.
40. Schmid SC, Geith A, Boker A, Tauber R, Seitz AK, Kuczyk M, et al. Enzalutamide after docetaxel and abiraterone therapy in metastatic castration-resistant prostate cancer. Adv Ther 2014;31:234–41.
41. Brasso K, Thomsen FB, Schrader AJ, Schmid SC, Lorente D, Retz M, et al. Enzalutamide antitumour activity against metastatic castration-resistant prostate cancer previously treated with docetaxel and abiraterone: A multicentre analysis. Eur Urol 2015;68:317–24.
42. Suzman DL, Luber B, Schweizer MT, Nadal R, Antonarakis ES. Clinical activity of enzalutamide versus docetaxel in men with castration-resistant prostate cancer progressing after abiraterone. Prostate 2014;74:1278–85.
43. Bianchini D, Lorente D, Rodriguez-Vida A, Omlin A, Pezaro C, Ferraldeschi R, et al. Antitumour activity of enzalutamide (MDV3100) in patients with metastatic castration-resistant prostate cancer (CRPC) pre-treated with docetaxel and abiraterone. Eur J Cancer 2014;50:78–84.
44. Salvi S, Casadio V, Conteduca V, Burgio SL, Menna C, Bianchi E, et al. Circulating cell-free AR and CYP17A1 copy number variations may associate with outcome of metastatic castration-resistant prostate cancer patients treated with abiraterone. Br J Cancer 2015;112:1717–24.
45. Ricci DS, Li W, Griffin TW, Gromley M, Henitz E, Ryan CJ, et al. Predicting response to abiraterone acetate (AA): mRNA biomarker analysis of study COU-AA-302. J Clin Oncol 2014;32:(abstract 5058).
46. Sun Y, Wang BE, Leong KG, Yue P, Li L, Jhunjhunwala S, et al. Androgen deprivation causes epithelial-mesenchymal transition in the prostate: Implications for androgen-deprivation therapy. Cancer Res 2012;72: 527–36.
47. Huber MA, Azoitei N, Baumann B, Grunert S, Sommer A, Pehamberger H, et al. NF-kappaB is essential for epithelial-mesenchymal transition and metastasis in a model of breast cancer progression. J Clin Invest 2004; 114:569–81.
48. Wang X, Belguise K, Kersual N, Kirsch KH, Mineva ND, Galtier F, et al. Oestrogen signalling inhibits invasive phenotype by repressing RelB and its target BCL2. Nat Cell Biol 2007;9:470–8.
49. Odero-Marah VA, Wang R, Chu G, Zayzafoon M, Xu J, Shi C, et al. Receptor activator of NF-kappaB Ligand (RANKL) expression is associated with epithelial to mesenchymal transition in human prostate cancer cells. Cell Res 2008;18:858–70.
50. Birnie R, Bryce SD, Roome C, Dussupt V, Droop A, Lang SH, et al. Gene expression profiling of human prostate cancer stem cells reveals a pro-inflammatory phenotype and the importance of extracellular matrix interactions. Genome Biol 2008;9:R83.
51. Kong D, Wang Z, Sarkar SH, Li Y, Banerjee S, Saliganan A, et al. Platelet-derived growth factor-D overexpression contributes to epithelial-

Published OnlineFirst December 19, 2016; DOI: 10.1158/1078-0432.CCR-16-2054

mesenchymal transition of PC3 prostate cancer cells. Stem Cells 2008;26: 1425–35.
52. Rajasekhar VK, Studer L, Gerald W, Socci ND, Scher HI. Tumour-initiating stem-like cells in human prostate cancer exhibit increased NF-kappaB signalling. Nat Commun 2011;2:162.
53. Campa VM, Baltziskueta E, Bengoa-Vergniory N, Gorrono-Etxebarria I, Wesolowski R, Waxman J, et al. A screen for transcription factor targets of glycogen synthase kinase-3 highlights an inverse correlation of NFkappaB and androgen receptor signaling in prostate cancer. Oncotarget 2014; 5:8173–87.
54. Jeganathan S, Zoubeidi A, Gleave M, Wouters BG, Joshua AM. Using functional and chemical genomics to identify mechanisms of Enzalutamide resistance in prostate cancer. Cancer Res 2015;75:(supp: abstract 732).

Published OnlineFirst December 19, 2016; DOI: 10.1158/1078-0432.CCR-16-2054

Clinical Cancer Research

Characterization of an Abiraterone Ultraresponsive Phenotype in Castration-Resistant Prostate Cancer Patient-Derived Xenografts

Hung-Ming Lam, Ryan McMullin, Holly M. Nguyen, et al.

Clin Cancer Res 2017;23:2301-2312. Published OnlineFirst December 19, 2016.